Modulation of the Tumor Microenvironment To Overcome Glioblastoma Treatment Resistance

Mohammed Ahmed

Thèse de doctorat

NNT : 2021UPASL037

université PARIS-SACLAY

Modulation du microenvironnement tumoral pour contourner la résistance du glioblastome aux traitements

Modulation of the tumor microenvironment to overcome glioblastoma treatment resistance

Thèse de doctorat de l'université Paris-Saclay

École doctorale n°582 Cancérologie, biologie, médecine, santé (CBMS)
Discipline : Recherche clinique, innovation technologique, santé publique
Unité de recherche : Institut du Cerveau (ICM)
Référent : Faculté de médecine

Thèse présentée et soutenue à Paris-Saclay

le 28/05/2021, par

Mohammed AHMED

Composition du Jury

Pr Alexandre CARPENTIER PU-PH, HDR, Sorbonne Université	**Président**
Dr Hélène CASTEL Directeur de Recherche, Université de Rouen	**Rapporteur & Examinatrice**
Dr Monique DONTENWILL Directeur de Recherche, Université de Strasbourg	**Rapporteur & Examinatrice**
Dr Gilles HUBERFELD MCU-PH, HDR, Sorbonne Université	**Examinateur**

Direction de la thèse

Pr Ahmed IDBAIH PU-PH, HDR, Sorbonne Université	**Directeur de thèse**

`

`

`

List of Tables

`

List of Figures

`

`

Acknowledgement

I want to express my deep gratitude to all people who made this thesis possible. Firstly, I would like to acknowledge Marie Curie Action Plans for their funding of the GLIOTRAIN consortium and my project. Special thanks go to Dr. Alice O'Farrell, who made our training valuable with the courses she organized during the last three years. Additionally, I would like to thank the jury members for their agreement to evaluate my work, Dr. Hélène CASTEL, and Dr. Monique DONTENWILL as referees and Dr. Gilles HUBERFELD, and Pr. Alexandre CARPENTIER as examiners.

My deep appreciations go to Pr. Ahmed IDBAIH and Dr. Maite VERREAULT who supervised me during my doctoral training and supported me personally and academically. Their patience, knowledge, support, encouragement, and efforts cannot be summarized in a few sentences. I want to extend my sincere thanks to Pr. Marc SANSON and Dr. Emmanuelle HUILLARD who welcomed me to the Genetics and Development of Nervous System Tumors at Paris Brain Institute, allowing me to work in a quality scientific environment.

Additionally, I would like to give my deep appreciation for Carthera members who provided me with technical and scientific support during the last three years. Dr. Guillaume BOUCHOUX and Dr. Charlotte SCHMITT.

During the flow cytometry experimental design, I had the chance to work with a great collaborator Dr. Coralie Guerin, the head of the cytometry platform in Institute Curie. She provided us with enough support and efficient planning for our flow cytometry results.

I am grateful to everyone who supported me in the GLIOTEX team Nolwenn LEMAIRE, Emie QUISSAC. Thank you for your continuous help. Many thanks to my Ph.D. colleagues in the office: Yanis, Quentin, Isaias, Irma, and Alexa, for all the fun that we had and all the unforgettable moments that we had.

`

For the women who treated me and raised me to be a man, my Mum “Rabaa” no words express my deep love for you, may Allah bless you. My sisters Manal, Rana, Faten, Doaa, my brother Fady, my brother-in-law Muneeb, and all family members. Finally, I would like to express my gratitude to my family-in-law and the deepest gratitude for my wife “Sara” who supported me in every step during my thesis. You were with me in the darkest times and the happiest ones, and you are the angel behind all this work.

`

Resume

Le glioblastome (GBM) est le cancer cérébral primitif le plus fréquent chez l'adulte avec une incidence estimée entre 2 et 5 nouveaux cas par an et pour 100000 habitants en Amérique du Nord et en Europe. Le GBM représente plus de 50% des tumeurs cérébrales primitives malignes. Le pronostic des patients souffrant de GBM est globalement sombre. Le traitement standard de première ligne chez les patients souffrant d'un GBM nouvellement diagnostiqué repose sur une résection neurochirurgicale aussi complète que possible suivie d'une radiochimiothérapie concomitante et d'une chimiothérapie adjuvante.

Malgré cette stratégie thérapeutique lourde, la majorité des GBM récidivent. Depuis 2015, le témozolomide est la chimiothérapie standard de première ligne. Au cours des dernières décennies, des efforts importants ont été menés pour développer de nouveaux traitements plus efficaces et mieux tolérés, notamment des thérapies moléculaires ciblées, des immunothérapies et des dispositifs médicaux.

Tout d'abord, dans le cadre de cette thèse nous avons synthétisé le rôle des membres de la superfamille des protéines ABC exprimées au sein de la barrière hémato-encéphalique (BHE) et leur implication dans la résistance des GBM à la chimiothérapie. Nous avons résumé les stratégies développées pour contourner la résistance à la chimiothérapie médiée par les transporteurs ABC dans le GBM. Ces stratégies correspondent soit à une inhibition partielle ou complète, chimique ou physique, des transporteurs ABC soit à un contournement des pompes d'efflux ABC : (i) des nanotransporteurs, (ii) des anticorps conjugués et (iii) des ultrasons. L'inhibition des transporteurs ABC empêche l'efflux des agents thérapeutiques des cellules endothéliales vers la circulation sanguine et augmente leur pénétration dans le cerveau sain et le cerveau tumoral. En plus des inhibitions chimique ou pharmacologique des protéines ABC, des

`

approches physiques permettent également de contourner la BHE. En effet, récemment, il a été montré que les ultrasons étaient capables d'inhiber l'expression des transporteurs ABC. Les ultrasons peuvent réduire l'expression de la protéine ABCB1 dans les vaisseaux cérébraux sans affecter l'intégrité des autres protéines. Des études complémentaires sont nécessaires pour préciser le rôle des ultrasons dans le contournement de la BHE et dans l'augmentation de l'efficacité des chimiothérapies contre le GBM.

Ensuite nous avons étudié l'expression des protéines des checkpoints immunitaires CD80 et CD86 et leur valeur pronostique chez les patients présentant un GBM nouvellement diagnostiqué et traité selon le standard de soins. CD80 et CD86 sont exprimés dans les cellules tumorales des GBM mais également dans les cellules du microenvironnement. L'expression CD80 et CD86 semblent prédominer dans les cellules tumorales de GBM. Néanmoins des études complémentaires sont nécessaires pour apprécier précisément l'expression de CD80 et CD86 dans les différentes populations cellulaires composant le GBM (i.e., cellules tumorales et cellules du microenvironnement). Une faible expression de CD80 et une faible expression de CD86 sont associées à un meilleur pronostic en termes de survie sans progression chez les patients souffrant d'un GBM nouvellement diagnostiqué. CD80 et CD86 sont des inhibiteurs des lymphocytes T. Nous supposons que les GBM exprimant faiblement CD80 et CD86 limitent moins l'action anti-tumorale dans lymphocytes T cytotoxiques. Parallèlement, les GBM exprimant fortement CD80 et CD86 pourraient répondre de manière plus importante aux anticorps immunothérapeutiques anti-CTLA-4. Bien que nous ne soyons pas parvenu à démontrer, probablement en raison d'un manque de puissance statistique de notre cohorte d'entrainement, une valeur pronostique indépendante de l'expression de CD80 et CD86 chez les patients souffrant d'un GBM nouvellement diagnostiqué, une tendance est observée. Notre étude encourage à l'étude du microenvironnement tumoral à la recherche de biomarqueurs, pertinents, pronostiques et/ou prédictifs de la réponse aux traitements.

`

En effet, des biomarqueurs composites associant données cliniques, données tumorales et données du microenvironnement pourraient être très puissant pour guider l'évaluation pronostique et le traitement des patients souffrant de GBM.

Enfin, deux des obstacles à l'efficacité des traitements anti-tumoraux conventionnels contre le GBM est la BHE et le microenvironnement tumoral immunodéprimé. Notre thèse s'est focalisée sur le contournement de la BHE pour moduler le microenvironnement tumoral pour une meilleure efficacité thérapeutique.

L'ouverture, médiée par les ultrasons, de la BHE (OBMU) a été évaluée dans des modèles précliniques pour contourner la BHE et augmenter la pénétration intracérébrale de plusieurs types d'agents thérapeutiques. Les ultrasons pulsés de faible intensité peuvent être délivrés en direction du cerveau afin d'induire une cavitation de microbulles délivrées quant à elles par voie intraveineuse. Cette mise en cavitation des microbulles permet d'ouvrir les jonctions serrées localisées entre les cellules endothéliales de la BHE. Plusieurs médicaments ont été testés en combinaison avec l'OBMU pour le traitement des GBM, notamment le témozolomide, la carmustine, l'irinotecan, le carboplatine, la doxorubicine et, les liposomes chargés de médicaments. Récemment, l'OBMU a été évaluée dans le cadre d'essais cliniques qui ont permis de confirmer sa sécurité et sa tolérance chez les patients et plus particulièrement les patients souffrant d'un GBM en récidive.

Les immunothérapies et notamment les inhibiteurs des checkpoints immunitaires (ICI) et les thérapies cellulaires ont révolutionné le traitement de plusieurs types de tumeurs solides via une stimulation de l'immunité anti-tumorale. Les premiers essais cliniques évaluant le nivolumab en monothérapie ou en combinaison avec l'ipilimumab ont été décevants avec une efficacité limitée et une certaine toxicité. L'essai clinique de phase III CheckMate-143 a comparé le nivolumab au bevacizumab. Malheureusement, le nivolumab ne s'est pas montré supérieur en termes d'efficacité par rapport au

`

bevacizumab chez les patients souffrant de GBM. Plusieurs raisons peuvent expliquer la faible efficacité des ICI dans le GBM : (i) la faible charge mutationnelle des cellules de GBM, (ii) l'absence de biomarqueurs prédictifs de réponse au ICI guidant la prescription, (iii) la faible pénétration des ICI dans le parenchyme cérébral, (iv) la faible activation immunitaire périphérique dans les ganglions lymphatiques, (v) l'immunosuppression locale et, (vi) la faible pénétration des lymphocytes dans le cerveau normal et tumoral.

Notre travail a confirmé l'efficacité modeste des ICI chez des souris souffrant de GBM GL261 et Nfpp10. Nous avons donc étudié l'efficacité des ICI combinés à l'OBMU dans des modèles précliniques murins de GBM.

Les paramètres des ultrasons (i.e. la pression acoustique, les temps, la quantité de microbulles, la fréquence des ultrasons) influent la sécurité et l'efficacité de l'OBMU. La sécurité et l'efficacité de l'OBMU ont été évaluées chez des souris C57BL/6 greffées orthotopiquement avec des cellules de GBM GL261. L'OBMU a été optimisée pour cibler l'hémisphère cérébral droit dans lequel sont greffées les cellules tumorales GL261. L'optimisation a porté sur les paramètres des ultrasons et la fréquence de l'ouverture de la BHE.

La concentration du nivolumab dans le cerveau est augmentée de 28 fois lorsqu'il est combiné à l'OBMU versus lorsqu'il est utilisé sans ouverture de la BHE. Dans l'autre sens, l'OBMU permet également le passage de molécules tumorales de la tumeur vers la circulation sanguine. En effet, une quantité significative d'ADN tumoral a été identifié dans le sang des souris souffrant de GBM et traitées par OBMU. De plus, nous avons montré que la BHE limite l'efficacité dans anticorps immunothérapeutiques anti-PD-L1 chez les souris souffrant de GBM GL261. De manière intéressante, l'efficacité des anti-PD-L1 est nettement augmentée quand ils sont combinés à une OBMU avec 76% de souris souffrant de GBM-GL261 survivantes à plus dans 100 jours versus seulement 26% (4/15) pour souris traitées par anti-PD-L1 seul. Enfin, nous avons montré une plus grande activation des

`

cellules microgliales chez les souris traitées par OBMU versus les souris traitées par anti-PD-L1 seul.

`

Abbreviations

Full name	Abbreviations
Chromosome arms 1p and 19q	1p/19q
Depatuxizumab Mafodotin	ABT-414
Antibody-drug conjugates	ADC
X-linked adrenoleukodystrophy	ALD
Alternative lengthening of telomeres	ALT
Adenosine triphosphate	ATP
Alpha thalassemia/mental retardation syndrome X-linked chromatin remodeler	ATRX
Blood-brain barrier	BBB
Carmustine	BCNU
Breast cancer resistance protein	BCRP
Bone morphogenetic protein 7	BMP7
Blood-tumor barrier	BTB
Carbonic Anhydrase XII	CA XII
Cyclin dependent kinase inhibitor 2A	CDKN2A
Convection enhanced delivery	CED
Central nervous system	CNS
Computed tomography	CT
Cytotoxic T-lymphocyte-associated antigen-4	CTLA-4
Dendritic cells	DC
Endothelial cells	EC
Extracellular matrix	ECM
Epidermal growth factor receptor	EGFR
Fluid-attenuated inversion recovery	FLAIR
Food and Drug administration	FDA
Gamma-aminobutyric acid receptor subunit alpha-1	GABRA1
Glioma-associated neovascularization	GAN
Glioblastoma	GBM
Glioblastoma stem cells	GSC
Gray-radiation	GY
Histone H3 mutation	H3K27m
hypoxia-inducible factor-1 alpha	HIF-1α
Immune checkpoint blocking antibodies	ICB
Isocitrate dehydrogenase	IDH
Interferon	IFN
Immunohistochemistry	IHC
Interleukin	IL
Kilo Dalton	Kda
Karnofsky Performance Scale	KPS
MRP1 and MRP4 I inhibitor	MDM2
Multidrug resistance	MDR
Proto-oncogene, receptor tyrosine kinase	MERTK

`

O6-Methylguanine-DNA Methyltransferase	MGMT
Major histocompatibility complex	MHC
An inhibitor of ABCC1 and ABCC4	MK571
Magnetic resonance imaging	MRI
Monoclonal antibodies	MAbs
Multidrug resistance-associated protein	MRP
Molecular weight	MW
Nucleotide-binding domains	NBD
Neurofilament Light	NEFL
Not otherwise specified	NOS
Overall survival	OS
OncoNeuroTek database	ONT
Programmed death-1 receptor	PD-1
Patient-derived cell line	PDCL
Platelet-derived growth factor receptor A	PDGFRA
Programmed death ligand-1	PD-L1
Positron emission tomography	PET
Progression-free surival	PFS
P-glycoprotein	P-gly
Phosphatase and tensin homolog	PTEN
Tumor suppressor retinoblastoma	pRB
Proto-oncogene, NF-KB subunit	RELB
Role of 5	RO5
Receptor tyrosine kinase	RTK
Src homology 2	SHR2
Solute carrier family 12-member 5	SLC1245
Single nucleotide polymorphism	SNP
Synaptotagmin 1	SYT1
Tumor associated macrophages	TAM
The Cancer Genome Atlas	TCGA
T cells receptor	TCR
Transforming growth factor-beta	TGF-B
Trans membranous domain	TMD
Tumor microenvironment	TME
Temozolomide	TMZ
Tumor necrosis factor receptor 1 superfamily Member 1A	TNFRSF1A
Tumor necrosis factor receptor type 1-associated death domain protein	TRADD
T regulatory lymphocytes	Tregs
Tumor treating fields	TTF
Ultrasound-mediated blood-brain barrier opening	UMBO
World health organization	WHO

`

Introduction

1. Classification of primary brain tumors in adults

1.1 Primary brain tumors in adults

The definition and the classification of primary brain tumors advanced over the last decades. The classification of primary brain tumors was initially based on histo-morphological features with three major categories: (i) gliomas (including glioblastomas, GBM), (ii) meningiomas and, (iii) rare primary brain tumors **(Figure 1).**

The most common primary malignant brain tumors are diffuse gliomas. Diffuse gliomas account for almost 30% of all primary central nervous system (CNS) tumors and 80% of all malignant primary CNS tumors. The heterogeneity of diffuse gliomas was an obstacle to define specifically subcategories of diffuse gliomas with clinical relevance (Finch et al., 2021). During the 20th century, several researchers described a classification of diffuse gliomas. Kernohan et al. (1949) suggested that diffuse gliomas are originated from adult glial cells that mutate and acquire malignancy. In 1979, the World Health Organization (WHO) established a classification for diffuse glioma based on tumor cell phenotype (*i.e.,* astrocytic, oligodendroglial or oligoastrocytic) and grade of malignancy (from II to IV). The grade of malignancy integrates tumor cell density, tumor cell differentiation, necrosis, mitosis and endotheliocapillary proliferation.

WHO classification was revised in 1993, 2000, 2007, and recently in 2016 (Louis et al., 2016, Stoyanov and Dzhenkov, 2018). The novelty of the WHO 2016 classification was the implementation of molecular features for classification of diffuse gliomas (Louis et al., 2016). In addition to the phenotype and the grade of malignancy, molecular markers are now required for accurate and comprehensive diagnosis: (i) Isocitrate dehydrogenase

`

(*IDH*) mutational status, (ii) chromosome arms 1p/19q status and, (iii) histone H3 mutational status.

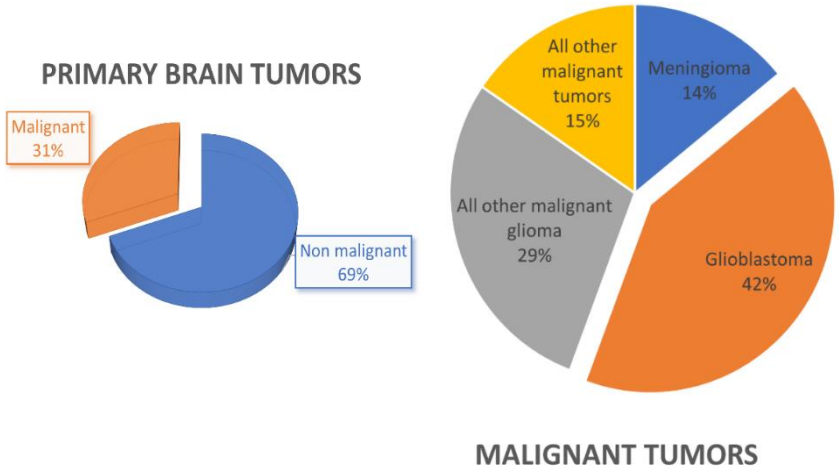

Figure 1: Incidence of primary brain tumor's subtypes illustrated as percentage. Adapted from (Ostrom et al., 2017).

Table 1: Simplified classification of diffuse gliomas according to the WHO 2016 publication

Tumor type and grade		IDH mutant	IDH wildtype	IDH mutant 1p/19q co-deletion	H3K27M mutation	NOS
Grade IV	Glioblastoma	X	X			X
	Diffuse midline glioma				X	
Grade III	Astrocytoma	X	X	X		X
	Oligodendroglioma					X
	Oligoastrocytoma					X
Grade II	Astrocytoma	X	X			X
	Oligodendroglioma			X		X
	Oligoastrocytoma					X

Abbreviations: 1p/19q: chromosome arms 1p and 19q; H3K27M: histone H3 mutation. NOS (not otherwise specified) is a "diagnosis in the current (2016) WHO classification of CNS tumors and denotes a diffuse glioma with astrocytic features and anaplasia, microvascular proliferation and/or necrosis consistent with a WHO grade IV glioblastoma but with inconclusive or unavailable IDH mutation status"

`

1.2 Glioblastoma IDH wildtype

1.2.1 Epidemiology

GBM incidence ranges from 2 to 5 cases per 100,000 people in North America and Europe, accounting for more than 50% of primary malignant CNS tumors cases. The number of new cases of GBM per year is estimated around 250,000 worldwide. GBM, the most common primary CNS malignancy, is characterized by high morbidity and mortality. Since 2020, the cIMPACT-NOW consortium (the consortium to inform molecular and practical approaches to CNS tumor taxonomy) categorizes GBM as grade IV IDH wildtype CNS tumors (Louis et al., 2020).

1.2.2 Clinical presentation and diagnosis of GBM

The clinical presentation of GBM is variable, rapidly progressive, and can present up to a couple of months depending on the size of the tumor and location. The most common clinical presentation is headache that arises from an elevation of the intracranial pressure. Other symptoms such as blurred vision, progressive focal neurological deficits, seizures, and/or cognitive disturbances are frequent (Rajaratnam et al., 2020).

The diagnosis of GBM starts with brain imaging to determine the tumor location, size, and radiological features. The most common and available medical techniques for brain imaging are computed tomography (CT) scan and magnetic resonance imaging (MRI). CT scan is the oldest technique available for brain imaging. It provides an exact location of the tumor and assesses tumor morphology. MRI with and without gadolinium infusion provides a higher quality of imaging than CT scan. It allows an exact location of the tumor, the surrounding structures, and guides surgical planning for biopsy or surgical removal of the tumor (Lundy et al., 2020)

Gadolinium is a contrast agent for MRI imaging that appears as hyper-intense in T1-weighted MRI images. T1-MRI sequence allows visualization of the tumor body, including

`

the necrotic, angiogenic and edema areas. T2-weighted MRI image series are widely used to test the size, shape, and position of cancerous tumors. A T2-weighted MRI image with a fluid-attenuated inversion recovery (FLAIR) sequence visualizes abnormalities such as the edematous areas surrounding the tumor and the presence of invasive tumor cells. Several other possible MRI approaches are validated and offer more detailed images (*e.g.* diffusion-weighted MRI and perfusion-weighted)(Lundy et al., 2020).

Although imaging examinations can guide the diagnosis, only the histo-molecular analysis will determine the final diagnosis of GBM. They will be established from neuropathological and molecular examinations of a tumor sample according to the pathological criteria published by the classification of WHO 2016 combined with cIMPACT-NOW (Louis et al., 2020)

`

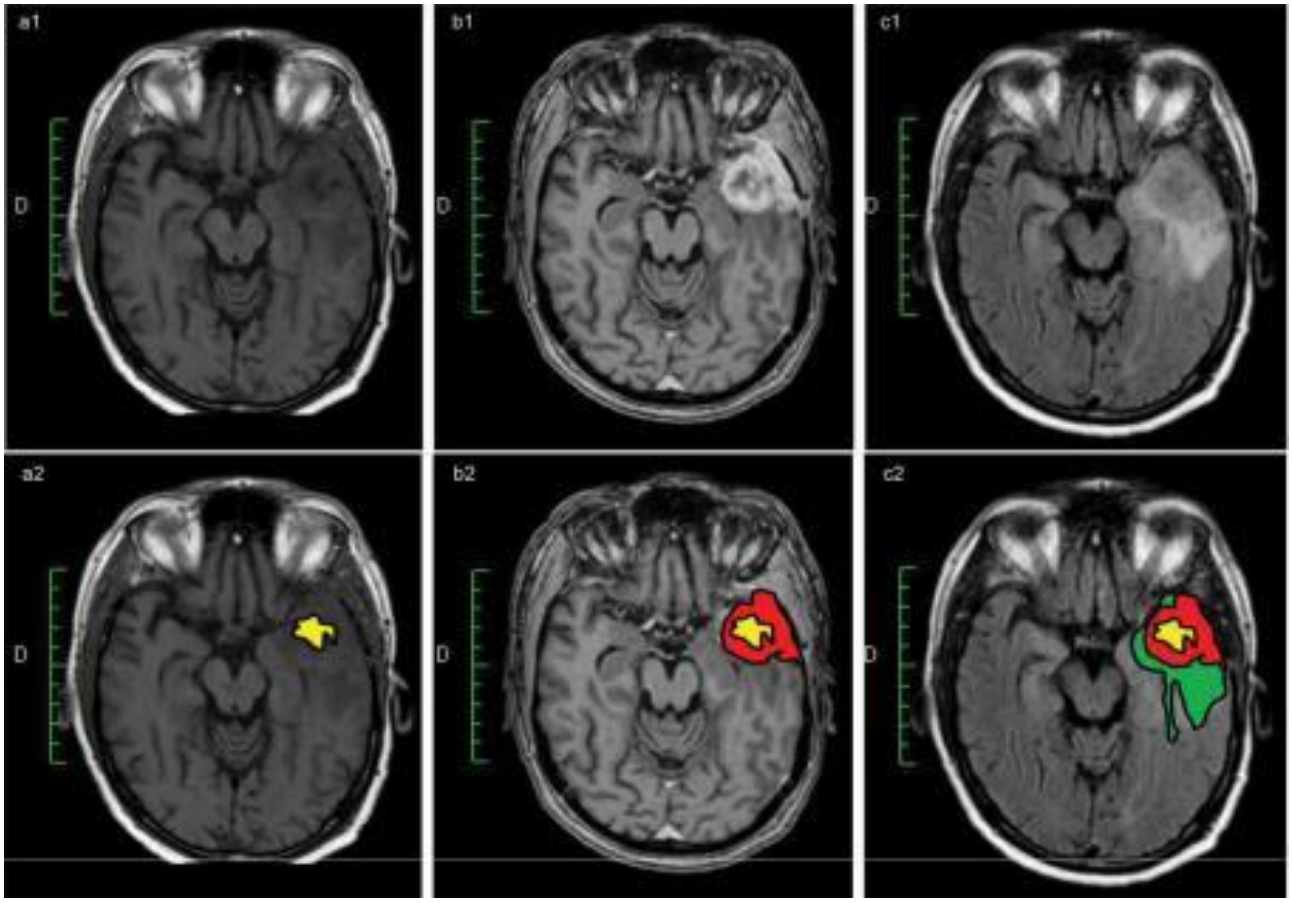

Figure 2: MRI imaging of GBM patient. Panel a1: T1-weighted MRI imaging. Panel a2: the central necrotic area is stained in yellow. Panel b1: T1-weighted MRI imaging with gadolinium contrast enhancement. Panel b2: The contrast uptake zone colored in red corresponds to the proliferative zone of the tumor. Panel c1: FLAIR T2-weighted MRI imaging. Panel c2: The area colored in green corresponds to an area of vasogenic edema in which tumor cells are present (Drean et al., 2016).

`

1.2.3 Standard treatment of GBM

I. In newly diagnosed GBM

The standard first-line treatment for newly diagnosed GBM includes major cancer treatment modalities (Elham et al., 2017). As other solid tumors, a safe maximum surgical resection, radiotherapy, and chemotherapy are usually applied in the treatment of GBM. Irradiation induces both direct and indirect effects on tumor growth. Direct effects of irradiations manifest as DNA damage. DNA damage can appear as cellular replication errors and mutations, leading to an episode of mitotic catastrophe and tumor cell's death. Indirect effect of radiotherapy is linked to the host's antitumor immune responses. Damage-associated molecular patterns from radiated cells alert antigen presenting cells and naïve T-lymphocytes. Furthermore, radiation induces blood brain barrier (BBB) disruption and allows drugs to reach CNS tumors (Sia et al., 2020). Finally, chemotherapy aims to eradicate tumor cells with cytotoxic agents that target crucial stages of the cell cycle.

The standard first-line protocol was developed in 2005 (Stupp et al., 2005) for the treatment of newly diagnosed GBM, and it includes the following specific modalities:

- A maximum safe surgical resection is performed depending on the tumor location and the surrounding functional brain regions. In GBM, a total surgical resection is nearly impossible due to the invasive nature of GBM tumors.
- Radio-chemotherapy is then used to treat marginal cells surrounding the resection area and reach the invasive GBM cells. Fractional x-ray radiation therapy at 2 gray (Gy) daily is applied five days a week for a total of 6 weeks (60 Gy). Radiotherapy is accompanied by concomitant chemotherapeutic alkylating agent, temozolomide (TMZ) at a dose of 75 mg per square meter of body surface area (mg/m^2).

`

- Adjuvant chemotherapy with TMZ is then continued with six cycles at 150-200 mg/m^2 daily for five days per 28-day cycle.

In early 1980, TMZ has been synthesized as a novel derivative of imidazotetrazinones. Mitozolomide, a prodrug with a higher antitumor activity than TMZ, was initially developed but clinical trials reported severe thrombocytopenia as an adverse drug reaction for mitozolomide limiting its usefulness in clinical practice. TMZ, a 3-methyl derivative of mitozolomide, showed a more acceptable toxicity profile with similar antitumor activity. TMZ is an alkylating agent with a small molecular weight (194.15 g/mol) that readily passes the BBB. A high systemic bioavailability of TMZ was reported following an oral administration with about 20-30% drug concentration crossing the BBB to reach GBM cells (Drean et al., 2016). Overall, these therapeutic characters nominated TMZ for further clinical trials until was approved in 2005 (Friedman et al., 2000, Stupp et al., 2005).

Recently, tumor treating fields (TTF) is a new method to eradicate cancer cells by using mild electrical field travelling through the skin and disrupting the ability of cancer cells to replicate. TTF disrupt cell division and induce GBM cell apoptosis and was shown to improve prognosis of newly diagnosed GBM patients in good clinical conditions after the surgical and the radio-chemotherapy concurrent steps (Stupp et al., 2017).

II. At tumor recurrence

The majority of GBM will relapse regardless of the first line treatments used (described above). Surgical intervention can be considered as a second-line treatment plan when possible. In the same line, a limited number of patients are candidates for second irradiation. Few chemotherapies agents can be used in recurrent GBM cases, *i.e.*, Lomustine with or without Bevacizumab (anti-vascular endothelial growth factor A -VEGF-A- therapeutic antibody) (Wick et al., 2017) **(Table 2)**.

`

Table 2: Therapies for recurrent GBM patients

Therapies for recurrent GBM patients	
Carmustine (BCNU) wafers	A biodegradable polymer containing 3.85% carmustine applied in the surgical lesion when patients are candidate for second surgery (Xiao et al., 2020).
Bevacizumab	10 mg/kg once every two weeks (Wick et al., 2017)
BCNU	150-200 mg/m^2 (single dose or divided over two days) over six weeks OR 75-100 mg/m^2/day for two days over six weeks
Lomustine (CCNU)	110 mg/m2 orally every six weeks (Jakobsen et al., 2018)

III. Innovative therapies

TMZ remains today the standard first-line chemotherapeutic agent in GBM treatment(Brat et al., 2020). For over five decades, significant efforts have been put into the development of new anti-cancer therapies for GBM including anti-neoplastic agents (Atiq and Parhar, 2020), molecular targeted drugs (Touat et al., 2017), immunotherapeutic approaches (Weenink et al., 2020), and medical devices (Idbaih et al., 2019). Indeed, multiple of these innovative therapies are currently under investigations in the setting of clinical trials **(Table 3)**.

`

Table 3: Examples of molecular and innovative therapeutic strategies used in clinical trials for GBM treatment are summarized from the clinicaltrial.gov official website (21/03/2021)

Intervention	Experimental	Status	Phase	Clinical trial reference
Molecular targeted therapies	Marizomib (proteasome inhibitor)	Active, not recruiting	III	NCT03345095
	Regorafenib (pan-Tyrosine kinases inhibitor)	Recruiting	II/III	NCT03970447
Passive and active immunotherapy	Autologous dendritic cells vaccination	Recruiting	II	NCT04115761
	Nivolumab (anti-PD-1) and Ipilimumab (anti-CTLA-4)	Active, not recruiting	II	NCT03367715
	EGFRvIII and chimeric antigen receptor T cell	Completed	I/II	NCT01454596
Medical devices	Ultrasound mediated BBB opening (Sonocloud 9) in combination with albumin-bound Paclitaxel	Recruiting	I/II	NCT04528680

Abbreviations: *EGFRvIII:* Epidermal growth factor receptor variant III; PD-1: programmed death-1; CTLA-4; cytotoxic T-lymphocyte-associated antigen-4

`

1.2.4 Prognostic factors in GBM patients

Patients with GBM have a dismal outcome with a median overall survival below 18 months with the current standard of care (Stupp et al., 2005). In the past few years, several clinical and molecular biomarkers have been identified as reliable prognostic factors in GBM, as shown in **(Table 4)**

A standard evaluation of a patient's capacities to perform an ordinary activity is referred to as a Karnofsky Performance Status (KPS) score. The KPS score ranges from 0-100, where 100 is the highest capacity to perform ordinary activities. A KPS score of 70 (*i.e.*, the patient can perform daily life activities at home but is unable to work) or above was associated with a better prognosis in GBM patients. The KPS score is therefore used as a tool to evaluate the eligibility and stratification of GBM patients in clinical trials.

It has been noted that age is also a significant predictor of GBM patient prognosis. Indeed, Li et al. discovered that "≤ 70 years of age" was an independent beneficial factor in GBM patients (Li et al., 2009, Kudulaiti et al., 2021).

Epigenetics can be defined as heritable gene expression changes that are not due to any alteration in the DNA sequence. These are reversible changes that can be induced and reversed through different environmental factors and are implicated in multiple diseases including cancer. The most widely studied epigenetic changes are DNA methylations, histone modification, and chromatin remodeling. Abnormal promoter sequence methylations are common in tumor cells and lead to gene stable transcriptional repression.

The most critical epigenetic change with clinical relevance in GBM affects O6-Methylguanine-DNA Methyltransferase (*MGMT*) expression. This enzyme is involved in DNA repair following the alkylation of guanine bases. In GBM, hypermethylation of the promoter of *MGMT* is frequently observed, leading to inhibition of the enzyme expression,

`

preventing it from fulfilling its role as DNA damage protector. *MGMT* promoter methylation status is widely recognized as a predictive marker of response to alkylating agents such as TMZ and as independent prognostic factor regardless the treatment prescribed **(Figure 3)** (Verhaak et al., 2010). However, this knowledge has led to minimal changes in how GBM patients are treated due to a lack of alternative therapy options and the variability in *MGMT* promoter methylation testing (Malmström et al., 2020).

The identification of a mutation in the gene encoding IDH1 influenced prognosis of GBM patients. IDH1 and IDH2 belong to the IDH enzyme family located in the cytoplasm (IDH1) and mitochondria (IDH2). Both enzymes are involved in a certain number of cellular processes, including oxidative phosphorylation, glutamine metabolism, lipogenesis, and the redox status regulations. IDH2 mutations are rarely reported in GBM. The aberrant function of mutated IDH1 is the conversion of alpha-ketoglutarate to the novel oncometabolite 2-hydroxyglutarate which leads to genome-wide epigenetic changes in human gliomas. Tumors with mutated *IDH1* and corresponding epigenetic changes demonstrated better prognosis than gliomas with wild-type *IDH1* (Li et al., 2021b).

Overall, these observations highlight the importance of *IDH1* mutations in the diagnosis, prognosis, and GBM treatment and have led to their inclusion in the latest WHO classification. Indeed, the WHO classification that previously relied on histopathological criteria to classify brain tumors was revised in 2016 to include vital molecular biomarkers such as *IDH* status. Efforts to further stratify *IDH*-wildtype tumors are continuously evolving (Louis et al., 2016). The cIMPACT-NOW consortium objectives is identifying new clinically relevant biomarkers to be incorporated to the upcoming WHO classification of primary CNS tumors (Louis et al., 2020).

`

Table 4: Prognostic factors in GBM patients

Marker	Outcome
The extent of surgical resection	Compared with sub-total resection, gross total resection (substantially) improves OS and PFS (Smrdel et al., 2018)
Age	Prognosis in patients younger than 70 years of age is relatively favourable, with a significant portion of these patients living for more than two years.
KPS	A KPS > 70 is a marker for a better prognosis (Lamborn et al., 2004)
***MGMT* promoter status**	Better OS and PFS in GBM treated with radio- and chemotherapy when *MGMT* promoter is methylated (Li et al., 2021b)

Abbreviations: PFS: progression free survival; OS: overall survival

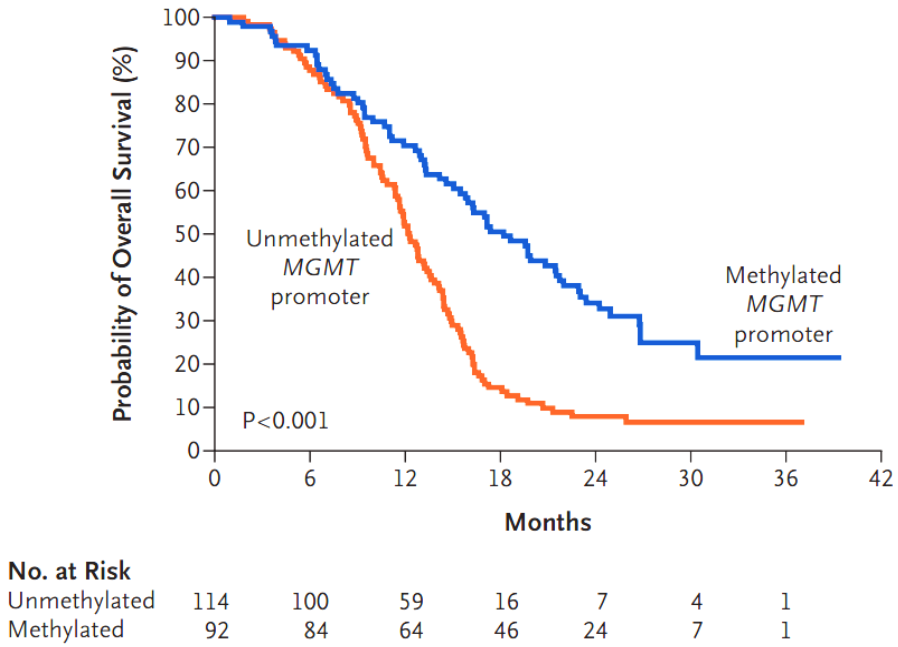

Figure 3: *MGMT* promoter methylation as a prognostic factor in GBM (Hegi et al., 2005).

`

2. GBM cell biology and their microenvironment

2.1 GBM cells and heterogeneity

2.1.1 Tumor cells origin, and intratumor cell heterogeneity

Virchow made the first description of intratumoral heterogeneity at the beginning of the 19th century (Balkwill and Mantovani, 2001). Since then, technological advances have brought to light different cell populations with distinct molecular alterations within the same tumor bulk. The acquisition and accumulation of oncogenic molecular alterations in a normal cell will result in obtaining neoplastic characters. Three main models have been proposed to explain intratumoral heterogeneity:

- The clonal evolution model that was described by Nowell (1976). He proposed that all tumor cells have originated from a single cell, and the acquisition of genetic and epigenetic alterations within a cell is responsible for the tumor progression. This model ignores the relevance of non-genetic variability and the potential functional interactions between the tumor cells and the tumor microenvironment (TME) (Nowell, 1976).
- Cancer stem cell (CSC) or GBM stem cell (GSC) model suggests a hierarchical organization whereby tumor growth is dependent on CSCs that are self-renewable and able to give differentiated tumor cells progenies. In GBM, cell identity responsible for carcinogenesis is not fully understood; however, accumulating evidence suggests that the origin could be an astrocyte, a glial progenitor, or a neural stem cell. Indeed, it was initially thought that GBM originates from astrocytes which differentiate into an immature progenitor state (Nair et al., 2017) however, there is controversy over this hypothesis. Recent studies suggest that transformed neural stem cells (NSC) into GSC is the origin of gliomagenesis. Since the 2000s, several teams have succeeded in isolating and cultivating GSC from cortical glial tumors, medulloblastoma and GBM.

`

This work made it possible to demonstrate the tumorigenic ability of GSC and to identify discriminating NSC-associated surface markers (e.g., CD133, A2B5, CD15, and CD44) or intracellular proteins (e.g., nestin and other the transcription factors SOX2, OLIG2, BMI1, and ASCL1) (Lathia et al., 2015).

- The third so-called "Big bang" model was proposed by Sottoriva et al. (2015). This model suggests a hierarchical organization with the existence of different clonal subpopulations. In addition to the common mutations inherited from the original transformed/neoplastic cell, these clones are said to have shared and/or unique molecular alterations. These would appear silently and permissively during replications, accumulate, and be expressed at a given time, which varies according to the clones. This model justifies several molecular subgroups, defined by Verhaak classification **(Table 5)** co-existing within the same tumor. Furthermore, it explains the variations in response to treatments observed within the same GBM due to heterogeneous subpopulation of clones with different genetic alterations and capacity to resist treatments (Sun et al., 2018).

`

Table 5: Molecular characteristics of identified subtypes (Verhaak et al., 2010)

Subtype	Molecular characteristics
Proneural	• Focal amplification, mutation, and high expression of *PDGFRA* • Mutations in *IDH* • *TP53* mutation or Loss of heterozygosity • Amplification of *EGFR* and deletion of *PTEN* less likely
Neural	• Expression of neuron markers, *e.g.*, *NEFL, GABRA1, SYT1, SLC12A5*
Classical	• Strong chromosome 7 (*EGFR)* amplification • *EGFRvIII* often present • Focal 9p21.3 deletion *(CDKN2A)*
Mesenchymal	• Focal homozygous deletion of 17q11.2 • Strong expression of genes from the NF-kB pathway (*e.g., TRADD, RELB, TNFRSF1A)* • Expression of mesenchymal markers *(MET)* • Expression of astrocytic markers *(CD44, MERTK)*

Abbreviations: PDGFRA: platelet-derived growth factor receptor A; EGFR: epidermal growth factor receptor; PTEN: phosphatase and tensin homolog; NEFL: neurofilament Light; GABRA1: gamma-aminobutyric acid receptor subunit alpha-1; SYT1: synaptotagmin-1; SLC12A5: solute carrier family 12 member 5; CDKN2A: cyclin dependent kinase inhibitor 2A); 17q11.2: chromosome 17q11.2 deletion; NF-kB; TRAAD: tumor necrosis factor receptor type 1-associated death domain protein; RELB: RELB proto-oncogene, NF-KB subunit; TNFRSF1A: tumor necrosis factor receptor 1 superfamily Member 1A; MET: proto-oncogene, receptor tyrosine kinase.

`

2.1.2 Four signaling pathways are disrupted in GBM

Genetic alterations in GBM such as amplification, deletion, and/or mutation modulate the oncogenic pathways. Accumulation of such genetic alterations activates oncogenesis. The most extensively studied signaling pathways alterations in GBM are summarized in **(Figure 4).**

The Receptor Tyrosine Kinase (RTKs) are high affinity cell surface receptors for large number of hormones, growth factors and cytokines. RTK pathways is altered in 88% of GBMs, resulting in decreased apoptosis, and promoting invasion and proliferation of GBM cells. Mutations in RTKs activate a series of signaling pathways and cascades modulate gene and protein expression. In GBM, RTKs show molecular abnormalities, such as gene amplification in a wide spectrum of RTKs, such as *EGFR* (60%- 70%), *PDGFRA* (12%-15%), and *MET* (5%). Furthermore, EGFRvIII variant is reported in 20% of GBM and is expressed heterogeneously across GBM cells part of EGFRvIII-positive tumors suggesting that its crucial contribution to gliomagenesis. It is possible that RTKs contribute to lead mitogenic cellular signaling pathways in GBM (Crespo et al., 2015).

TP53 is a major protein involved in tumorigenesis. TP53 signaling is affected in 87% of cases and mainly leads to defects in processes controlling apoptosis, senescence, or cell cycle progression. In healthy cells, its activation will lead to senescence or apoptosis induction. *TP53* loss of function (*i.e.*, mutation or deletion) is reported in 35% of GBM cases. Amplification of *MDM2* and *MDM4*, TP53 inhibitor proteins, are reported in 14% and 7% of GBMs, respectively (Pedrote et al., 2020).

The tumor suppressor retinoblastoma (pRB) signaling pathway is altered in 77% of GBMs. Loss of pRB expression is detected in 11% of GBM cases. In the G1 phase of the cell cycle, cyclin D/CDK4-dependent phosphorylation releases pRB, allowing cell cycle progression. In GBM, *CDKN2A* and *CDKN2B* are inactivated in 46.4 % cases, and *CDK4* and

`

CDK6 amplification have also been found in 13.4% of GBM showing that CDK4 and CDK6 contribute to GBM development (Cao et al., 2020).

Mutations in the *TERT* gene promoter are reported in 80% of GBMs, allowing activation of telomerase expression. The process of extending telomeres participates in immortalization of tumor cells. These mutations are mutually exclusive with mutations in the Alpha thalassemia/mental retardation syndrome X-linked chromatin remodeler (ATRX) *ATRX* gene. Alternative lengthening of telomeres (ALT) phenotype is positively correlated with IDH1 mutant protein, ATRX protein loss, strong TP53 expression and absence of *EGFR* amplification.

`

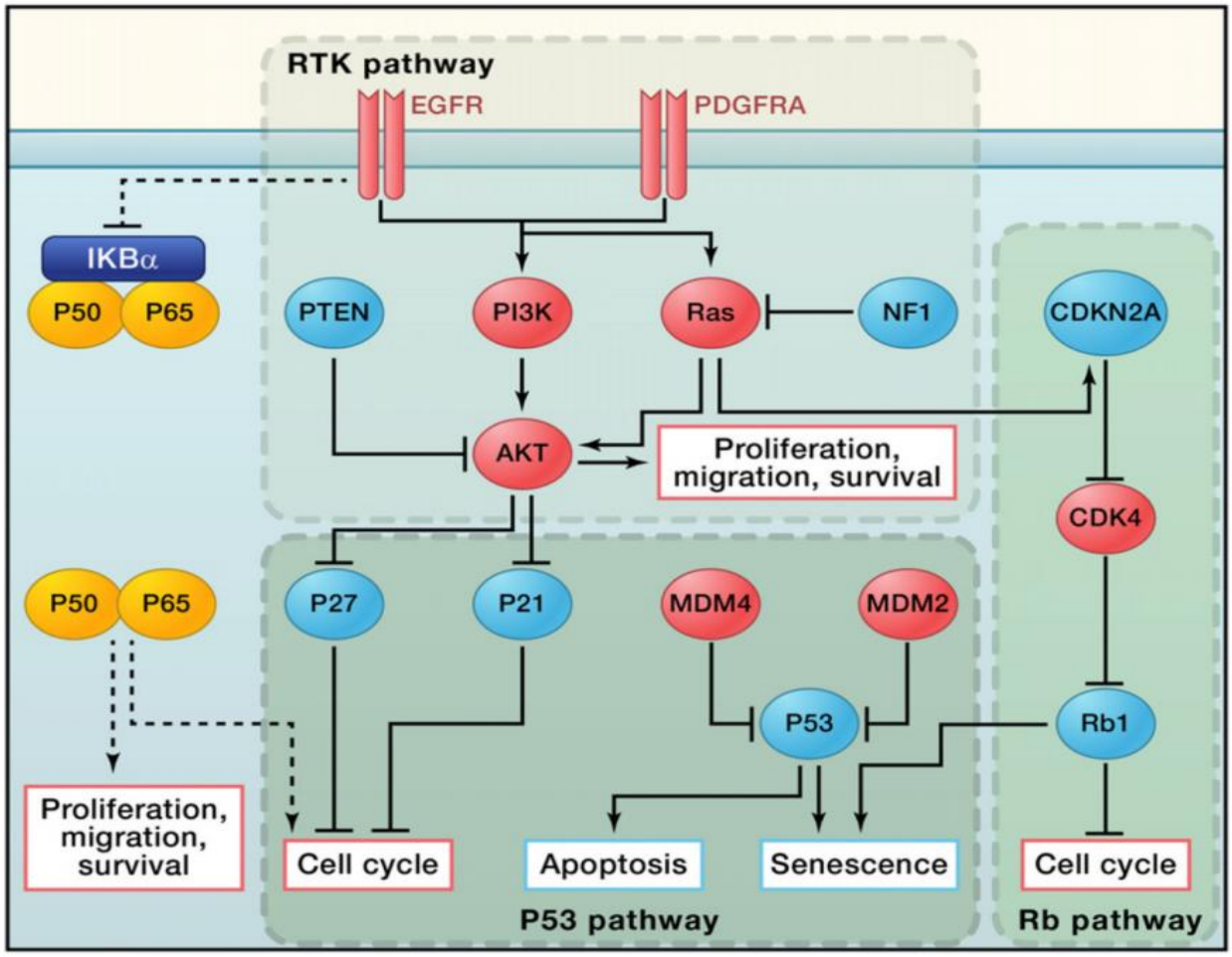

Figure 4: Main signaling pathways disrupted in GBM. RTK, TP53 and RB pathways and their implications on apoptosis, senescence, and cell cycle progression. In addition, *TERT* promoter mutations, not shown in this figure, are found in ~80% of GBM (Chen et al., 2012).

`

2.2 Tumor cell microenvironment

2.2.1 Niches and stem cells of GBM

GBM stem cells (GSC) are grouped together in specialized niches that provide signals that are essential for maintaining their phenotype and tumorigenic capacities. The discovery of these niches has made the study of GSCs more complex, both on their role within the tumor and on their regulation. Three niches have been described in GBM: (i) the perivascular niche, (ii) the hypoxic niche, and (iii) the invasive niche.

I. The perivascular niche

The perivascular niche is multi-cellular structure composed of neoplastic and non-neoplastic cells. The neoplastic cells are here tumor cells with varying degree of differentiation state, including GSC. One the other hand, the non-neoplastic cells include endothelial cells, pericytes, macrophages, neutrophils, myeloid-derived suppressor cells, reactive astrocytes, and infiltrating neural progenitor cells. Pericytes interact with tumor cells to promote their growth and to contribute to the blood tumor barrier (BTB), which has been described as leaky compared to the normal BBB. In contrast to normal brain micro-vessels, both astrocytes and pericytes coverage is incomplete in GBM vessels (Hambardzumyan and Bergers, 2015).

II. The hypoxic niche

In GBM, oxygen deprivation seems to be an essential regulator of GSC survival and the maintenance of their stemness. Therefore, hypoxic niches contribute to tumor progression via the stabilization of the factor hypoxia-inducible factor-1 alpha (HIF-1α), which allows the expression of angiogenesis, invasion, and survival promoting genes. These niches are located near necrotic areas, where oxygenation is sufficient to allow cell survival. The onset of hypoxia is highly dependent on the altered state of the

`

microvasculature, suggesting a relationship between the perivascular niches and the hypoxic niches. Instead of slowing down tumor development, impaired oxygen delivery act as a strong growth activator. Over the last years, accumulating evidence has pointed to hypoxia as a critical regulator of tumor cell survival, stemness, and immune surveillance in these niches.

III. The invasive niche

The invasive properties are thought to promote tumor cell aggressiveness; invading glioma cells make surgical resection incomplete and are partially responsible for tumor recurrence (Hambardzumyan and Bergers, 2015)

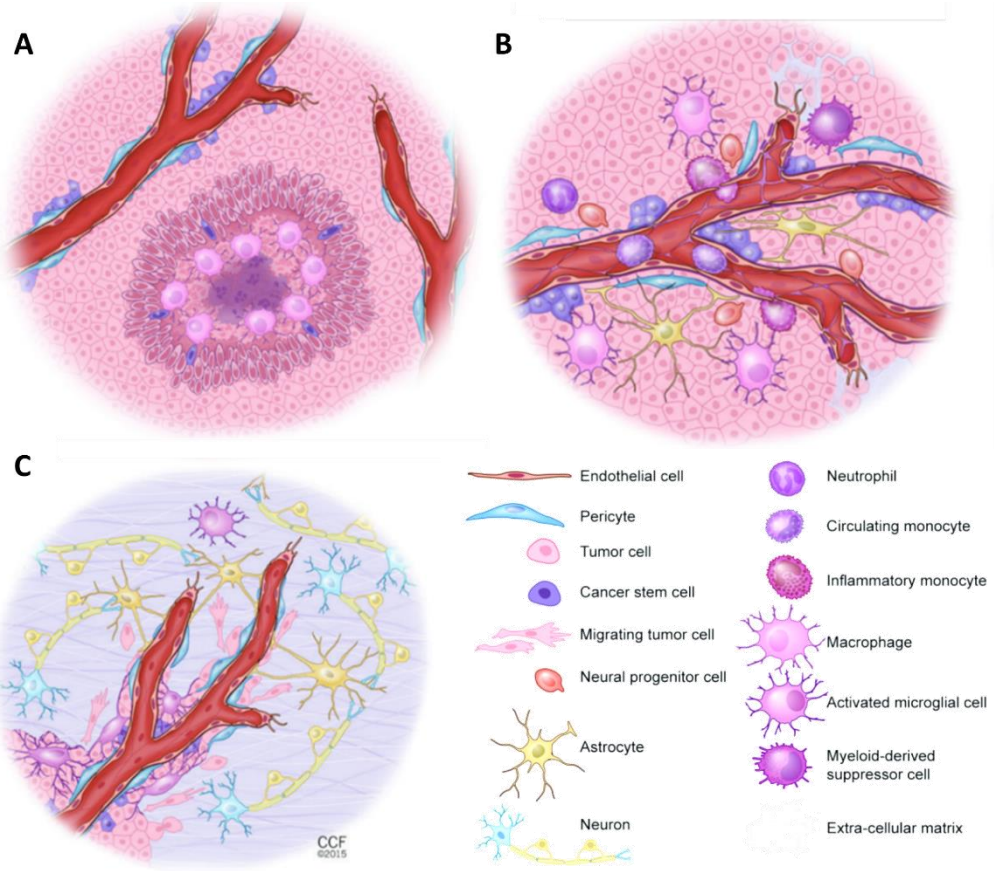

Figure 5: Niches in GBM. Panel A: Perivascular niche. Panel B: Hypoxic niche. Panel C: Invasive niche (Hambardzumyan and Bergers, 2015, Broekman et al., 2018).

`

2.2.2 Cellular components of TME

The CNS has long been considered an "immuno-privileged" organ due to the presence of the BBB limiting the exchanges between the brain and the blood vessels. Leukocytes are the main cellular contributor in protection against tumors and infections. Prior to their release to the blood stream, they are developed in hematopoietic organs such as the bone marrow or/and thymus. Leukocytes migrate to the specific infected tissues following an activation process. However, due to the BBB, their passage to the CNS is limited through few passage ways: (i) through the choroid plexus, (ii) across superficial leptomeningeal vessels into the subarachnoid space and (iii) through the perivascular space into the brain parenchyma (Ratnam et al., 2019). The passage of leukocytes to the brain parenchyma is partially restricted by the BBB. Indeed, endothelial cell (ECs) within the BBB and their tight junctions prevent the passage of cells to the brain. Furthermore, pericytes around the vascular structures of the parenchyma maintain and support the integrity of the BBB. In physiological conditions, leukocytes are not detected in the brain parenchyma. However, under pathological conditions i.e., GBM, the integrity of the BBB is compromised allowing lymphocytes to reach the GBM TME (Weenink et al., 2020)

Accumulating evidence have suggested that tumor development is not only due to the accumulation of intrinsic abnormalities but also to extrinsic signals from the TME. Indeed, the TME, which is defined as a cellular (*i.e.* blood vessels, immune cells and fibroblasts), molecular (*i.e.* intercellular signaling molecules, extracellular matrix –ECM-), and dynamic network surrounding tumor cells, plays a significant role in tumor biology (Broekman et al., 2018). The tumor and the TME are linked in a highly interactive manner **(Figure 6).** They influence each other through extracellular signals (Huang et al., 2020).

`

I. Microglia and macrophages

Microglia, the brain-specific immune cells, ensure immunosurveillance of the brain parenchyma. Since the discovery of a cerebral lymphatic system (De Leo et al., 2020) and leukocyte extravasation to the GBM TME, microglia gained interest as an immune cellular component in the brain. Macrophages are the most abundant immune cells found amongst circulating leukocytes. Microglia corresponds to the resident macrophages in the CNS, while circulating macrophages originate from monocytes recruited from the blood.

Immunosuppression within GBM is characterized by enhancement of immune-suppressive cytokines and inhibition of T-lymphocytes proliferation. The presence of several immune-suppressive cytokines characterizes the GBM TME (*e.g.*, Interleukins -IL-, IL-6 and IL-10, prostaglandin E2, IL-1, and transforming growth factor-beta -TGF-β). Each mediator affects the GBM immune TME in a specific matter. For example, TGF-β blocks the activation of T-lymphocytes, inhibits IL-2 production, and decreases NK-T lymphocytes activity. IL-2, a known immunosuppressive cytokine, is secreted mainly by macrophages and GBM cells within the TME. IL-2 enhances GBM cell growth and inhibits interferon-gamma (IFNγ) and tumor necrosis factor-alpha (TNF-α). It is also associated with a downregulation of major histocompatibility complex (MHC) class II and enhancement of CD80/CD86 expression on the surface of infiltrating T-lymphocytes as well as on GBM cells (Scheffel et al., 2020).

`

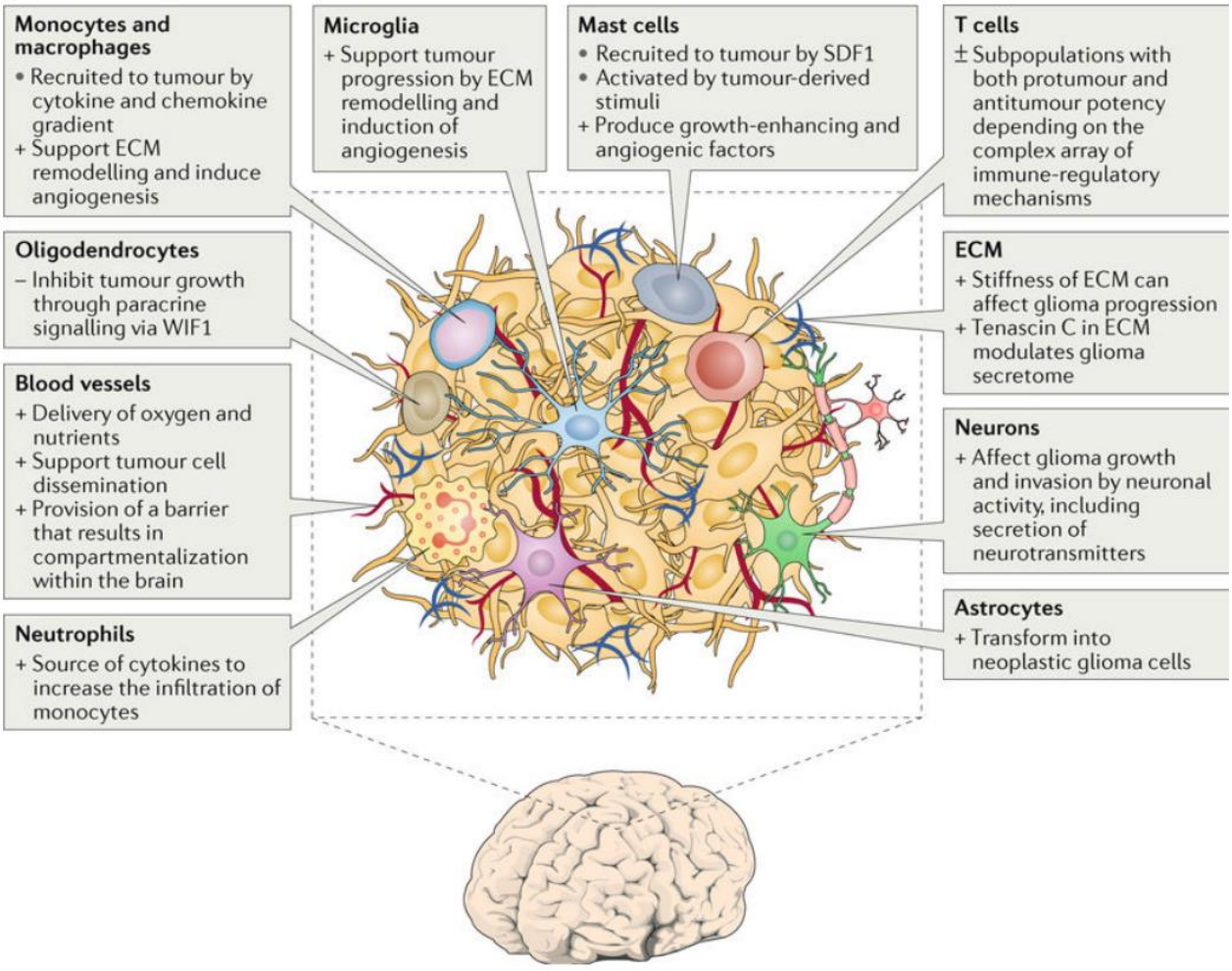

Figure 6: GBM microenvironment components. TME is defined as a cellular (blood vessels, immune cells, fibroblasts) and molecular (intercellular signalling molecules, extracellular matrix), and mechanical network surrounding tumor cells (Broekman et al., 2018).

`

II. Antigen presentation and tumor-associated macrophages (TAM)

Antigens released from tumor cells are processed by antigen presenting cells (APC) on MHC class I and presented to cytotoxic T-lymphocytes. Microglia cells have been identified with the ability to present antigens to T-lymphocytes within the CNS. However, the downregulation of APCs within the TME decreases microglia's ability to exert this role. In GBM, macrophages derived from monocyte precursors polarize into two distinct categories within the GBM TME. Exposure to INF-γ polarizes monocytes to M1 macrophages. The role of M1 macrophages are pro-inflammatory cytokines and chemokines secretion. Therefore, participate in the positive immune response and function as an immune monitor. On the other hand, M2 macrophages are involved in the anti-inflammatory cytokine's secretion therefore, reducing inflammation and contributing to immunosuppressive function and tumor growth (Grégoire et al., 2020).

M2 macrophages polarize through exposure to IL-4. TAMs are known to be capable of cross-presenting tumor antigens to T-lymphocytes and priming anti-tumor immune response (anti-inflammatory response). There is no definite answer about the importance of TAM in GBM antigen presentation. However, the presence of TAM is linked to GBM progression. Indeed, results from published articles reported that modulation of macrophage polarization has a regulatory effect on the GBM TME (Saha et al., 2017). The inhibitory effect of GBM TME rises from a regulatory link between M2 macrophages and tumor cells. Several factors such as colony-stimulating factor 1, TGF-β1, macrophages inhibitory cytokines-1, and IL-10 can polarize TAMs to M2 phenotype and inhibiting their phagocytic capacity (Grégoire et al., 2020).

`

III. Regulatory T-lymphocytes

Regulatory T-lymphocytes (Tregs) are considered a small population of $CD4^+$ T-lymphocytes expressing FoxP3 transcription factor. Tregs are a subpopulation of circulating lymphocytes with immune suppressive effects. Tregs also express CD25 and CTLA-4, and their role in GBM is still under investigation. Studies have shown that glioma associated Tregs are most likely originating from the thymus. They migrate within the GBM bulk *via* chemotactic attraction from the TME (González-Tablas Pimenta et al., 2021)

2.2.3 Glioma-associated neovascularization

Tumor vessels are structurally and functionally abnormal. The tumor vascularization is highly disorganized and shows several anomalies which are responsible for functional defects. These structural abnormalities include endothelial cell hyperplasia, a decrease in the number of pericytes in contact with endothelial cells, and tortuous vessel organization (Li et al., 2021a), all factors leading to increased vascular permeability. Glioma-associated neovascularization (GAN) is a complex and regulated process and is highly dependent on the balance between five separate pathways: (i) vascular co-option and (ii) angiogenesis, followed by (iii) vasculogenesis and (iv) vascular mimicry and finally (v) GBM-endothelial cell trans-differentiation.

Vascular co-option was reported for the first time in 1999 and was described as the first process involved in the organization of tumor cells around normal tissue vasculature. Holash et al. (1999) was the first person to report vascular co-option in a rat model of glioma. Early tumors were well vascularized, and it took at least four weeks for an angiogenic response to be observed at the tumor's edge. Winkler et al. (2009) discussed the invasive potential of glioma cells after being in close contact with the surrounding micro-vessels. Vascularization occurred via vascular co-option **(Figure 7-A)** but not angiogenesis. (Hardee and Zagzag, 2012).

`

Angiogenesis, a step following the vascular co-option, is known as new vessels developing from pre-existing micro-vessels. Angiogenesis processes were described in 1976 when Brem (1976) observed a high neovascularization process in GBM animal models. Hypoxic glioma cells around necrosis release proangiogenic factors, and other hypoxia independent mechanisms shift the angiogenic balance toward proangiogenic phenotype **(Figure 7-B).** GBM angiogenic phase is characterized by the formation of an irregular vascular network, with dilated and distorted arteries, abnormal branching, and shunts, contributing to abnormal perfusion. GBMs have immature vasculature with excessive leakage. GAN is driven by many key pathways identified (*e.g.*, erythropoietin and their receptor, macrophages migration inhibitory factor, basic fibroblast growth factor, and placental growth factor) (Xue et al., 2017)

Vasculogenesis has been identified to include mobilization, differentiation, and recruitment of marrow-derived cells known as endothelial progenitor cells **(Figure 7-C)**. Similarly, to the angiogenic process, vasculogenesis is induced by both hypoxia-dependent and independent mechanisms. The most well-known factors are the SDF-1 and CXCR4 pathways (Sun et al., 2019)

Vascular mimicry characterizes tumor cells that organize themselves with ECM to mimic the structure of a vessel (**Figure 7-D)**. Thus, the cells forming these structures do not express endothelial cell markers (CD31, CD34) but may show gene alterations specific to GBM cells *e.g.*, *EGFR* amplification. This vascular mimicry appears to be connected to functional blood vessels and, although permeable, would increase nutrient delivery to the tumor. However, it is accepted that the neovessels formed exhibit altered structures and functionalities.

The final step takes place as tumor cells align themselves to form ECs lining the vascular channels. The endothelial transformation happens at both the functional and the

`

molecular level, and is characterized by typical endothelial-specific biomarkers **(Figure 7-E)** (Hardee and Zagzag, 2012).

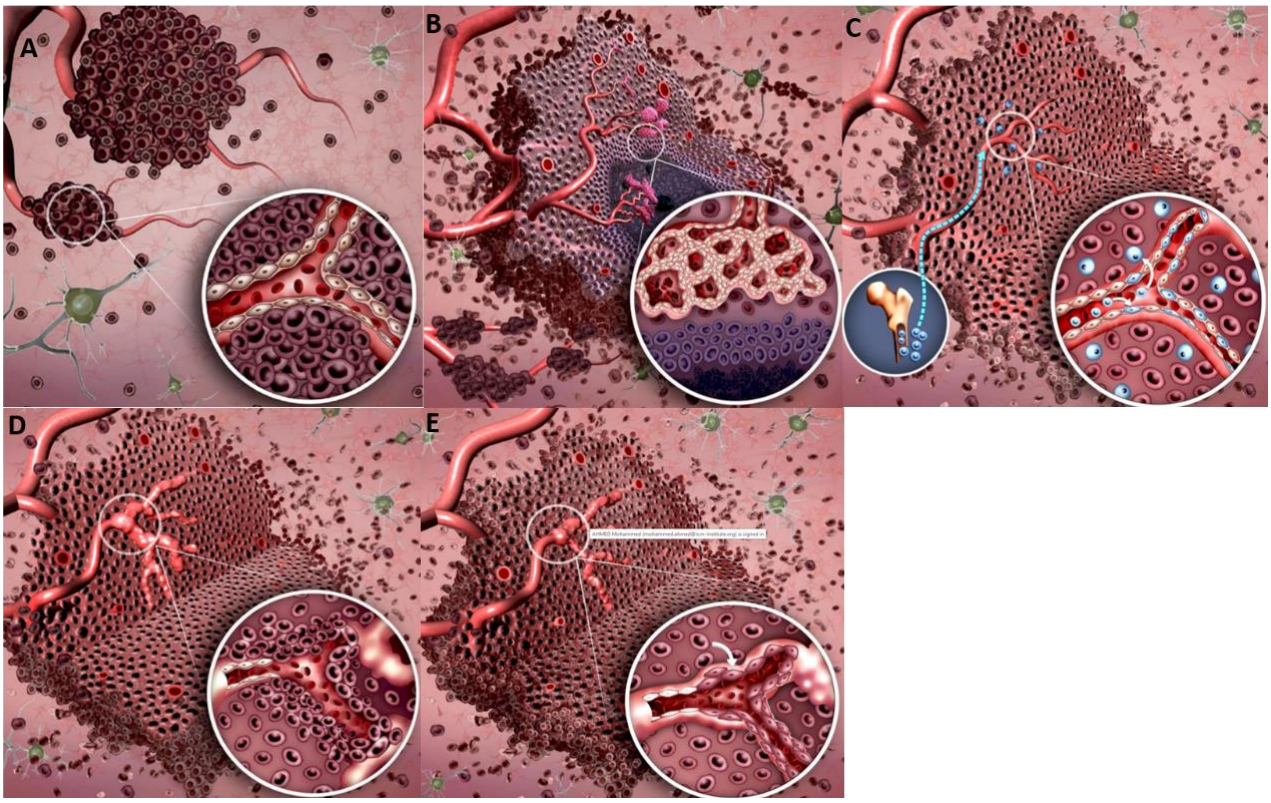

Figure 7: Several steps of glioma associated neovascularization: The first step starts with vascular co-option (A) followed by angiogenesis (B), vasculogenesis (C), vascular mimicry (D), and GBM-endothelial cell trans differentiation (E). Adapted from (Hardee and Zagzag, 2012).

`

2.2.4 The blood-brain barrier

The essential and complex organ which is the human brain is separated from the blood by the BBB. The BBB is a specificity of the CNS blood vessels. The BBB isolates the brain from the blood for protection purposes (Kadry et al., 2020). Indeed, it prevents potentially toxic molecules circulating in the bloodstream to access brain cells, while ensuring the supply of nutrients to maintain homeostasis (Al Rihani et al., 2021). Highly specialized brain capillary ECs form an important part of the BBB. In addition to ECs, various cells described in **(Figure 8)** contribute to the biophysical structure of BBB.

To date, five mechanisms are known to regulate the exchanges of molecules from blood to brain and *vice versa* and described in detail in (Role of Multi-Drug Resistance in Glioblastoma Chemoresistance: Focus on ABC Transporters)

BTB is referred to as a biological and physiological altered version of the BBB that with increased permeability to chemotherapies and/or other molecules. The structural changes in the GBM TME are responsible for the irregular, disorganized, large, and leaky micro-vessels that constitute the BTB. Despite the altered barrier functions of BTB within the tumor body, it is not completely open. Therefore, the penetration of chemotherapy is increased, but not to a level that is detected in non-cerebral tissues in a total absence of BBB. Furthermore, tumor cells present outside the zone of altered BTB *i.e.*, in the surrounding brain tissue, are protected as described previously in **(Figure 2)**

`

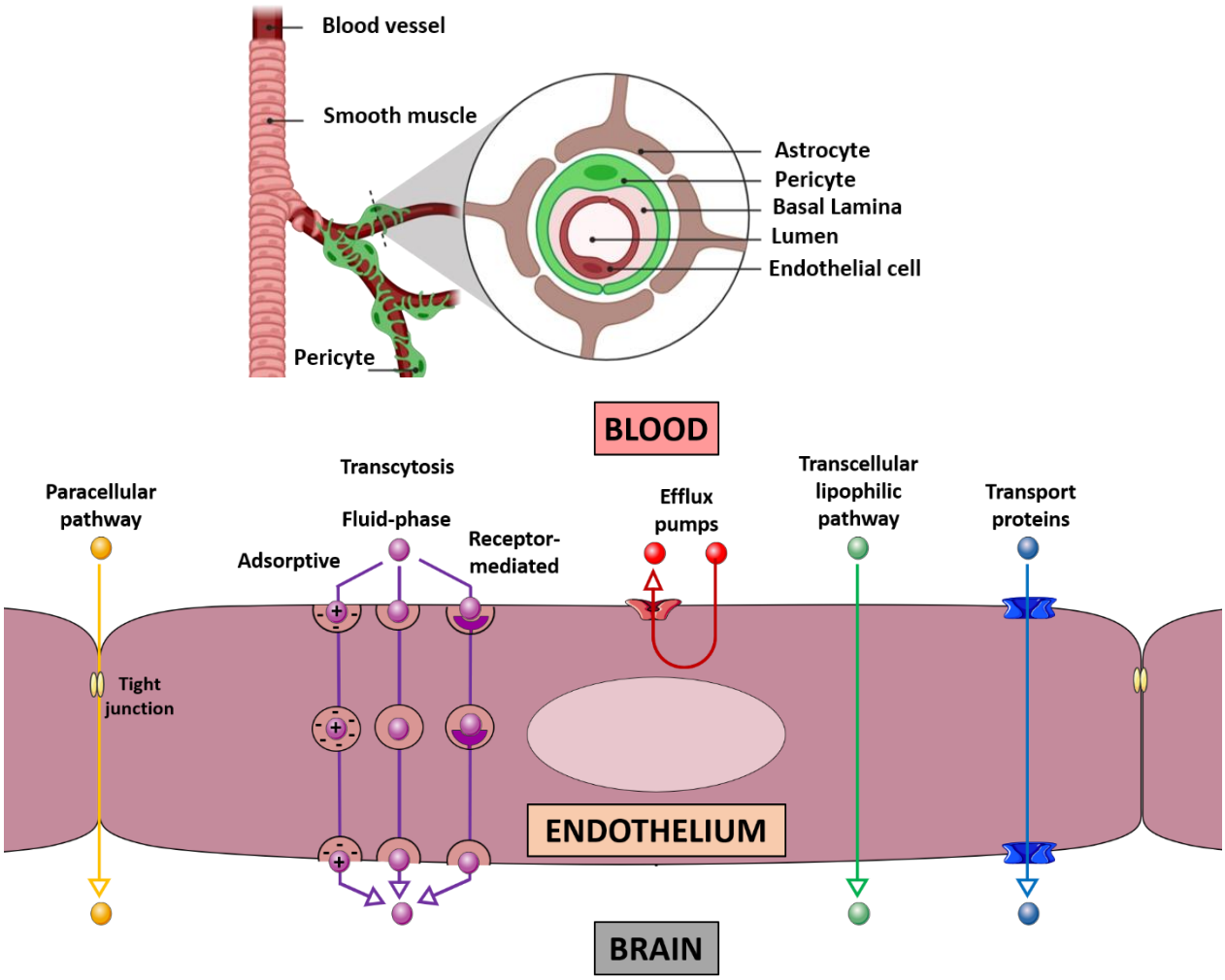

Figure 8: BBB is formed of different types of cells tightly knit together. Highly specialized ECs surround blood vessels and form part of the BBB. In addition to brain ECs, various cells contribute to the structure of BBB. Pericytes (represented in green) are attached to endothelium cells via gap junctions whilst astrocytes end feet (represented in purple) surround ECs of the BBB, providing structural and functional support to these cells. Adapted from (Drean et al., 2016).

`

Several factors influence the ability of a chemotherapeutic agents to cross the BBB. The physicochemical properties of the chemical agents highly influence the ability of compounds to cross the BBB. The main physicochemical properties are (i) size, (ii) liposolubility, (iii) electrical charge, (iv) interactions with plasma proteins, and (v) interactions with ABC efflux pumps. Based on these properties, compounds can be predicted to cross the BBB. *In silico* models have been developed to allow a prediction of the compounds that cross the BBB. However, none of these models allows accurate and consistent data with the *in vivo* models.

One of the well-accepted models to predict compounds' abilities to cross the BBB has been developed by analyzing 2500 compounds and called the rule of 5 (RO5). The RO5 states that compounds with molecular weight (MW) >500 Daltons, Log P >5, >10 hydrogen bond acceptors, five hydrogen bond donors, and compounds that are substrates for efflux pumps are predicted to have poor absorption and can hardly cross the BBB (Drean et al., 2016). A more recent tool was developed to evaluate the potential of molecules to cross the BBB with more precision than the RO5. The CNS Multiparameter Optimization Desirability (CNS-MPO) tool depends on six fundamental physicochemical properties: (i) lipophilicity, (ii) calculated distribution coefficient at pH 7.4, (iii) MW, (iv) topological polar surface area, (v) number of hydrogen-bond donors, and (vi) most basic center (Wager et al., 2016).

`

3. Therapeutic strategies to modulate the tumor microenvironment

3.1 Modulation of the immune system

3.1.1 History and concept of immune system's modulation

The relationship between immune functions and cancer cells was reported for the first time by Rudolf Virchow 150 years ago. He observed the presence of leukocytes within tumor tissue. Therefore, he suggested that the leukocyte infiltrate reflected that cancer's origin lies in chronic inflammation (Balkwill and Mantovani, 2001). William Coley hypothesized the concept that our immune system can effectively recognize and eliminate cancer cells. He injected living or inactivated bacteria in the intra-tumor regions. The idea of Coley's toxins generated several discussions between researchers and scientists. His hypothesis that activated phagocytes would kill both living bacteria and adjunctive tumor cells was accepted at that time, following evidence that injection of bacteria in the intratumor region led to cancer shrinkage. Although the concept showed an innovative idea regarding cancer treatment, the responses were heterogeneous, and the success rate was not promising (Carlson et al., 2020). Cancer is characterized by alterations in molecular pathways and cellular processes. These alterations result in diverse neoantigens presented by MHC class I on tumor cells' surface. These complexes can be recognized by $CD8^+$ T-lymphocytes in cancer patients.

Although cancer progression involves a variety of methods to overcome the host's immunity, immunotherapy can restore and even improve the patient's immune system. Many immunotherapeutic approaches have already shown efficacy in patients, while other new therapeutic approaches remain under development. Immune checkpoint blocking antibodies (ICBs) are currently under clinical investigation(Persico et al., 2021). To date, 1st of April 2021, 4 042 clinical trials of immunotherapy in all types of cancer are listed on ClinicalTrials.gov.

`

One of the most attractive immunotherapy features is its ability to target cancer cells and thus spare healthy tissue. This characteristic differentiates immunotherapy from other "traditional" therapies such as radiation therapy and chemotherapy. The efficacy of immunotherapy was first demonstrated in the treatment of melanoma and renal cell carcinoma with high doses of IL-2 and is now spreading to other haematological and solid cancers (Ventola, 2017).

3.1.2 Antitumor immune response

Our knowledge of fundamental cellular and molecular mechanisms of the immune system's innate and adaptive components has evolved. Cells from the innate system have receptors that can detect foreign microorganisms and dying cells. Macrophages and neutrophils provide early defense against microorganisms, while dendritic cells (DC) provide a linkage to the immune system's adaptive components. Immunological reactions against a growing tumor require an integrated response between the innate and adaptive immune responses. Based on our current knowledge of immune responses, several distinct steps must be completed, endogenously or therapeutically, to produce an effective antitumor response **(Figure 9)**. Oncogenesis processes in tumor cells generate neoantigens that start the initial step in antitumor immune response when DCs detect such neoantigens. Additionally, pro-inflammatory molecules, together with chemokines released by the tumor cells themselves, will recruit innate immune cells to this local source of "danger" (Pio et al., 2019). Initiation of the antitumor response occurs when innate immunity cells are alerted to the presence of a growing tumor. The following two steps occur when the captured antigens on MHC class I and MHC class II molecules are presented to T-lymphocytes by DCs, triggering the activation and the priming of effector T-lymphocytes against tumor-specific antigens. At this stage, the immune response is initiated, with the ratio of T effector lymphocytes to T-regulatory lymphocytes presenting a critical determinant in this response.

`

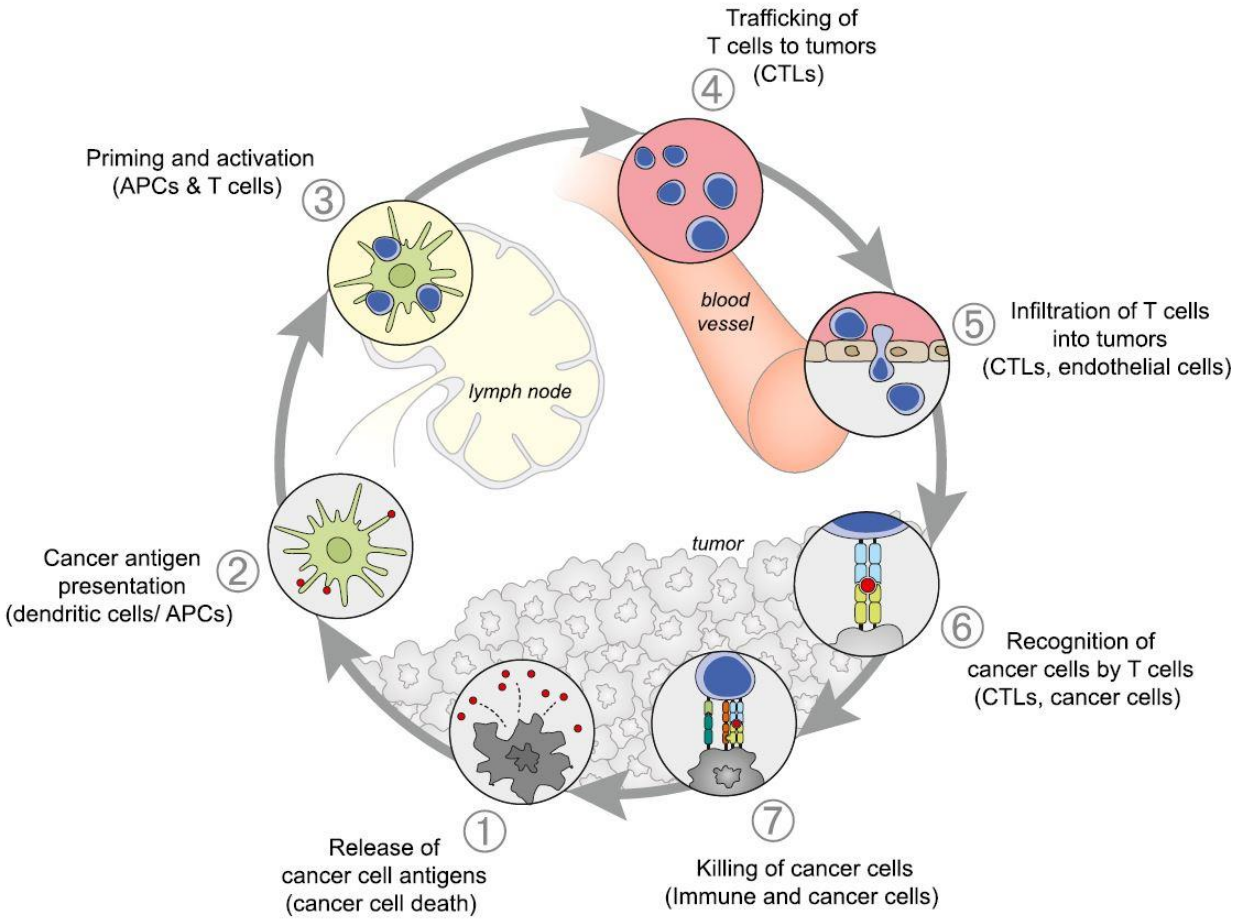

Figure 9: Anticancer immunity can be described as a cycle leading to an accumulation of immune-stimulating factors that enhance T-lymphocytes response (Chen and Mellman, 2013).

3.1.3 Tumor escape mechanisms

The term "cancer immunosurveillance" was discredited in 2003. This process was initially thought to be a protective function of the host immune system at the onset of malignant transformation of cells. However, it has been recognized that both the innate and adaptive immune compartments protect the host from tumor progression and edit the immunogenicity of tumors that might form. Therefore, the term "cancer immunoediting" has been proposed to emphasize the immune system's dual role in preventing tumor progression. This process is made up of three phases, called the "3Es": elimination, equilibrium, and escape. Once normal cells have been transformed to tumor cells by combining oncogenic processes and loss of intrinsic tumor suppressor

`

mechanisms, the immune system acts as an extrinsic tumor suppressor mechanism by eliminating tumor cells or by preventing their growth (Pearson et al., 2020)

In the elimination step, formerly known as immunosurveillance, innate and acquired immunity cells recognize cancerous cells and eliminate them, leading to a return to physiological tissue. However, if antitumor immunity is not able to eliminate tumor cells acquired immunity cells can modulate tumor growth without being able to eradicate it (equilibrium phase). Additional mutations are estimated at this point allowing tumor cells to escape recognition, destruction, and control by the immune system, leading to clinically detectable tumors (escape). The elimination phase represents the original concept of cancer immunosurveillance. If this phase makes it possible to completely eradicate the developing tumor, no progression occurs to the following phases. For this reason, cancer is more common in older people in whom immune function, and thus cancer immunosurveillance, begins to decline (Razavi et al., 2016).

During the equilibrium phase, the host's immune system and tumor cells that survived the elimination phase enter a dynamic equilibrium state. Lymphocytes and the IFN-γ factor exert a relentless selection pressure on tumor cells which may be sufficient to contain but not fully eradicate tumor cells. Although many original tumor cells are destroyed, new variants arise. These variants carry different mutations that allow tumor cells to resist and escape immune response. Equilibrium is probably the longest of the three phases and can last for several years in humans. For some solid tumors, it is estimated that 20 years may separate the initial exposure to the carcinogen and the tumor clinical detection. During this period, the heterogeneity and genetic instability of cancer cells that survive the elimination phase are probably the main factors that allow cancer to resist the host's immune system (Pearson et al., 2020).

`

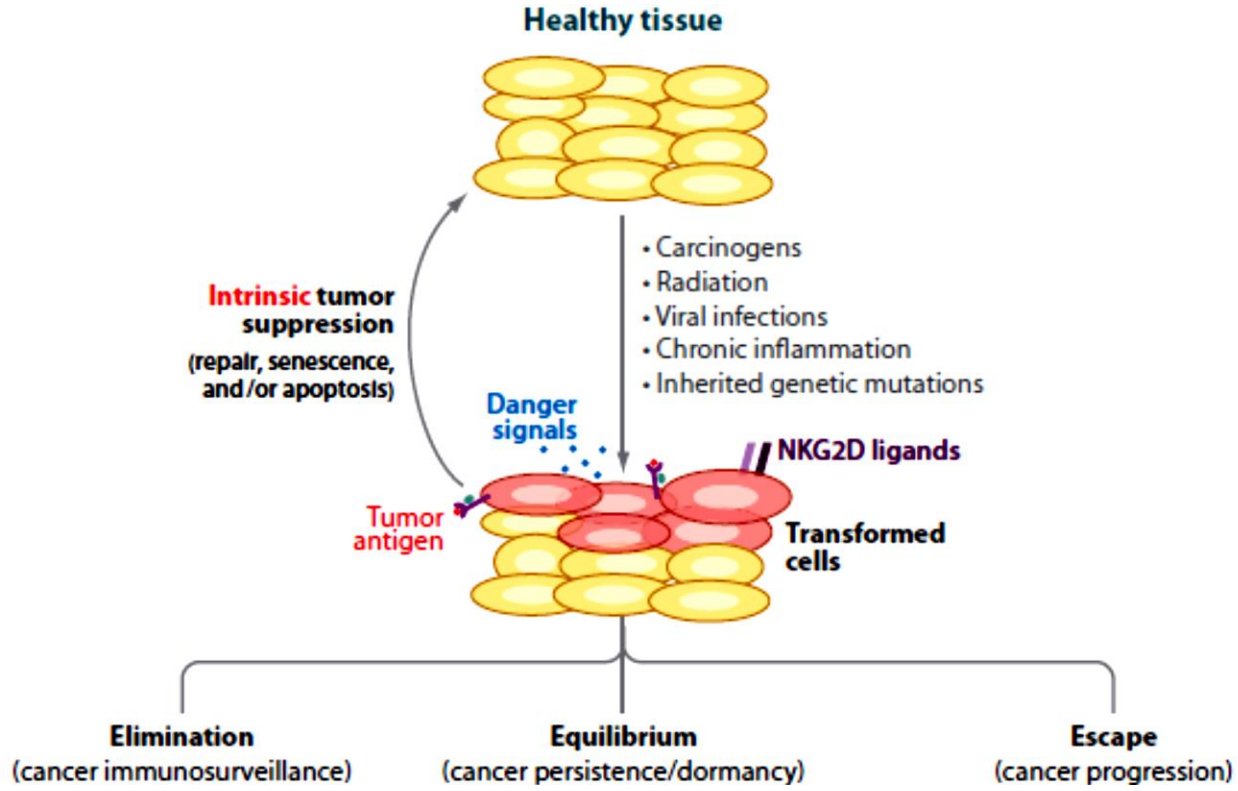

Figure 10: The concept of immunoediting. Adapted from (Vesely et al., 2011).

Escape from the immune system now represents one of the characteristics common to cancer cells. During the escape phase, tumor cells selected during the equilibrium phase can grow. This breach of the host's immune defenses likely occurs when genetic and epigenetic changes within tumor cells confer resistance to detection and elimination by the immune system. Tumor cells must employ multiple strategies to escape from the immune system innate and adaptive antitumor responses. Much work has focused on defining the molecular and cellular mechanisms of tumor escape. They operate at many levels and involve the tumor, the TME, and the innate and adaptive immunity components (Razavi et al., 2016). Some of the most well-determined escape mechanisms were described within the TME section and are summarized in **(Table 6).**

`

Table 6: Summary of GBM escape mechanisms Razavi et al. (2016)

Category	Biomarkers or Mechanism	Major source	Effect
CNS	BBB	Anatomical barrier	Decrease the chance of immune cells infiltration to the brain
TME	IL-6, IL-10, TGF-β, IL-1	Microglia/TAMs, GBM cells and endothelia cells.	Blocks T-cell activation and proliferation, suppresses NK cell activity, promotes Treg activity, promotes tumor growth and invasion
Immune checkpoints	PD-L1, CTLA-4	GBM cells, microglia/TAMs, T-Cells	Significantly reduce T-cell proliferation and increase T cell exhaustion
Regulatory T-lymphocytes	CCL22, CCL2	GBM cells	Modulate T cell activity and attracts Tregs to the tumor site
Tumor-associated macrophages	VEGF, IL-6, EGF, TGF-β1, MIC-1	Microglia/TAMs	Promote tumor growth, immunosuppression, and tumor vascularity

Abbreviations: IL-6: interlueikin-6; TGF-β : Transforming growth factor beta; CCL22: C-C motif chemokine 22; EGF: epidermal growth factor: MIC-1: macrophage inhibitory cytokine 1

`

3.1.4 Immunotherapy

The choice of the most appropriate immunotherapy depends on many factors, *i.e.*, the treatment's objectives (curative or palliative), the patient's status, the type of cancer, the rate of tumor progression, and the efficacy *versus* the adverse effects. Adverse effect reactions associated with immunotherapy may be moderate to severe and localized to systemic effects. Some immunotherapies activate the body's immune system in general, while others specifically target distinct tumor antigens. Another important consideration in using immunotherapy is the possibility of inducing a long-lasting antitumor immune response through the immune memory. While this effect can be beneficial, it could lead to long-lasting toxicities. The primary role of immunotherapy is to re-activate the host's deficient immune system to initiate and maintain immune reactions against tumor cells. The majority immune evasion mechanism used by TME represents therapeutic target points to restore immune control. Several immunotherapeutic approaches can be combined in some patients (Carlson et al., 2020).

3.1.5 Monoclonal antibodies

Monoclonal antibodies (MAbs) approved to be a significant strategy used in the treatment of solid tumors and hematological malignancies. They have a unique specificity for a specific antigen which allow them to bind to epitopes on the surface of cancer cells or immune cells. Therapeutic Abs are related to the immunoglobulin G family and composed of fragments that bind to their antigen. Furthermore, they are known as "naked," as they are not conjugated with another active principle such as chemotherapy or radiotherapeutic agent. The primary mechanisms of action of the majority of naked mAbs are antibody-dependent cellular cytotoxicity and complement-dependent cytotoxicity. Other mechanisms are also reported, such as the direct triggering of cell death or the blocking of angiogenesis and cell survival signaling pathways. All-human MAbs show lower immunogenicity compared to murine, chimeric, or humanized mAbs.

`

Therapeutic MAbs with a non-human sequence is more easily identified as foreign subjects and induce host immune responses. Reduced efficacy was observed in non-human MAbs mainly due to increased clearance and more adverse reactions, such as injection site reactions. The use of naked MAbs has significantly improved the treatment of certain solid tumors (Zahavi and Weiner, 2020).

3.1.6 Monoclonal antibodies against checkpoint proteins

MAbs that block immune checkpoints represent up-and-coming treatments for various cancer types as they have remarkable and long-lasting responses in some patients. Unlike chemotherapies, MAbs are well tolerated and provide long-term benefits on patient survival. A notable example is pembrolizumab's success, an anti-PD-1 antibody combined with surgery and radiation therapy have eradicated all melanoma traces in former President Jimmy Carter. The mechanism of action of ICBs was a breakthrough in the conception of cancer treatment and led for a Nobel Prize in Physiology (Huang and Chang, 2019). Chemotherapy and radiation therapy are directed to destroy cancer cells, while ICBs target the tumor-induced immunosuppression. These MAbs block checkpoint proteins on the surface of T-lymphocytes that are responsible for the immune response, resulting in prolonged antitumor responses (Desland and Hormigo, 2020).

Immunomodulatory antibodies can prevent checkpoint ligand/receptor interactions. They bind either to immune checkpoint proteins on T-lymphocytes, such as ：(i) cytotoxic T-lymphocyte-associated antigen–4 (CTLA-4) and its ligands CD80/CD86 or (ii) PD-1 and its ligands programmed cell death ligand 1 (PD-L1). These ICBs have demonstrated clinical efficacy, but many other ICBs have been identified and under developments **(Figure 11).** Stimulation of the immune system with ICBs *i.e.*, Ipilimumab, anti-CTLA-4, and atezolizumab, anti-PD-L1, showed promising effects alone or with other chemotherapies on treating multiple cancers. Ipilimumab was the first humanized anti-CTLA-4 approved

`

by the American federal drug administration (FDA) to treat inoperable melanoma (Tarhini, 2013).

Five years later, atezolizumab was the first humanized anti-PDL1 to be approved by the FDA to treat advanced or metastatic urothelial carcinoma (Hsu et al., 2017). However, the combination of nivolumab and ipilimumab with GBM in clinical trials ended with immune-related severe adverse effects and avelumab monotherapy, anti-PD-L1 has a small effect on progression-free survival. In preclinical settings, ICBs efficacy was enhanced when antibodies were delivered to brain tumors. (Guo et al., 2020). PD-L1 proteins are expressed as surface molecules by cancerous cells as GBM cells (Hao et al., 2020) and provide a tumor escape mechanism when binds to PD-1 proteins at the surface of activated T-lymphocytes leading to T lymphocytes exhaustion (Azoury et al., 2015).

On average, clinical data show that approximately 15-20% of patients respond to ICBs (Azoury et al., 2015). Currently, the responses observed with ICBs are more often partial responses at rates comparable to other targeted therapies or chemotherapies. ICBs have drastically reduced the tumor's size or even eliminated it in some patients allowing a surgical removal of the tumor. Besides, the duration of possible responses with ICBs can be extended to longer periods and patients sometimes considered completely cured. Anti-CTLA-4 stimulate circulating T-lymphocytes and their response may take months to activate enough T-lymphocytes to produce a favorable clinical outcome. In contrast, anti-PD-1/PD-L1 produces a faster response as these antibodies act on activated T lymphocytes which are directed against tumors (Wei et al., 2018).

I. Anti-CTLA-4

Anti-CTLA-4 was the first ICB to be tested in the clinic. This receptor is exclusively expressed on T-lymphocytes' surface, and its primary function is to regulate the amplitude of early activation of T-lymphocytes. B7-1 and B7-2 proteins bind to CD28 at the surface

`

of T-lymphocytes and promote the activation of T-lymphocytes by amplifying T-cell receptors (TCR) signals resulting in co-activation signal. On the other hand, CTLA-4 has a higher affinity for B7-1/2 than CD28 and inhibits T lymphocytes activation by providing inhibitory signals and competing with CD28 for binding to B7-1/2 (Rowshanravan et al., 2018).

The exact molecular signaling pathway amplified by CTLA-4 binding remains unclear, however, studies reported a kinase signals' disruption triggered by CD28 and TCR. Furthermore, CTLA-4 appears to activate (*i.e.,* src homology-2 domain-containing protein tyrosine phosphatase-2 (SHP2) and protein phosphatase 2A), which oppose the phosphorylation cascade initiated by the activation of TCR and CD28, therefore, leading to the opposing of T-lymphocytes activations. Activation of CTLA-4 also increases the immunosuppressive action of Tregs while decreasing the production of IL-2 and the expression of its receptor. It is proposed that anti-CTLA-4 reduces the ability of Tregs to control the anticancer immune response and autoimmunity. Overall, the mechanism of action of anti-CTLA-4 involves both the elevation of T lymphocytes activity and the inhibition of Treg activity.

II. Anti PD-1 and anti PD-L1

The programmed cell death (PD-1) protein is a type 1 transmembrane receptor that was identified in 1992 (Ishida, 2020). A negative regulatory function for PD-1 was first proposed when mice deficient of PD-1 developed spontaneous autoimmune phenotype. PD-1 receptor, present on the surface of activated $CD8^+$ T lymphocytes. The primary role of PD-1 is to regulate peripheral T-lymphocytes activity and to prevent autoimmunity during an inflammatory response. PD-1 binding with its ligands PD-L1 and PD-L2 results in a decreased proliferation, apoptosis, and decreased cytokine production. Like CTLA-4,

`

PD-1 is strongly expressed on Tregs' surface and induces their proliferation, therefore suppressing the functions of $CD4^+$ and $CD8^+$ T-lymphocytes.

The PD-1 pathway may also regulate T-lymphocytes activation to a state of immune tolerance in secondary lymphoid tissues during the early immune response. The expression of PD-1 is broader than that of CTLA-4 because it is not limited to T-lymphocytes and affects other activated cells such as B lymphocytes and NK lymphocytes, limiting their lytic activity. PD-1 regulates the activation of T-lymphocytes through the inhibition of kinases. When PD-1 binds to its ligand, the SHP2 phosphatase is inhibited. It can, therefore, no longer dephosphorylate the TCR signaling molecules. Unlike CTLA-4 ligands, PD-L1 and PD-L2 are overexpressed on cancer cells and in the TME. Therefore, the expression of PD-L1 is described in many types of cancer, including solid tumors. PD-L1 is also commonly expressed on myeloid cells of the TME. As a result, blocking PD-1/PD-L1 leads to a more active and prolonged antitumor immune response. Blocking PD-1 with ICBs induces and increases the activation, expansion, and the effector functions of T-lymphocytes. Furthermore, it may increase antitumor responses by reducing the number and the immunosuppressive activity of Tregs in the TME.

`

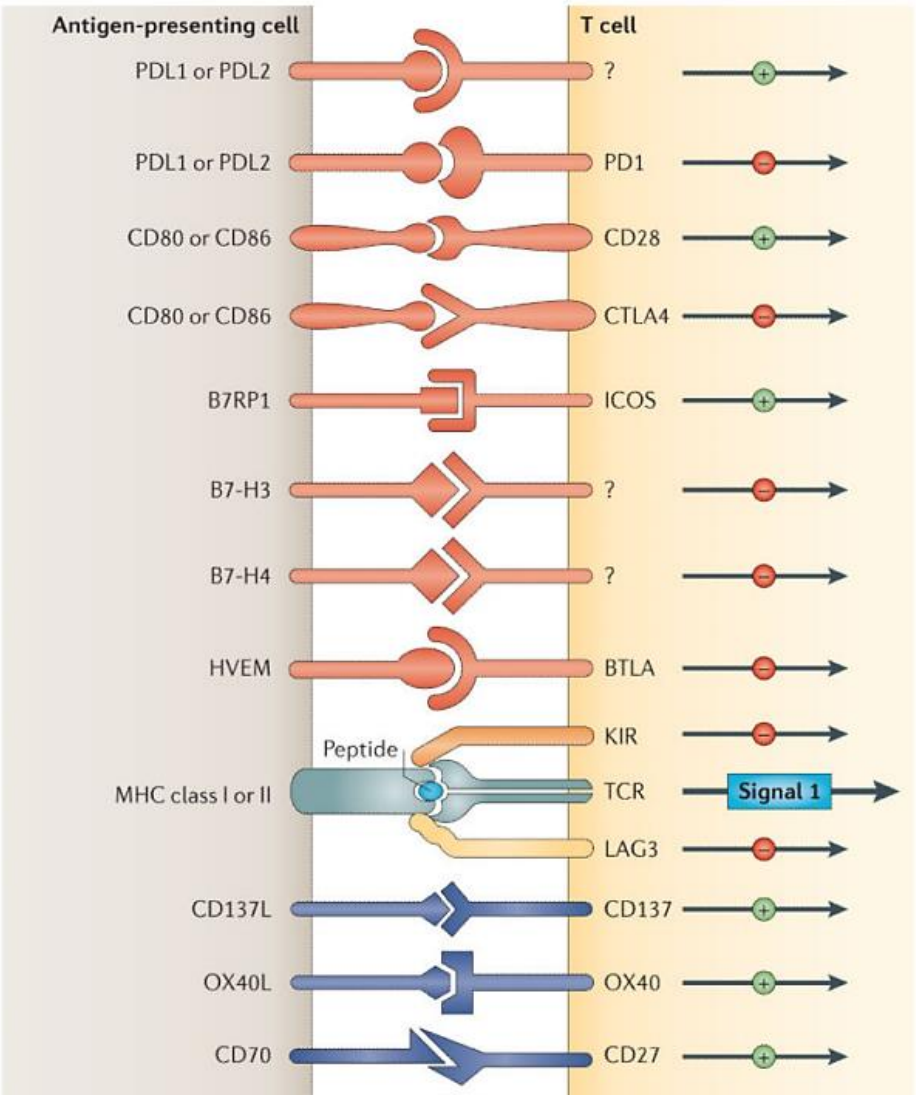

Figure 11: A list of the therapeutic antibodies currently available and associated with their potential targets of immune checkpoint pathways on T-lymphocytes and antigen presenting cells. PD-1, CTLA-4, PD-L1 and CD80 are targets with available antibodies to block their activity.

`

3.2 Overcoming, disrupting, or bypassing the BBB

3.2.1 The BBB limits drug penetration into normal and tumor tissue

It is estimated that 20% of small molecules crosses the BBB while none of the large therapeutic agents (*i.e.*, antibodies) crosses it in physiological conditions. In neuro-oncology, many studies have measured the capacity of therapeutic compounds to cross the BBB. For examples, studies show that ~25% of TMZ reaches the brain following oral administration. Furthermore, nitrosoureas have a similar percentage of brain penetration (~25%). On the other hand, compounds such as etoposide and platinum derivatives are less likely to reach the brain (Drean et al., 2016). Therefore, several innovative strategies are continuously evolving to overcome the BBB by increasing drug delivery (*i.e.*, systemic, or local administration of chemotherapy) or by increasing the drug penetration either by drug chemical modification or BBB modulation.

I. Intra-tumor injection

A local delivery of chemotherapy is possible through catheter insertion during MRI imaging to allow a proper insertion procedure. The main advantage of the catheter-mediated local delivery is to reduce systemic toxicity of chemotherapies. Almost all chemotherapies can be delivered by this method. However, some adverse neurotoxic effects as seizure may be observed, therefore limiting the use of certain medications (*i.e.*, taxanes and platinum derivatives). A clinical trial administering DTI-015 (BCNU in 100% ethanol) directly to patients with recurrent malignant gliomas showed that BCNU stabilized the tumor growth in 72% of patients. However, the reported three deaths in the clinical trial limited the success of this method (Hassenbusch et al., 2003).

`

II. Convection enhanced delivery

Edward Oldfield's group developed convection enhanced delivery (CED) in 1990. CED is based on the insertion of a catheter during neurosurgical procedure. The catheter is placed with a positively pressured pump that allow the drug to be delivered slowly over a specific time. Several antineoplastic agents were tested using CED (*e.g.*, cisplatin, methotrexate, paclitaxel, nimustine, topotecan and carboplatin). The success of CED is highly dependent on several factors but mainly the drug itself and the tumor site became the major concern in this technique. A recent clinical trial reporting the efficacy of carboplatin delivered by CED showed that it reduced recurrent GBM tumor size in 58% of patients and enhanced their clinical conditions (Barua et al., 2016).

III. *In situ* biodegradable wafers

Drug-loaded polymer wafers (*e.g.,* Gliadel®) have been developed and used for the direct delivery of antineoplastic agents to brain tumors. One of the disadvantages of this method is an effect called the sink effect in which the concentration of the drug declines rapidly after their release from the polymer. A systematic review that analyzed all clinical trials on the efficacy of Gliadel® wafers combined with systemic administration of TMZ suggested a positive additive effect on survival without increased toxicity in GBM patients (Ashby et al., 2016).

IV. BBB and efflux pumps modulations

Using partial or complete inhibitors of ABC transporters can be combined with their substrates to enhance their CNS penetration and anticancer activity. A variety of modulators were tested to suppress activity of efflux proteins, mainly (ABCB1 and ABCG2) and few were successful enough to reach clinical trials. In GBM, a limited number of clinical trials were initiated to modulate ABC proteins. To date, these trials failed to show significant clinical benefit, which could be related to a few reasons. Firstly, the study design

`

was not optimal *i.e.*, in the early clinical trials, the patients were not stratified based on high expression of ABC proteins, and a precise evaluation of the role of ABCB1 and ABCG2 transporters in patients could not be conducted. Secondly, modulators of ABC proteins could change the pharmacokinetics of other drugs reducing their anti-tumor properties. Thirdly, the dose that was selected to inhibit the ABC proteins was not sufficient or a higher dose could not be applied safely in patients.

V. Drug modification

Drug modification strategies using nanocarriers (nanocapsules, liposomes, micelles, or dendrimers) were developed to allow drugs to enter the BBB via endocytosis, and/or to improve drug half-live and protection from clearance mechanisms (Zhao et al., 2020). One clinical study investigated pegylated liposomal doxorubicin's efficacy when administered with TMZ and radiotherapy in newly diagnosed GBM patients. This study showed that the pegylated liposomal doxorubicin form is safe and tolerable. However, no meaningful efficacy was observed from the addition of liposomal doxorubicin to TMZ treatment (NCT00944801) (Beier et al., 2009). Another study evaluated the safety and the pharmacokinetics of a liposomal form of irinotecan, the study confirmed the safety of this formulation. However, the efficacy is still under investigation (Clarke et al., 2015).

Antibody-drug conjugates (ADCs) were also evaluated against a variety of targets in GBM and this approach is currently under investigation (Gan et al., 2017). ADCs are a newly developed biopharmaceutical compounds that allow the targeting of tumor cells while sparing healthy cells. This method is based on the use of an antibody to carry the substrate when binding to its ligand. In 2017, a published clinical trial showed a promising efficacy of depatuxizumab mafodotin (ABT-414), an ADC targeting wild-type or mutant forms of *EGFR* to selectively deliver a cytotoxic agent, in *EGFR*-amplified recurrent GBM patients with manageable adverse effects (Reardon et al., 2017).

`

VI. Ultrasound-mediated BBB opening (UMBO)

UMBO was used in pre-clinical models to bypass BBB and to increase brain penetration of a wide variety of therapeutics. Low-intensity pulsed ultrasound can be delivered to the brain to induce a safe oscillation of intravenously injected microbubbles within blood vessels (Hynynen et al., 2001). Oscillation of these microbubbles opens the BBB by reversibly disrupting the tight junctions between ECs. A range of drugs has been tested for use with UMBO for treating gliomas and include temozolomide, carmustine, irinotecan, carboplatin, doxorubicin, and drug-loaded liposomes (Beccaria et al., 2016, Goldwirt et al., 2016). UMBO has recently moved to clinical trials where its clinical safety was confirmed: Sonocloud-induced UMBO was found to be safe and tolerable among recurrent GBM patients (Carpentier et al., 2016). Two other phase 1 and phase 2 clinical trials are currently in progress to evaluate UMBO's efficacy in combination with carboplatin in patients with recurrent GBM (NCT03744026).

3.2.2 Role of ultrasound-mediated BBB opening

I. Ultrasound mediated BBB opening

In 2001, Hynynen laboratory developed a method of UMBO which has proven to be safe and effective. UMBO relies on a mechanism termed cavitation, where ultrasound propagate through the tissue and encounter micron-size bubbles (listed in **Table 7**), making them expand at low acoustic pressure and contract at higher pressure. Indeed, UMBO is highly dependent on the emission of low intensity ultrasound waves that alter the conformation of microbubbles. The interaction between the microbubbles and the ultrasound waves results in a microbubbles expansion and contraction within the capillaries. The expansion of the microbubbles fills the capillary lumen resulting in a mechanical stretching on the micro-vessels wall. This results in the opening of the tight junctions. Furthermore, the microbubbles may decrease the blood flow, allowing a

`

compensatory mechanism of BBB opening due to ischemia. It is believed that UMBO can enhance the main four known mechanisms that regulate the exchanges of molecules from blood to brain and vice versa. Transcytosis, trans-endothelial openings, opening of the tight junctions and the free passage of molecules through the permeable endothelium can be all be enhanced by UMBO and be responsible for the increased delivery of chemotherapies and molecules into the brain parenchyma **(Figure 12).**

The sub-harmonic (SH) acoustic emission leads to the oscillation regime of microbubbles called "stable cavitation", which is generally associated with a safe BBB disruption. On the other hand, broad-band (BB) acoustic emission is linked with the cavitation regime called "inertial cavitation", where the bubbles collapse. This type of cavitation is often associated with side-effects **(Figure 14)**(Dauba et al., 2020). Therefore, this value should remain low during the UMBO protocol to maintain a safe and effective UMBO **(Figure 12).**

Table 7: Available commercial microbubbles. Each type of microbubbles differs in its composition (capsule and gas), size, half-life, and concentration.

	SonoVue®	**Definity®**	**Optison®**
Company	Bracco Diagnostics	Lantheus	E-Cardio
Encapsulated gas	Hexafluoride sulphide	Octafluoropropane	Octafluoropropane
Capsule	Phospholipids	Phospholipids	Albumin
Diameter of microbubbles (µm)	2.5	1.1 - 3.3	2-4.5
Concentration (bubbles/ml)	1 - 5 x 10^8	1.2 x 10^{10}	5 - 8 x 10^8
Half-life (minutes)	2	1.9	1.3

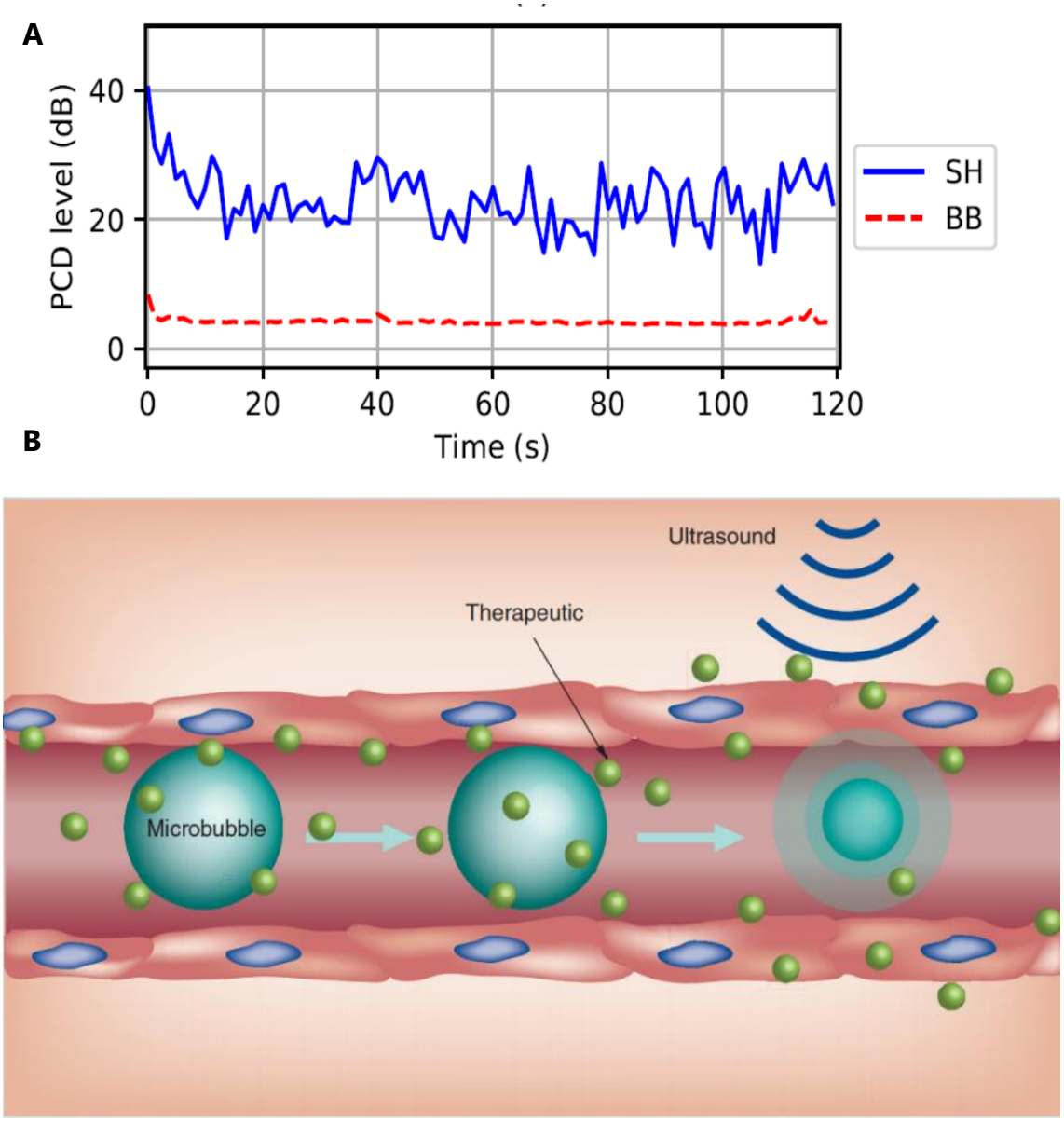

Figure 12: Mechanisms of UMBO. Panel A: represent the values of SH acoustic emission in blue detected in real-time (Sonocloud device for small animal). On the other hand, BB in red, is maintained with low values to reduce adverse effects. Panel B: Although the mechanisms potentially involved in UMBO in combination with microbubbles are poorly understood, accumulative evidence suggest that the mechanism of stable cavitation is responsible for the transient opening of the BBB. Adapted from (Beccaria et al., 2020)

`

II. Parameters affecting UMBO

The extent of UMBO is usually assessed through the injection of optical or fluorescent dyes that cannot cross the BBB (*e.g.* Evans blue dye is ~70 KDa when bound to albumin *in vivo*) (Yao et al., 2018). When UMBO is applied, Evans's blue will cross the BBB and is detected in the brain parenchyma. Other methods include post-gadolinium MRI acquisition and two-photon live microscopy **(Figure 13).** Furthermore*, in vivo* imaging using two-photon microscopy in combination with a dye (dextran-conjugated 10 KDa) was used as a method to evaluate the passage of a dye following UMBO . Gadolinium does not cross the BBB in physiological conditions (500-900 Daltons). Following UMBO, post gadolinium MRI images show a significant enhancement of the contrast agents across the brain (Idbaih et al., 2019).

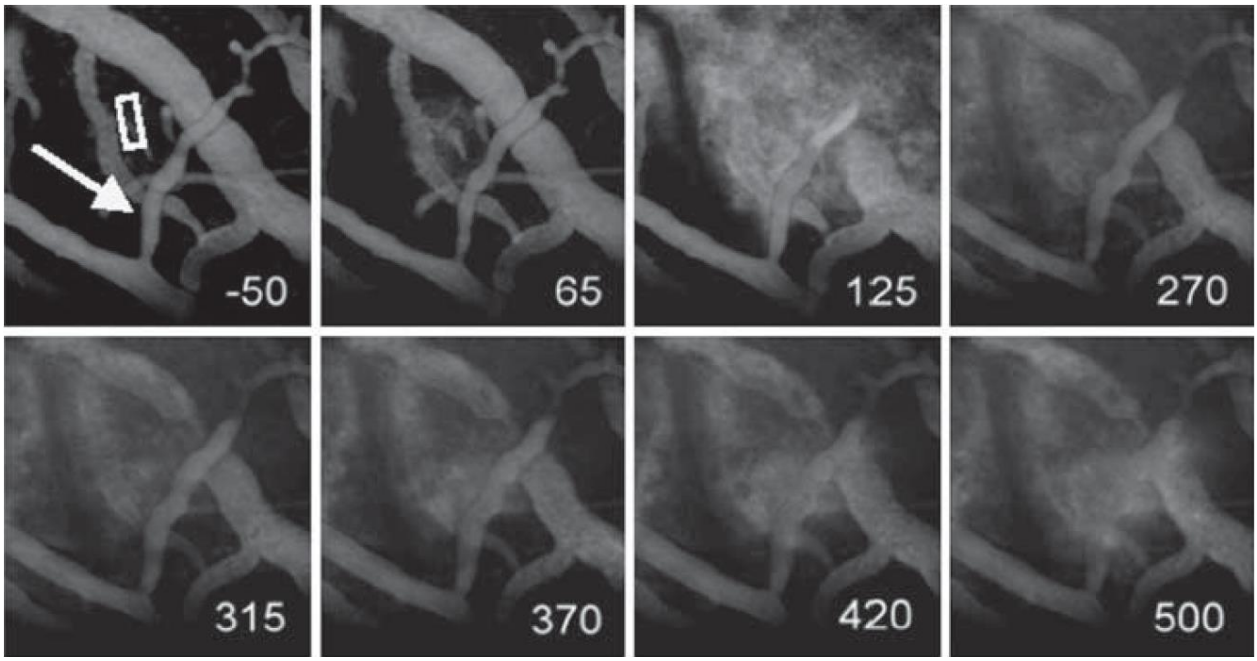

Figure 13: Two photon microscopy to visually follow the leakage of a Dextran-conjugated Texas Red (10 KDa) through a micro-vessel wall after UMBO. Numbers correspond to the time in second following UMBO (Cho et al., 2011).

Prior to clinical application, the safety of UMBO protocols must be established, showing no adverse effects or tissue damages with a successful BBB opening **(Figure 14)**

`

Type of ultrasound (focused or unfocused), pulse frequency, repetition and duration, the amplitude, the total exposure time, the microbubbles used **(Table 7)** and their dose must be optimized. These parameters will define the effectiveness and the safety of the opening. Possible side-effects that must be avoided include vasogenic edema, extravasation of red blood cells leading to fatal hemorrhages or tissue damages.

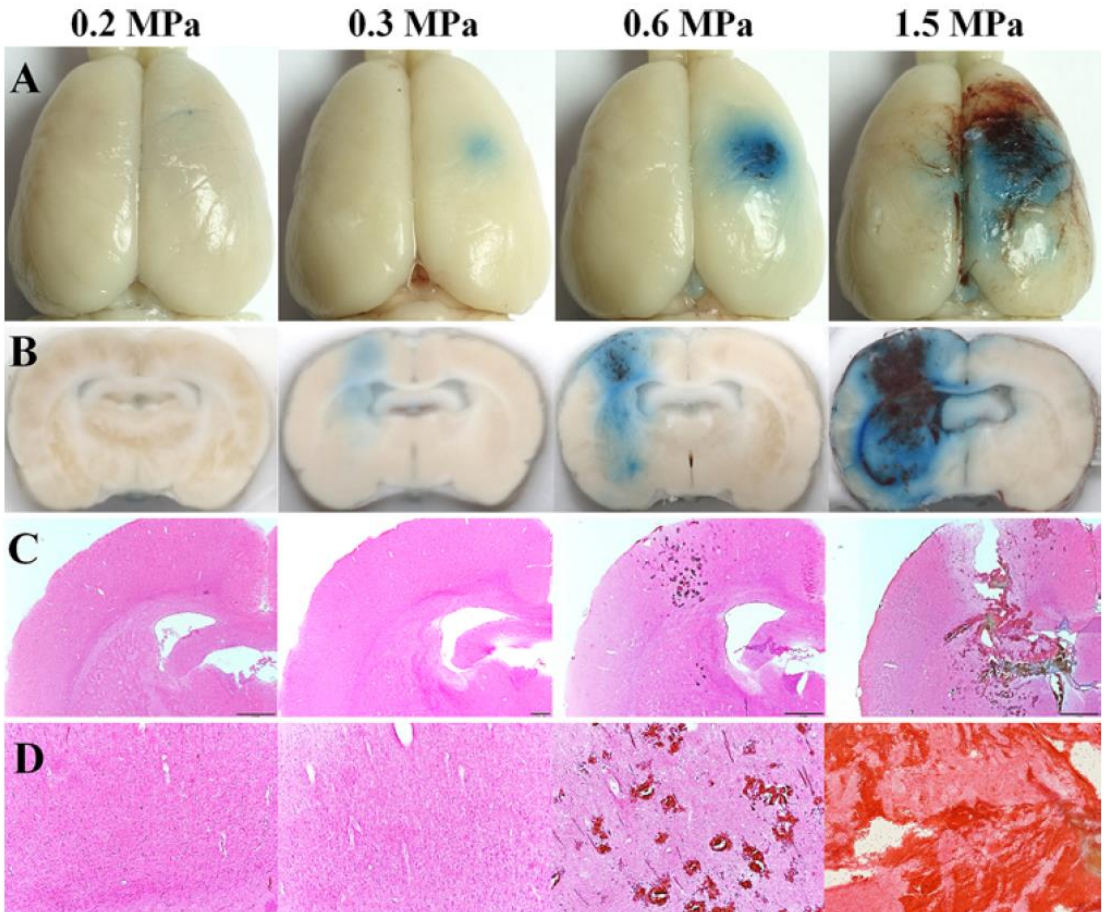

Figure 14 Example of efficacy/safety: impact of acoustic pressure on treated rats. High acoustic pressure induces large UMBO with a significant tissue damage and associated hemorrhage. Consistent with such effect, duration of sonication (long sonication's time is associated with tissue damage) and microbubbles doses. The opening is visible by the entry of Evans blue into the brain parenchyma on the right hemisphere of a rat brain. Hematoxylin and eosin stains of brain sections allow identification of tissue damage (Shin et al., 2018)

`

3.2.3 UMBO and antibodies delivery to the brain

The first two studies that showed the possibilities to enhance antibodies delivery by focused ultrasound to the brain were published in 2006. Both studies were conducted in healthy rodents, and they aimed to prove the concept of antibody delivery using UMBO. Anti-D4 receptor antibody was successfully detected using immunohistochemistry (IHC). Furthermore, IHC detection of the delivered antibody was consistent with Evans blue passage following UMBO (Kinoshita et al., 2006a). In 2013, another published study reported a reduction in glioma tumor size following antibody loaded microbubbles and UMBO targeting VEGF (Fan et al., 2013).

Interestingly, results were published in 2016 reporting that bevacizumab concentration was increased up to 57-fold with UMBO. UMBO at 0.8 MPa facilitates the passage of bevacizumab for up to 57-fold. However, this acoustic pressure is not safe. At a safer UMBO parameter, up to 5-fold bevacizumab concentration was reported (Liu et al., 2016). A very recently published study reported enhancing delivery of high molecular weight dextran's (70 and 500 KDa) with UMBO at different acoustic pressure (Valdez et al., 2020). Recent articles that evaluated UMBO in combination with antibodies and large molecules are summarized in **(Table 8)**.

`

Table 8: Original research articles that combined UMBO with antibodies and macromolecules delivery.

Antibody	Model	Results	Reference
Herceptin	Healthy mice	Proof of concept of safety and efficacy of Herceptin delivery	(Kinoshita et al., 2006a)
Anti-D4 receptor antibody	Healthy mice	Enhanced the delivery of anti-D4 receptor antibody in the brain	(Kinoshita et al., 2006b)
VEGF-targeting, drug-loaded MBs	C-6 Glioma rat model	Reduction in tumor volume with enhanced overall survival	(Fan et al., 2013)
Trastuzumab and Pertuzumab	Brain metastasis in rat model	Combination of focused ultrasound and antibodies enhanced the overall survival	(Kobus et al., 2016)
Bevacizumab	Glioma mouse model	Significant enhancement of bevacizumab concentration (5-57 folds) and increased survival	(Liu et al., 2016)
Anti-β-amyloid protein antibody	Alzheimer's model in rabbits (high-cholesterol diet)	Focused ultrasound decreased B amyloid plaque	(Alecou et al., 2017)
Tau-specific antibody	Alzheimer's Mouse model	Focused ultrasound increased the local delivery of tau antibody in the brain parenchyma	(Janowicz et al., 2019)
Macromolecule (dextrans MW 3, 70 and 500KDa)	Healthy mice	Focused ultrasound enhanced the delivery of different dextran sizes in the brain.	(Valdez et al., 2020)

`

3.2.4 Ultrasound mediated BBB opening in clinical settings

During the last two decades, Sunnybrook Research Institute in Canada established and developed transcranial ultrasound systems to open the BBB under MRI guidance. A commercial transcranial ultrasound system implementing this approach was developed by the company Insightec® and is currently evaluated in clinical trials for several neurological disorders, including GBM (NCT03712293). The noninvasive system's main disadvantage compared to the implantable SonoCloud-9® device is its cost (including a 3-hour MRI immobilization per treatment) and the limited BBB disruption volume. The company NaviFUS® developed another noninvasive transcranial system. They recently launched a neuronavigational-guided clinical trial to open the BBB to enhance bevacizumab delivery in GBM patients (NCT04446416). The device's main strength is that it uses the neuronavigational system to target a specific brain region. It provides a cheaper alternative than the Insightec device; however, this device is still under testing and validation.

The SonoCloud-9 UMBO device, developed by CarThera®, can be implanted after resection surgery, limiting the number of eligible patients. It can also be implanted during a dedicated surgery, but it can become a limitation compared with less invasive approaches. The SonoCloud® approach is very well integrated with the standard oncology procedures, as it only requires five minutes of activation before or after the drug administration. The volume treated with this device is significant for large infiltrative GBM tumors as in the current clinical trial (NCT03744026).

`

Thesis Objectives

This thesis aims to evaluate the modulation of GBM TME, including the BBB and the immune system, to increase efficacy of anti-tumor therapeutic strategies in both GBM patients and preclinical mouse models. Therefore, the study objectives are divided into three parts:

A. Firstly, reviewing the literature to understand the role of ABC transporters in GBM resistance to chemotherapy.
B. Secondly, exploring the expression of immune checkpoint proteins, mainly CD80 and CD86, in the GBM TME and their role as prognostic markers in newly diagnosed GBM patients.
C. Finally, evaluating the role of the UMBO to improve and to understand response to ICB GBM mouse model.

`

A. Review of the literature to understand the role of ABC transporters in GBM chemo-therapy resistance

GBM is the most frequent and the most aggressive primary cancer of the brain in adults. Without doubt, therapeutic strategies to overcome GBM resistance are continuously failing. Not to mention, after initial efficacy, GBM cells acquire resistance to TMZ and other chemotherapeutic agents *via* multiple mechanisms, including the expression of ATP-binding cassette (ABC) efflux proteins. These transporters are involved in normal physiological functions, *i.e.*, physiological cholesterol transport and elimination of toxins, but also it plays a role in pathological conditions, *i.e.*, chemotherapies drug resistance. In humans, each ABC protein has specific tissue locations and specific functions.

In this review, I used publicly available data obtained from PubMed and Google Scholar. Original published articles were selected using the keywords: ABC transporters, glioblastoma, temozolomide, and chemotherapy. A total of 36 selected articles was used for further reviewing. I described the most-commonly investigated ABC proteins members (ABCB1, ABCC1 and ABCG2) and their role in the resistance of GBM cells to chemotherapy. The review article was submitted for publication and is listed in the **results** section.

`

B. Exploring the expression of immune checkpoint proteins, mainly CD80 and CD86, in GBM TME and their role as a prognostic factor in newly diagnosed GBM patients

GBM patients have a dismal outcome with a median OS of 15 months after initial diagnosis with known prognostic factors such as age, KPS and *MGMT*. Immunotherapies have dramatically improved the prognosis of multiple non-neurological cancers. In the setting of primary brain cancers, the results of clinical trials are still disappointing. Nonetheless, specific GBM patients respond to these therapies, supporting the need for identifying biomarkers to guide the prescription of immunotherapies.

Checkpoint proteins such as the Cluster of Differentiation CD80 (also known as B7-1) and CD86 (known as B7-2) are expressed on the surface of tumor cells (Ville et al., 2015). Furthermore, CD80 protein expression was observed in infiltrative tumor lymphocytes in melanoma (Hersey et al., 1994). CTLA-4 and the Cluster of Differentiation CD28 are located on the surface T-lymphocytes. CTLA-4 has a higher affinity to CD80 and CD86, and when bound to these ligands, T-lymphocytes remain inactive and exhausted (Rowshanravan et al., 2018). Antibodies targeting CTLA-4 were used preclinical studies in multiple solid tumors, followed by several ongoing clinical trials (Letendre et al., 2017). Ipilimumab (anti-CTLA-4) has also shown responses in patients with brain metastases, highlighting efficacy within the CNS (Amaral et al., 2020).

The expression of PD-L1 was inversely correlated with OS in GBM patients (Nduom et al., 2016). Here, I investigated whether the expression of CD80 and CD86 in GBM tissues could be used as a biomarker to predict the efficacy of ipilimumab among GBM patients. I studied the RNA and protein expression of checkpoint proteins CD80 and CD86 in GBM patient samples and their possible correlation with clinical outcome in newly diagnosed GBM patients aged below 70 and with good performance status and treated with the standard of care.

`

C. Evaluating the role of UMBO and its potential to be combined with immune checkpoint blockers, i.e., anti-PD-L1, to overcome GBM resistance to ICB

The existence of BBB as a specificity of the CNS blood vessels prevents most systemic therapeutics from reaching the brain (Drean et al., 2016). In GBM, structural and functional changes of the BBB are frequent and lead to the generation of the BTB, allowing larger chemotherapies to reach the tumor. Although BTB enhances the delivery of some chemotherapeutic agents, large therapeutic antibodies have no chance to reach the brain at their therapeutic levels (Veldhuijzen van Zanten et al., 2019) Several innovative strategies are known to enhance the delivery of chemotherapeutic agents and therapeutic antibodies (Drean et al., 2016).

UMBO using low-intensity pulsed ultrasound (LIPU) is one of the safe and effective methods to enhance the delivery of chemotherapeutic agents in both animals and patients. In clinical trials, UMBO showed adequate safety and efficacy among recurrent GBM patients (Idbaih et al., 2019). LIPU is delivered to the brain simultaneously with an intravenous injection of micron-sized bubbles for a few minutes, allowing microbubbles oscillation. Microbubbles oscillation produces a mechanical stretching on the vessel walls that allow the opening of tight junctions (Chen et al., 2019a).

The choice of therapeutic agents to deliver after UMBO is crucial and remains a point of discussion among researchers and regulators. Stimulation of the immune system with anti-CTLA-4 and anti-PD-L1 showed promising effects in multiple cancers. However, the combination of anti-PD-1 and anti-PD-L1 in GBM clinical trials ended with severe immune-related adverse effects. Therefore, there is a need to explore strategies to improve the efficacy of these immune modulators in GBM.

The third objective of my thesis is to study biological and therapeutic impacts of ICBs delivered with UMBO in GBM preclinical mouse models.

`

Results

- **Manuscript 1 (Submitted): Mohammed AHMED**, Maite VERREAULT, Xavier DECLAEVE, Ahmed IDBAIH 2021. Role of Multi-Drug Resistance in Glioblastoma Chemoresistance: Focus on ABC Transporters, Elsevier Publishing Company
- **Manuscript 2 (Submitted): Mohammed AHMED**, Isaias. HERNANDEZ., Franck BIELLE, Maite VERREAULT, Julie LEROND, Agusti ALENTORN, Marc SANSON, Ahmed IDBAIH 2021. CD80 and CD86: expression and prognostic value in newly diagnosed glioblastoma. Pathology and Oncology Research Journal
- **Manuscript 3 (in Preparation): Mohammed AHMED**, Mohammed Ahmed1,2*, Nolwenn LEMAIRE, Emie QUISSAC, Rana SALAM, Isaias HERNANDEZ, Coralie L GUERIN, Lea GUYONNET, Noël ZAHR, Laura MOUTON, Mathieu SANTIN, Alexandra PETIET, Charlotte SCHMITT, Guillaume BOUCHOUX, Marc SANSON, Maite Verreault, Alexandre Carpentier, Ahmed IDBAIH, 2021. Increased brain delivery of anti-programmed death-ligand 1 using low-intensity pulsed ultrasound-mediated blood-brain barrier opening is associated with increased anti-tumor efficacy and microglia activation in glioblastoma mouse models.

`

Role of Multi-Drug Resistance in Glioblastoma Chemoresistance: Focus on ABC Transporters

Mohammed Ahmed[1,2], Maite Verreault[1], Xavier Declaeves[3,4], Ahmed Idbaih[5]

[1]Sorbonne Université, Institut du Cerveau - Paris Brain Institute - ICM, Inserm, CNRS, APHP, Hôpital de la Pitié Salpêtrière, Paris, France

[2]Faculté de Médecine Paris-Sud - Université Paris-Saclay, 91190, Saint-Aubin, France.

[3]Inserm, UMR-S 1144, Université Paris Descartes - Paris Diderot, Variabilité de Réponse Aux Psychotropes, Paris, F-75006, France.

[4]Biologie du Médicament et Toxicologie, Hôpital Cochin, Assistance Publique-Hôpitaux de Paris, Paris, F-75014, France.

[5]Sorbonne Université, Institut du Cerveau - Paris Brain Institute - ICM, Inserm, CNRS, AP-HP, Hôpital de la Pitié Salpêtrière, DMU Neurosciences, Service de Neurologie 2-Mazarin, F-75013, Paris, France

Corresponding author

Ahmed Idbaih. Department of Neurology 2-Mazarin, Pitié-Salpêtrière University Hospital. 47-83, Boulevard de l'Hôpital, 75013 Paris, France. Tel : 01-42-16-03-85. Fax : 01-42-16-04-18. Email : ahmed.idbaih@psl.aphp.fr

`

Abstract

Glioblastoma (GBM) is the most frequent and the most aggressive primary cancer of the brain in adults. Despite aggressive therapeutic interventions, the median overall survival is below 18 months after initial diagnosis. The current standard of care of newly diagnosed GBM includes concurrent administration of temozolomide (TMZ) and radiotherapy followed by adjuvant TMZ. Since 2005, TMZ remained the first-line chemotherapy in treating GBM patients with its ability to cross the blood-brain barrier. However, after initial efficacy, GBM cells acquire resistance to TMZ and other chemotherapeutic agents *via* multiple mechanisms, including the expression of ATP-binding cassette (ABC) efflux proteins. These transporters are involved in normal physiological functions, i.e., physiological cholesterol transport and elimination of toxins, but also it plays a role in pathological conditions, i.e., chemotherapies drug resistance. In humans, each ABC protein has specific tissue's locations and specific functions. In this review, we highlight the role of ABC proteins superfamily members ABCB1, ABCC1 and ABCG2 in the resistance of GBM cells to chemotherapy.

Keywords: Glioblastoma, ABC transporters, multidrug resistance, chemotherapies, P-glycoprotein, the clinical role of ABC proteins

`

Introduction

Glioblastoma (GBM) is the most common and the deadliest primary brain cancer in adults with a median overall below 18 months after initial diagnosis (Ostrom et al., 2017). The current standard of care in newly diagnosed GBM patients, established in 2005, relies on concurrent administration of temozolomide (TMZ) and radiotherapy regimen followed by adjuvant TMZ alone (Pace et al., 2017). Despite remarkable efforts in the neuro-oncology field to develop new treatments, TMZ remains today the standard first-line chemotherapy in GBM patients 'treatment (Ostrom et al., 2017, Pace et al., 2017). TMZ is an alkylating agent with a small molecular weight (194.15 g/mol) that readily passes the blood-brain barrier (BBB) (Information, 2020).

The essential and complex organ, which is the human brain, is separated from the BBB's blood. The BBB is a specificity of the central nervous system (CNS) blood vessels. The BBB isolates the brain from the blood for protection purposes (Saunders et al., 2014). Indeed, it prevents potentially toxic molecules circulating in the bloodstream to access brain cells while ensuring the supply of nutrients to maintain homeostasis (Shen and Zhang, 2010). Highly specialized brain capillary endothelial cells (ECs) form an essential part of the BBB. In addition to ECs, various cells contribute to the biophysical structure of BBB described in **(Figure 15)**. To date, five mechanisms are known to regulate the exchanges of molecules from blood to brain and vice versa. Passive diffusion of molecules through the BBB can occur paracellularly for very low molecular weight molecules (*e.g.,* inorganic ions, water, gazes) and transcellularly for lipophilic compounds. An active transport can also occur either by : (i) transcytosis for some proteins (*e.g.,* leptin, insulin, transferrin) or (ii) carrier-mediated proteins belonging to two major transporter superfamilies for small molecules. The solute carrier (SLC) superfamily contains more than 400 transporters that allow exchanges of small molecules through the BBB while ATP-binding cassette (ABC) transporters limit CNS penetration of small molecules by effluxing

`

substrates from the brain ECs directly into the bloodstream **(Figure 15)** (Saunders et al., 2014, Chaves et al., 2014, Drean et al., 2016).

GBM cells acquire resistance to anticancer drugs via multiple mechanisms without being exhaustive: (i) acquisition of mutation in DNA repair genes, (ii) activation of alternative signaling pathways, (iii) immune escape, (iv) invasive switch from angiogenic growth and, (v) multidrug resistance mechanism (MDR) (Gillet and Gottesman, 2010, Ramirez et al., 2013) (Franceschi et al., 2018). MDR phenotype is observed in many types of cancers and induces : (i) increased efflux of drugs outside tumor cells and, (ii) reduced influx of drugs inside tumor cells (Turk et al., 2009). ABC transporters are efflux pump proteins involved in MDR. To date, 49 members of ABC proteins have been identified to be involved in different biological mechanisms within the human body, and are classified in seven subfamilies; ABCA (12 proteins), ABCB (11 proteins), ABCC (13 proteins), ABCD (4 proteins), ABCE (1 protein), ABCF (3 proteins), and ABCG (5 proteins) (Drean et al., 2018b).

ABC transporters are expressed in various tissues such as the liver and the intestine and have a distinct role in absorption, distribution, and excretion of drugs. Some ABC transporters are predominantly expressed in ECs of the BBB (Mahringer and Fricker, 2016). Indeed, ABCB1 and ABCG2 are expressed in ECs of the BBB, while others (ABCC, ABCG2) can be found in other cells such as astrocytes and neurons (Linton and Higgins, 2007, Shen and Zhang, 2010, Mahringer and Fricker, 2016). In humans, each ABC protein is expressed in specific locations and exhibit specific functions. i.e. ABCA subfamily members are expressed mainly in the CNS while ABCB subfamily members are mainly expressed in the BBB and liver (Lockhart et al., 2003). ABC proteins were studied in several types of cancers (Schinkel and Jonker, 2003). In GBM, three proteins (ABCB1, ABCC1 and ABCG2) were extensively studied and were shown to impact GBM cells biology. In this review, we highlight the role of ABC protein family mainly (ABCB1, ABCC1 and ABCG2) in resistance of GBM cells to chemotherapy.

`

Structure and Functions of ABC Proteins

Structure of ABC Proteins

The BBB was described for the first time in the 20th century when an intravenous injection of Evans blue significantly stained all tissue except the CNS while a direct intrathecal injection could stain only the brain tissue. This staining pattern highlighted the possibility of a barrier, termed the BBB, that prevents the dye to reach the brain tissue (Saunders et al., 2014). The BBB's integrity is preserved throughout life to maintain homeostasis and regulate the influx and efflux of nutrients/metabolites between the blood and the brain (Pulgar, 2018). ABC transporters, within the BBB, play a pivotal role in brain protection by eliminating harmful agents.

The ABC transporters' primary function is to actively transport their substrates, ranging from low molecular weight molecules to polypeptides, outside cells. Despite the large number of ABC transporters, they share structural similarities. In general, a typical ABC protein includes two functional units called transmembrane domain (TMD) and nucleotide-binding domains (NBD) (Figure 16). The NBDs are the ATPs binding units, and they contain the Walker A motif – a phosphate-binding structure-, Walker B motif, and Walker C motif. C motif is specific for ABC proteins while Walker A and B are present in all ATP dependent proteins. The TMDs include six or ten transmembrane helices depending on ABC superfamily members. There are two types of transmembrane helices: the inward part (open to the cytoplasm) and the outward part (open to the extracellular environment). These helices determine the direction of transport of the ABC transporters i.e. importer or exporter (Zolnerciks et al., 2011, Linton and Higgins, 2007).

Functions of ABC proteins

Several physiological functions are reported for each ABC subfamilies. However, ABC proteins' main function is to actively transport cytotoxic xenobiotics and endobiotics against their concentration gradient (Zolnerciks et al., 2011). According to their location,

`

they transport many substrates including anions, metal ions, peptides and lipophilic compounds (Mahringer and Fricker, 2016). ABCA subfamily is mainly responsible for lipids and cholesterol transport while ABCB, ABCC and ABCG subfamily members are mainly associated with drug resistance and elimination of xenobiotics. Genetic variants in ABC proteins are linked to genetic disorders *e.g.* a pathogenic variant in the ABCD2 is responsible for 95% of cases of X-linked adrenoleukodystrophy (ALD) disorder. **(Table 9)** summarizes the physiological functions of each ABC subfamilies.

Mechanisms of action of ABC transporters

ABC proteins hydrolyze ATP to efflux chemical agents against their concentration gradient. The active transport cycle starts with binding a substrate, *e.g.,* xenobiotic to a high-affinity structure formed by the TMDs and two ATP molecules binding NBDs. A conformational contribution forms the ATP binding sites at the NBDs residues from each NBD monomer. As a result, a conformational change in TMDs occurs from either outward to inward (importer) or *vice versa* (exporter) allowing the NBD units to form a dimer. The NBD dimer induces a major conformational change on the TMDs, allowing the xenobiotic to be translocated across the plasma membrane. The hydrolysis of ATP allows the NBD dimers to be dissociated and again inducing the TMDs conformational change, resulting in the xenobiotic to be released. A final step of restoration of the open NBD-dimer conformation then takes place **(Figure 17)** (Mahringer and Fricker, 2016, Vasiliou et al., 2009, Tivnan et al., 2015, Linton and Higgins, 2007, Zolnerciks et al., 2011).

ABC transporters in glioblastoma

Our review used public data obtained from PubMed and Google Scholar. Original published articles were obtained using the keywords (ABC transporters, glioblastoma, TMZ, and chemotherapy). 151 articles appeared in the results from the search engines. Another step was carried out to exclude the duplicated and review articles. Following the removal of duplicated article and review articles, 91 abstracts were reviewed (abstract

`

review), and only articles that studied ABC transporters in glioblastoma were selected. Full texts were obtained for all 36 selected articles using access from https://universiteparissud.focus.universite-paris-saclay.fr/ and https://insermbiblio.inist.fr/ using personal access. **(Figure 18)** summarizes the methodology used in the reviewing processes.

ABCB1 (MDR1, P-Glycoprotein)

ABCB1 which is also known as MDR1 and P-glycoprotein (P-GP) was identified by Victor Ling in 1976 (Juliano and Ling, 1976) making it the first studied protein among all ABC proteins. ABCB1 protein is a 170 KDa glycoprotein highly expressed in endocrine tissues, liver, gallbladder and brain, and it is usually co-expressed with the ABCG2 protein (Atlas, 2020). The physiological impact of ABCB1 protein was accidentally identified in 1994 by Schinkel et al. (1994), who found that a homozygous knockout of ABCB1 in laboratory mice induced a 100-fold increase in susceptibility to antiparasitic medications (Borst and Schinkel, 2013).

In humans, ABCB1 protein is encoded by the *ABCB1* gene. An update was published in 2011 to illustrate the role of *ABCB1* genetic polymorphisms, which accounts for more than 65 exon related single-nucleotide polymorphisms (SNPs) (Wolf et al., 2011). These SNPs could be responsible for the differences in drug response and toxicity in several types of cancers (Lockhart et al., 2003). In brain, ABCB1 is localized in the luminal membrane of ECs of the BBB (Mahringer and Fricker, 2016). It has an essential role protecting the brain from a possible brain uptake of toxic molecules or metabolic substances with a wide range of known substrates including TMZ (de Gooijer et al., 2018b).

Schaich et al., investigated the role of three different SNPs of ABCB1 in GBM patients treated with TMZ. He showed that the rs1128503 SNP in *MDR1* exon 12 is an independent predictive biomarker of response to TMZ. Patients with GBM exhibiting the homozygous allele (C/C allele) have better survival compared to their heterozygous variant counterparts

`

(Schaich et al., 2009). However, more recently, another large clinical cohort analyzed the clinical impact of four SNPs variants (rs2229109, rs1128503, rs2032582 and rs1045642) in patients with newly diagnosed GBM patients treated with the standard of care. They did not find any clinical value of the SNPs investigated in a large Swedish cohort, hence could not validate the results obtained from Schaich study (Malmstrom and Lysiak, 2019). One pilot clinical trial tried to evaluate ABCB1 protein among glioma patients. They measured the uptake of (^{11}C) N-desmethyl-loperamide ((^{11}C)dLop) using positron emission tomography (PET) imaging as a marker of ABCB1 activity. The clinical study aimed to recruit ten patients, however, only two registered patients are available in the clinical trial database, suggesting that early termination of the trial was due to the lack of patients that fits the inclusion criteria of the study.

Several studies have investigated the role of ABCB1 in the context of TMZ treatment in GBM preclinical models. ABCB1 downregulation was associated with increased efficacy of TMZ in U87 cell lines (Zhang et al., 2015, Munoz et al., 2015b). Two recent studies showed that that downregulation of ABCB1 also increases efficacy of TMZ *in vitro* and *in vivo* in GBM preclinical models (Tso et al., 2015, Zhang and Chen, 2018). Furthermore, an in *vivo* study reported a higher concentration of irinotecan in the brain of *Mdr1a* (-/-) mice *versus* wild-type when both exposed to the same dose of irinotecan (Goldwirt et al., 2014). The antitumor efficacy of TMZ against three intracranial tumor GBM models was significantly enhanced when *Abcb1a/b* and *Abcg2* were genetically deficient or pharmacologically inhibited (de Gooijer et al., 2018b, de Gooijer et al., 2018a). ABCB1 expression can be altered by several compounds including carbonic anhydrase XII (CAXII), Bone morphogenetic protein 7 (BMP7) and TMZ (Riganti et al., 2013, Salaroglio et al., 2018, Tso et al., 2015). Tso *et al* found that BMP7 sensitizes GBM stem cells to clinically relevant doses of TMZ (Tso et al., 2015) while Riganti and Salaroglio have found that GBM exposure to TMZ downregulates the expression of ABCB1 (Riganti et al., 2013). A recent study

`

showed that CAXII could also reduce ABCB1 activity and sensitize GBM cells to TMZ (Salaroglio et al., 2018). **(Table 9)** summarizes the xenobiotic that alters the function of ABCB1, ABCG2 and ABCC1 transporters in GBM.

ABCC1 (MRP1)

The multidrug resistance-associated protein 1 (MRP1) is encoded by the *ABCC1* gene. It was described for the first time by Cole et al. (1992). ABCC1 protein is a 180-190 KDa protein and is ubiquitously expressed in many tissues in humans. It is highly expressed in intestine, kidney and testis, while a lower expression is detected in the lung, colon and brain (Uhlen et al., 2015). ABCC1 protein has a wide range of substrates including anticancer drugs tested in GBM cell lines. *i.e.,* vinca alkaloids (vincristine and vinblastine) and topoisomerase inhibitors (mitoxantrone) (Yin and Zhang, 2011, Peignan et al., 2011). Many genetic alterations were detected in ABCC1 gene, and most of them are SNPs in non-coding sequences and introns. A complete list of all ABCC1 SNPs can be obtained from available public database accessible from the national center for biotechnology information.

In the literature, ABCC1 inhibitors including KIAP –an anti-apoptotic protein– reduce ABCC1 activity and sensitize U251 GBM cell line to TMZ (Liu et al., 2015b). Two in *vitro* studies found that ABCC1 inhibition sensitizes cells to vincristine and etoposide but not to TMZ (Peignan et al., 2011). Furthermore, a study showed that MK571, an inhibitor of ABCC1 and ABCC4, increased the anti-tumor efficacy of vincristine and etoposide in primary GBM cell lines (Tivnan et al., 2015). On the other hand, the overexpression of both ABCB1 and ABCG1 in GBM cell lines (U87 and U251) is associated with resistance to TMZ (Liang et al., 2017).

ABCG2, Breast Cancer Resistance Protein (BCRP)

The ABCG2 protein was the first MRP-associated protein to be discovered. This 72 KDa protein was first identified in 1998 after being cloned from a human breast cancer

`

cell line, which led to its alias, BCRP (Doyle et al., 1998). It is highly expressed in the small intestine, colon, rectum, placenta, and smooth muscles in humans while a lower expression is detected in adrenal and thyroid glands, lung and cerebral cortex (Atlas). In isolated brain microvessels and cortex biopsies from 12 patients with epilepsy or glioma, the expression of ABCG2 protein was 1.6 folds the expression of ABCB1 (Shawahna et al., 2011). ABCG2 protein is a ABC half transporter, therefore it requires the dimerization of two NBDs to function as a drug efflux pump (Mao and Unadkat, 2015). Many SNPs were identified in the *ABCG2* gene. The frequency of SNPs in ABCG2 gene is highly variable among ethnic groups, potentially associated with heterogeneous drug responses among these groups (Hira and Terada, 2018)

In 2017, a study enrolling 50 caucasian GBM patients found a correlation between expression of 8 different proteins (ABCG2, XIAP, MGMT, MSH2, pATM, pTP53, pAKT, Nestin) including ABCG2 and they reported a correlation between ABCG2 and the poor prognosis among GBM patients treated with the TMZ (Emery et al., 2017). To study the role of ABCG2 protein in *vitro*, they used GBM stem cells (GSC) and noticed an enhanced efficacy of TMZ following the inhibition of ABCG2. Therefore, they considered ABCG2 a promising therapeutic target in GBMs (Emery et al., 2017). However, another study reported that ABCG2 knockdown results in the upregulation of other drug transporters (ABCB1 and ABCC3) when treated with TMZ (Chua et al., 2008), suggesting that there might compensate mechanisms between transporters.

Several studies reported the importance of ABCG2 in drug response in GBM. An in *vivo* study reported that ABCG2 knockout in mice is associated with a better overall survival compared to wild-type mice when treated with dasatinib, a Src inhibitor (Agarwal et al., 2012). Another study showed that melatonin enhanced ABCG2 promoter methylation and sensitized GBM cell lines to mitoxantrone, doxorubicin and TMZ (Martin et al., 2013). Consistently with this study, the overexpression of ABCG2 in human GBM cell

`

lines is found to be associated with mitoxantrone resistance (Rao et al., 2005). It was also reported that dual knockout of *ABCB1* and *ABCG2* improves efficacy of TMZ therapy in spontaneous GBM mouse models (Lin et al., 2014). Finally, TMZ exposure, in U87 and T89G cells, was found to increase ABCB1 and ABCG2 mRNA expression. Therefore, exposure to TMZ itself could modulate the levels of ABC proteins and could induce TMZ resistance among patients (Munoz et al., 2014).

Clinical Value

To date, several strategies are developed to overcome the ABC transporters mediated MDR. These strategies are summarized in (**Figure 19**) and they vary from partial/complete inhibition to bypass approaches: (i) nanocarriers technologies, (ii) antibody-drug conjugates -ADC-, and (iii) ultrasound-mediated BBB opening (UMBO).

Using partial or complete inhibitors of ABC transporters can be combined with their substrates to enhance their CNS penetration and anticancer activity. Variety of modulators were tested to suppress activity of efflux proteins mainly (ABCB1 and ABCG2) and few were successful enough to reach clinical trials. In GBM, a limited number of clinical trials were initiated to modulate ABC proteins. To date, these trials failed to show significant clinical benefit, which could be related to a few reasons. Firstly, the study design was not optimal *i.e.*, in the early clinical trials, the patients were not stratified based on high expression of ABC proteins, and a precise evaluation of the role of ABCB1 and ABCG2 transporters in patients could not conducted. Secondly, modulators of ABC proteins could change the pharmacokinetics of other drugs reducing their anti-tumor properties. Thirdly, the dose that was selected to inhibit the ABC protein was not sufficient or a higher dose could not be applied safely in patients.

The selection of cancer cell line is a crucial step in *in vitro* studies dedicated to GBM. Many commercial human cells lines are available for GBM. However, a study from our laboratory has tested ABC proteins expression in GBM patient-derived cell lines (PDCL)

`

and their parental tumors (Drean et al., 2018a). The study showed that PDCLs recapitulated better ABC gene expression pattern of human GBM compared to commercial cell lines and can thus be considered a better model to test the biology of ABC proteins in GBM. In addition, we found that fetal bovine serum that is usually added to cell culture medium for commercial GBM cell lines modulates resistance to TMZ. Recently, a study highlighted the importance of using low passage number PDCL and serum-free medium when studying the role of ABC transporters in *vitro*. The high passaging number of commercial GBM cell lines could change the expression level of ABC protein and could lead to conclusions irrelevant to newly diagnosed human tumor (Tamaki et al., 2011, Drean et al., 2018a, Leonard et al., 2003).

Furthermore, sophisticated strategies using nanocarriers (nanocapsules, liposomes, micelles, dendrimers) for ABC protein substrates were developed to allow these substrates to enter via endocytosis, improving drug half-live and drug protection (Zhao et al., 2020). One clinical study investigated pegylated liposomal doxorubicin's efficacy when administered with TMZ and radiotherapy in newly diagnosed GBM patients. This study showed that the pegylated liposomal doxorubicin form is safe and tolerable however, no meaningful efficacy was observed from either the prolongation of TMZ therapy or the addition of liposomal doxorubicin (NCT00944801) (Beier et al., 2009). Another study evaluated the safety and the pharmacokinetics of a liposomal form of irinotecan, the study confirmed the safety of liposomal form of irinotecan. However, the efficacy still under investigation (Clarke et al., 2015). Therefore, the nanocarrier forms' utilisation could be effective tools in future clinical studies (Zhao et al., 2020).

Another strategy consists in the use of antibody-drug conjugates (ADCs) against a variety of targets in GBM and this approach is currently under investigation (Gan et al., 2017). ADCs are a newly developed biopharmaceutical compounds that allow the targeting of tumour cells while sparing healthy cells. This method is based on the use of

`

an antibody to carry the substrate when binding to its ligand. In 2017, a published clinical trial showed a promising efficacy of depatuxizumab mafodotin (ABT-414), an ADC specific for the activated form of EGFR to selectively deliver a cytotoxic, in *epidermal growth factor receptor* (*EGFR*)-amplified recurrent GBM patients with manageable adverse effects (Reardon et al., 2017). Another clinical trial was designed to evaluate its efficacy in newly diagnosed GBM patients (NCT02573324).

Finally, UMBO was used in pre-clinical models to bypass BBB efflux transporters and increase the brain's penetration of a wide variety of therapeutics. Low-intensity pulsed ultrasound can be delivered to the brain to induce a safe oscillation of intravenously injected microbubbles within blood vessels (Hynynen et al., 2001). Oscillation of these microbubbles opens the BBB by reversibly disrupting the tight junctions between ECs. A range of drugs have been tested for use with UMBO for treating gliomas and include TMZ, carmustine, irinotecan, carboplatin, doxorubicin, and drug-loaded liposomes (Beccaria et al., 2016, Drean et al., 2016). A new study showed that UMBO could decrease the expression of ABCB1 protein in cerebral vessels without affecting the integrity of other proteins (Choi et al., 2019). UMBO has recently moved to clinical trials where its clinical safety was confirmed: Sonocloud-induced UMBO was found to be safe and tolerable among GBM patients (Idbaih et al., 2019). Two other phase 1 and phase 2 clinical trials are currently in progress to evaluate UMBO's efficacy in combination with carboplatin in patients with recurrent GBM (NCT03744026).

Conclusion

GBM is an aggressive primary brain tumour with dismal prognosis. Over the last 15 years, no new drugs were found to be superior to TMZ. The long-term limited efficacy of TMZ is explained, at least partly, by the effect of MDR proteins (ABCB, ABCC1 and ABCG2). Accumulating evidence are rising to connect the effect of chemotherapies and ABC proteins. The clinical role of ABC proteins is still under investigation and the failure of

`

previous clinical trials raised several questions regarding the strategies to overcome MDR in GBM. A few clinical recommendations are currently being reported in the literature regarding future clinical trials. Firstly, all drugs that are going to be used in the trials should be tested against the major ABC proteins (ABCB, ABCC1 and ABCG2). A wide range of in *vitro* and *in vivo* models could allow a precise testing of the novel drugs (Tamaki et al., 2011). Secondly, newly available non-invasive diagnostic imaging approaches *i.e.* PET scanning have the potential to determine whether ABCB1 or other transporters are functioning to reduce drug accumulation and whether inhibition can change drug uptake in solid tumours (Fomichov et al., Bauer et al., 2016). Furthermore, dual ABC inhibitors with a high specificity could be developed. Indeed, for example, the ABCB1 specific inhibitor zosuquidar enhanced sunitinib brain concentration in mice, but not to the same level as the dual inhibitions of ABCB1 and ABCG2 (Oberoi et al., 2013). Following these recommendations could lead to the design of clinical trials that might successfully demonstrate the therapeutic potential of ABC protein inhibition in GBM treatment.

`

Acknowledgments

This work was supported by the European Union's Horizon 2020 research and innovation program under the Marie Skłodowska-Curie grant agreement #766069 (GLIO-TRAIN). We would like to acknowledge the online BioRender platform that provided all the tools and icons to draw the manuscript's graphs.

The research leading to these results has received funding from the program Investissements d'avenir" ANR-10-IAIHU-06. Institut Universitaire de Cancérologie. INCA-DGOS-Inserm_12560 (SiRIC CURAMUS) benefits from support from Institut National du Cancer, ministère des Solidarités et de la Santé and Inserm.

Authors' contributions

MA performed the literature analysis, drawing of the figures, writing of the manuscript and final approval of the final version. AI participated in the original concept of the article, reviewing, and editing of the figures, reviewing the manuscript and final approval of the manuscript. MV and XD participated in reviewing the figures, reviewing the manuscript and final approval of the manuscript.

Conflicts of interest

No potential conflicts of interest were disclosed

AI reports grants and travel funding from Carthera (September 2019), research grants from Transgene, research grants from Sanofi, research grants from Air Liquide, travel funding from Leo Pharma

`

Table 9: Analysis of published studies that show the effects of ABC transporters on chemotherapeutic agents used in GBM.

Effect	ABC Transporter involved	Drug involved	Reference
High dose of cyclosporine[1] doubles the plasma concentration of etoposide among glioma patients	**ABCB1**	Cyclosporine	(Lum et al., 1992)
Nimodipine[2] enhances sensitivity to procarbazine in viability tests in vitro using PDCLs obtained from glioblastoma patients	**ABCB1 and ABCG2**	Nimodipine	(Durmaz et al., 1999)
Paclitaxel in combination with valspodar[3] significantly decreases the tumour volume of U-118 MG tumors compared to the control and paclitaxel groups in mice	**ABCB1**	Valspodar	(Fellner et al., 2002)
Vincristine exposure induces an elevated expression of ABCG1 in rats' brain. This effect could lead to the assumption that ABCB1 is partially responsible for the observed resistance of a relapsing tumours.	**ABCB1**	Vincristine	(Balayssac et al., 2005)
Overexpression of ABCG2 in human GBM cell lines is associated with mitoxantrone resistance.	**ABCG2**	Mitoxantrone	(Rao et al., 2005)
GBM cell lines overexpressing ABCB1 exhibit high resistance to carmustine, carboplatin and etoposide	**ABCB1**	Carmustine, carboplatin and Etoposide	(Nakai et al., 2009)
Elacridar[4] sensitizes GBM cell lines to dasatinib. Homozygous knockout of ABCG2 in mice results in a better overall survival compared to the wild type when treated with dasatininb	**ABCB1 and ABCG2**	Elacridar	(Agarwal et al., 2012)

`

Similar brain-to-plasma concentration was observed for sunitinib in both ABCB1 and ABCG2 knockout mice model and with elacridar treatment in mice. However, mild effect was observed with the zosuquidar[5] and no effect with KO143[6]	**ABCB1 and ABCG2**	Elacridar, KO143 and Zosuquindar	(Oberoi et al., 2013)
Inhibition of ABCB1 and ABCG2 with ABT-888 improves the efficacy of TMZ therapy in GBM patients.	**ABCB1 and ABCG2**	ABT-888	(Lin et al., 2014)
Mdr1-/- mice show a higher concentration of irinotecan compared to mdr1a+/+ mice when both exposed to the same dose of irinotecan.	**ABCB1**	Irinotecan	(Goldwirt et al., 2014)
MRP1 inhibition enhanced Vincristine and Etoposide but not TMZ chemotherapeutic effect however the combined inhibition of MRP1 and P glycoprotein (P-gp) using Reversan[7] increased TMZ response in GBM PDCLs	**ABCC1**	MK571 and Etoposide	(Tivnan et al., 2015)
Inhibition of ABCB1 and ABCG2 with verapamil and KO143 increases the efficacy of TMZ when combined with MGMT inhibitors.	**ABCB1 and ABCG2**	Verapamil and KO143	(Tomaszowski et al., 2015)
Melatonin enhances ABCG2 promoter methylation hence sensitizes GBM cell lines to mitoxantrone, doxorubicin, TMZ	**ABCG2**	Melatonin	(Martin et al., 2013)
Limited drug delivery into brain tumors may significantly limit the efficacy of rucaparib[8] combined with TMZ in GBM	**ABCB1 and ABCG2**	Rucaparib	(Parrish et al., 2015)
AZD2461[9] has a limited brain permeability in *vivo* due to its efflux by ABCB1 protein.	**ABCB1**	AZD2461	(de Gooijer et al., 2018a)
Downregulation of ABCB1 and ABCG2 by Bone morphogenetic protein 7 sanitize the GBM stem cells to the clinically relevant dose of TMZ.	**ABCB1 and ABCG2**	BMP7	(Tso et al., 2015)
ABCE1 downregulation enhance the efficacy of TMZ in GBM cells (U87 and A172).	**ABCE1**	TMZ	(Zhang and Chen, 2018)
ABCG2 knockdown in several GBM cell lines resulted in upregulation of other drug transporters ABCB1 and ABCC3 when treated with TMZ.	**ABCG2**	TMZ.	(Chua et al., 2008)
KIAP -anti apoptotic protein- sensitizes U251 cells to TMZ through reduction of the ABCC1 expression	**ABCC1**	TMZ	(Liu et al., 2015b)

`

The study was not conclusive. Only 7% of the 125 cases studied showed detectable MDR1 expression, suggesting that ABCB1 was not a major contributor to drug resistance in the selected cohort	**ABCB1**	TMZ	(Fruehauf et al., 2006)
Histone-lysine N-methyltransferase (EZH2) enzyme silencing decreases the ABCB1, ABCC1 and ABCG2 mRNA and protein levels, which would lead to reduce efflux pump activity	**ABCC1, ABCB1 and ABCG2**	EZH2	(Fan et al., 2014)
TMZ treatment upregulate the expression of ABCC3 compared to control mice. ABCC3 protect natural killers from TMZ. A GL261 syngeneic mouse model was used in this study.	**ABCC3**	TMZ	(Pessina et al., 2016)
LRIG1, human EGFR inhibitor, reversed MDR in GBM cell lines (U87 and U251) by inhibiting EGFR and secondary ABCB1 and ABCG2	**ABCB1 and ABCG2**	TMZ	(Liu et al., 2015a)
CDK6 knockdown in GBM cell line (U251) resulted in significant downregulation of MDR1, MRP which enhanced the TMZ response	**ABCB1, ABCC1**	TMZ	(Li et al., 2012)
The antitumor efficacy of TMZ against three different intracranial tumor models was significantly enhanced by a homozygous knockout of Abcb1a/b and Abcg2 genes.	**ABCB1 and ABCG2**	TMZ	(de Gooijer et al., 2018b)
The single nucleotide polymorphism (SNPs) in the MDR1 gene exon12 C1236T is an independent predictive factor for prediction of the TMZ treatment in GBM patients.	**ABCB1**	TMZ	(Schaich et al., 2009)
Overexpression of MDR and MRP in GBM cells (U87, U251, U373) is associated with a high resistance to TMZ.	**ABCB1 and ABCC1**	TMZ	(Liang et al., 2017)
Activated EGFR kinase enhanced the ability of GBM cells (U87 and T98G) to resist TMZ through the upregulation of MDR1	**ABCB1**	TMZ	(Munoz et al., 2014)
Loss and gain of function for MDR1 showed an enhanced and reduced efficacy of TMZ in GBM cell lines (U87 and T98G)	**ABCB1**	TMZ	(Munoz et al., 2015b)
Inhibition of ABCG2 enhanced the efficacy of TMZ and is considered a promising therapeutic target in GBMs	**ABCG2**	TMZ	(Emery et al., 2017)
TMZ downregulate the expression of ABCB1 in GBM stem cells	**ABCB1**	TMZ	(Riganti et al., 2013)
MDR1 and ABCG2 is responsible for the resistant of recurrent GBM to TMZ. Following a TMZ exposure in U87 and T89G cells 8 folds expression MDR1 and 4 folds for ABCG2 in the cells compared to naive cells was recorded using real time PCR.	**ABCB1 and ABCG2**	TMZ	(Munoz et al., 2015a)
Multiple inhibition of the MDR1 protein showed no enhanced associated with an enhanced sensitivity of TMZ in GBM cell line (T98G)	**ABCB1, ABCB1**	TMZ	(Peignan et al., 2011)

`

Downregulation of p-glycoprotein enhance the efficacy of TMZ in GBM U87 cell line	**ABCB1**	TMZ	(Zhang et al., 2015)
ABCA13 overexpression is associated with a decreased progression free survival in univariate and multivariate analyses in GBM patients.	**ABCA13**	TMZ	(Drean et al., 2018a)
Carbonic anhydrase XII (CAXII) sensitizes primary GBM cells to TMZ by reduction of ABCB1 protein activity.	**ABCB1**	TMZ	(Salaroglio et al., 2018)

[1] Immunosuppressant medication with ABCB1 blocking activity
[2] Calcium channel blockers with ABCB1 blocking activity
[3] An experimental cancer drug with ABCB1 inhibition properties. It is a derivative of cyclosporine.
[4] An experimental small molecule that has a dual ABCB1 and ABCG2 inhibition
[5] A potent ABCB1 inhibitor, has reached clinical trials.
[6] Experimental drugs with ABCG2 inhibition activity.
[7] It is an experimental drug with ABCC1 and ABCB1 inhibition.
[8,9] Poly (ADP ribose) polymerase (PARP) inhibitors

`

Table 10: Identified subfamilies of ABC transporters and their physiological functions.

ABC Subfamily	ABC proteins	Physiological functions	Reference
ABCA	**12**	• Lipid and cholesterol transport, ABCA2 is involved in drug resistance	(Vasiliou et al., 2009)
ABCB	**11**	• Elimination of toxins • Inhibition of apoptosis • Volume dependent Cl^- channel regulator • Phospholipid translocation (can translocate short-chain phospholipids) • Maintenance of plasma membrane cholesterol esterification • Drug resistance	(Johnstone et al., 2000, Vasiliou et al., 2009)
ABCC	**13**	• Anion efflux. • Drug resistance • Nucleoside transport	(Vasiliou et al., 2009)
ABCD	**4**	• Mainly expressed in peroxisomes. • ABCD2 fatty acid transport and a major modifier locus for clinical diversity in X-linked ALD	(Vasiliou et al., 2009)
ABCE/ABCF	**1 ABCE** **3 ABCF**	• Along with ABCE1, ABCF members have ATP-binding domains, but no transmembrane domains, making transporter function unlikely • Mainly regulate protein synthesis or expression	(Vasiliou et al., 2009)
ABCG	**5**	• Transport of diverse drug substrates, sterols, and lipids • ABCG4 is expressed in macrophages • Drug resistance	(Vasiliou et al., 2009)

`

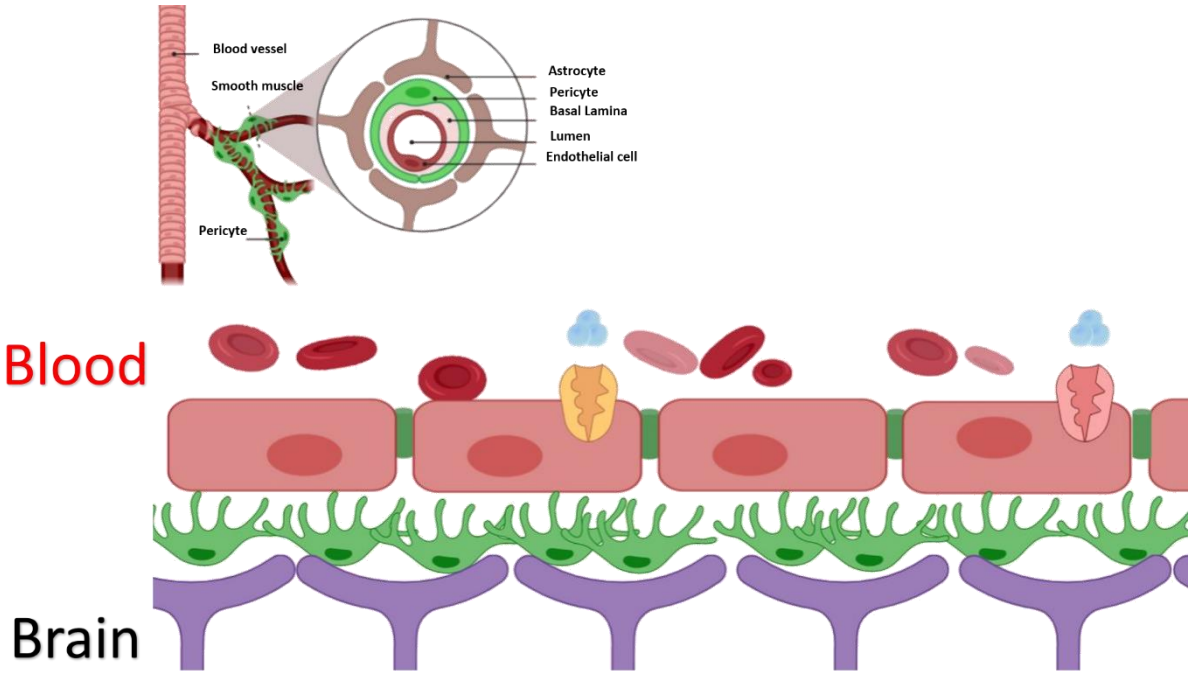

Figure 15: The blood-brain barrier (BBB) is formed of different types of cells tightly knit together. Highly specialized endothelial cells (ECs) surround blood vessels and form part of the BBB. In addition to brain ECs various cells contribute to the structure of BBB. Pericytes (represented in green) are attached to endothelium cells via gap junctions whilst astrocytes end feet (represented in purple) surround endothelial cells of the BBB, providing structural and functional support to these cells. Five mechanisms are known to regulate the entry of molecules to the brain. The efflux pumps pathway is considered a mechanism of active transport through the BBB (Drean et al., 2016).

`

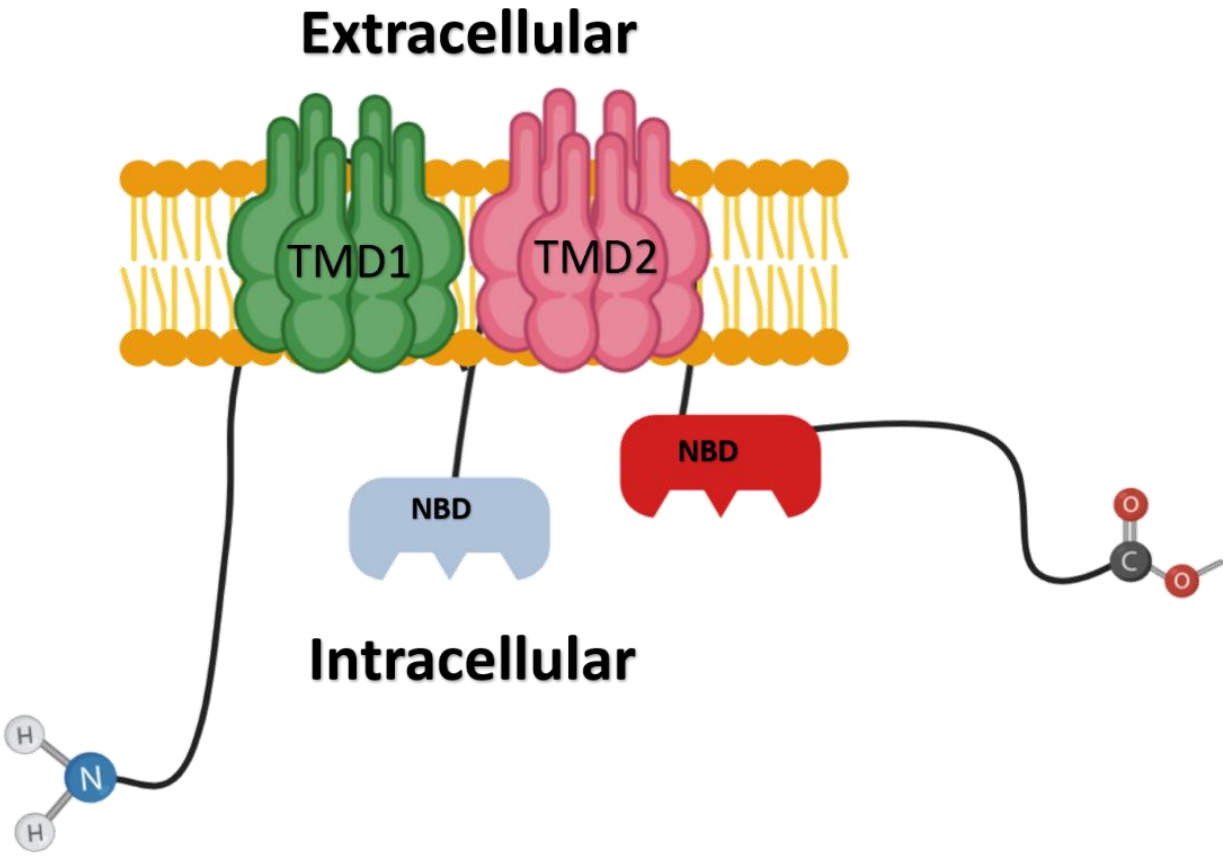

Figure 16: A full ABC transporter consists of four building units. The first two building units called TMDs are formed by six transmembrane segments. TMD1 and TMD2 are colored in green and pale red, respectively. The two other building units are called NBDs, NBD1 (pale blue) and NBD2 (red). ABC half transporters have only one TMD and one NBD and need to dimerize to become a functional protein. Additionally, some other ABC transporters have an additional TMD unit that is conjugated to the N-terminus of the protein and called "Long" ABC transporter (Deeley et al., 2006).

`

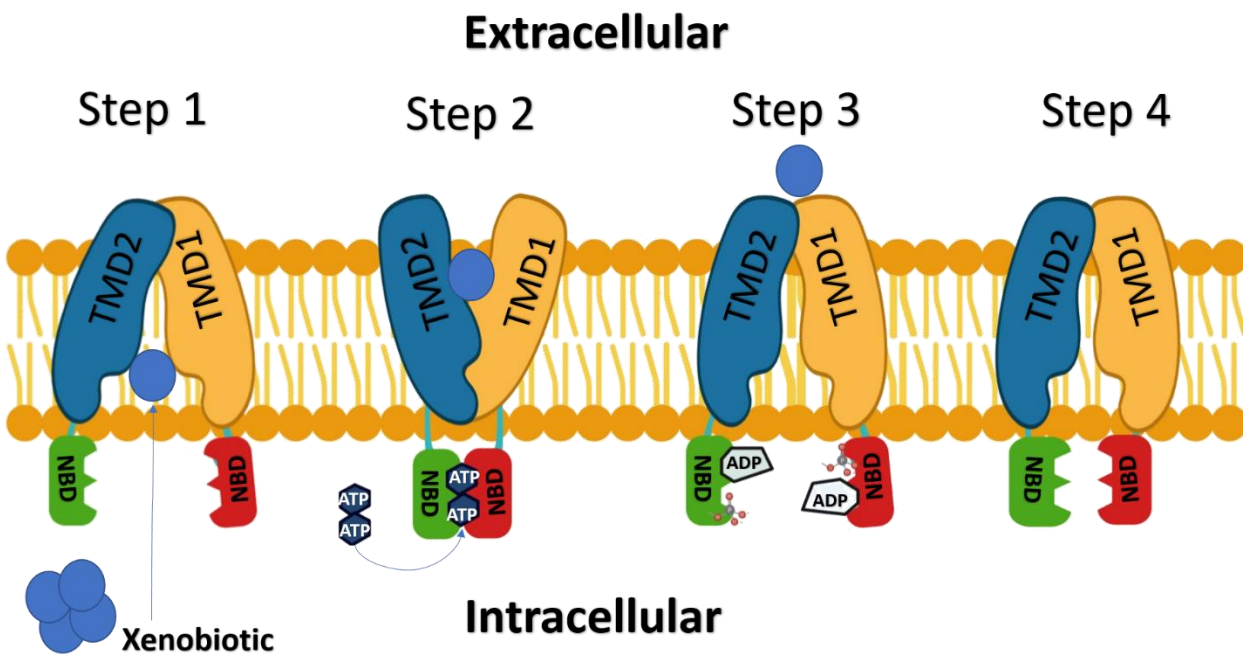

Figure 17: ABC transporters are transmembrane proteins capable of actively transporting a xenobiotic from the intracellular to the extracellular compartments. This active transport requires the hydrolysis of ATP to provide the energy necessary for the transport. The active transport cycle starts with the binding of the xenobiotic to a high-affinity structure formed by the TMDs (step 1). As a result, a conformational change makes the NBD units more exposed for ATP binding. The NBD dimer induces a major conformational change on the TMDs allowing the xenobiotic to be translocated (step 2). The hydrolysis of ATP allows the NBD dimers to be dissociated and again induces a TMDs conformational change (step 3). A final step of restoration of the open NBD-dimer conformation then takes place (step 4) (Linton and Higgins, 2007, Zolnerciks et al., 2011).

`

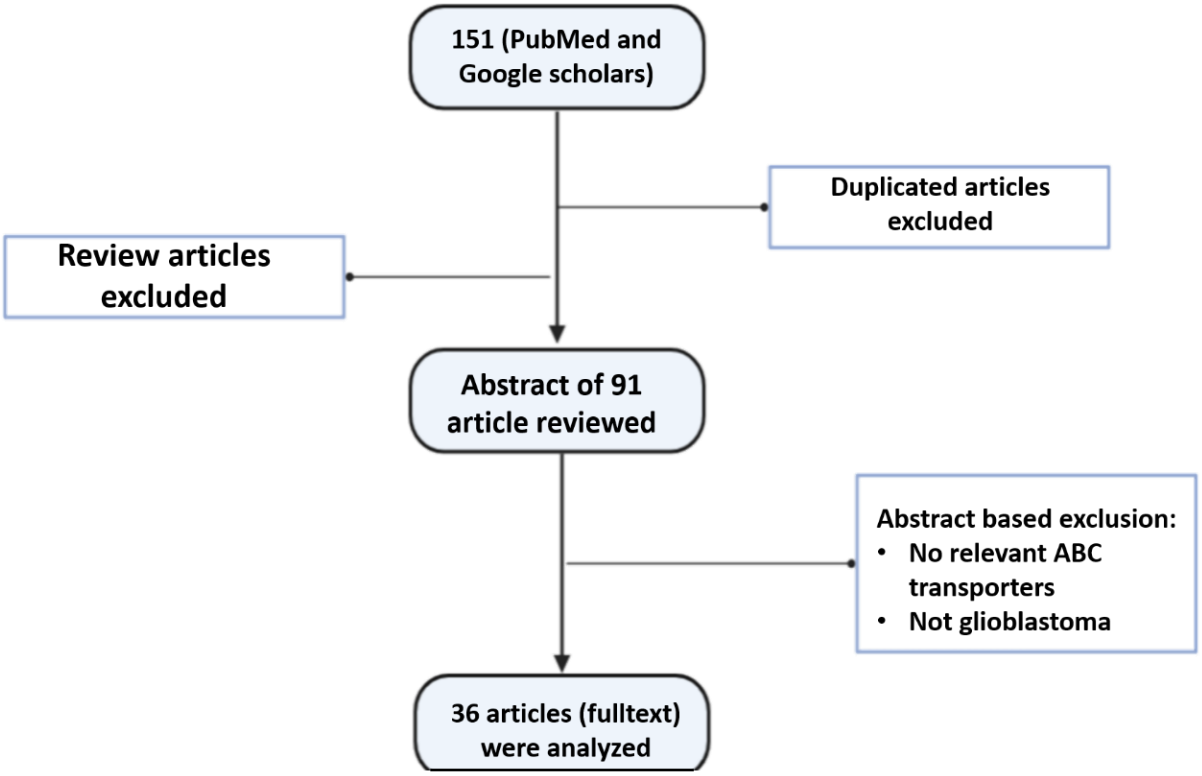

Figure 18 Represents the methodology of this literature review. The key words (ABC transporters, glioblastoma, TMZ, and chemotherapy) were used in PubMed and Google scholar search engines. 151 articles appeared in the results, then a few steps were carried out to exclude the duplicated and review articles. 91 abstracts were then reviewed and from the abstract, only articles that studied ABC transporters or GBM were selected. Full texts were obtained for all 36 selected articles.

`

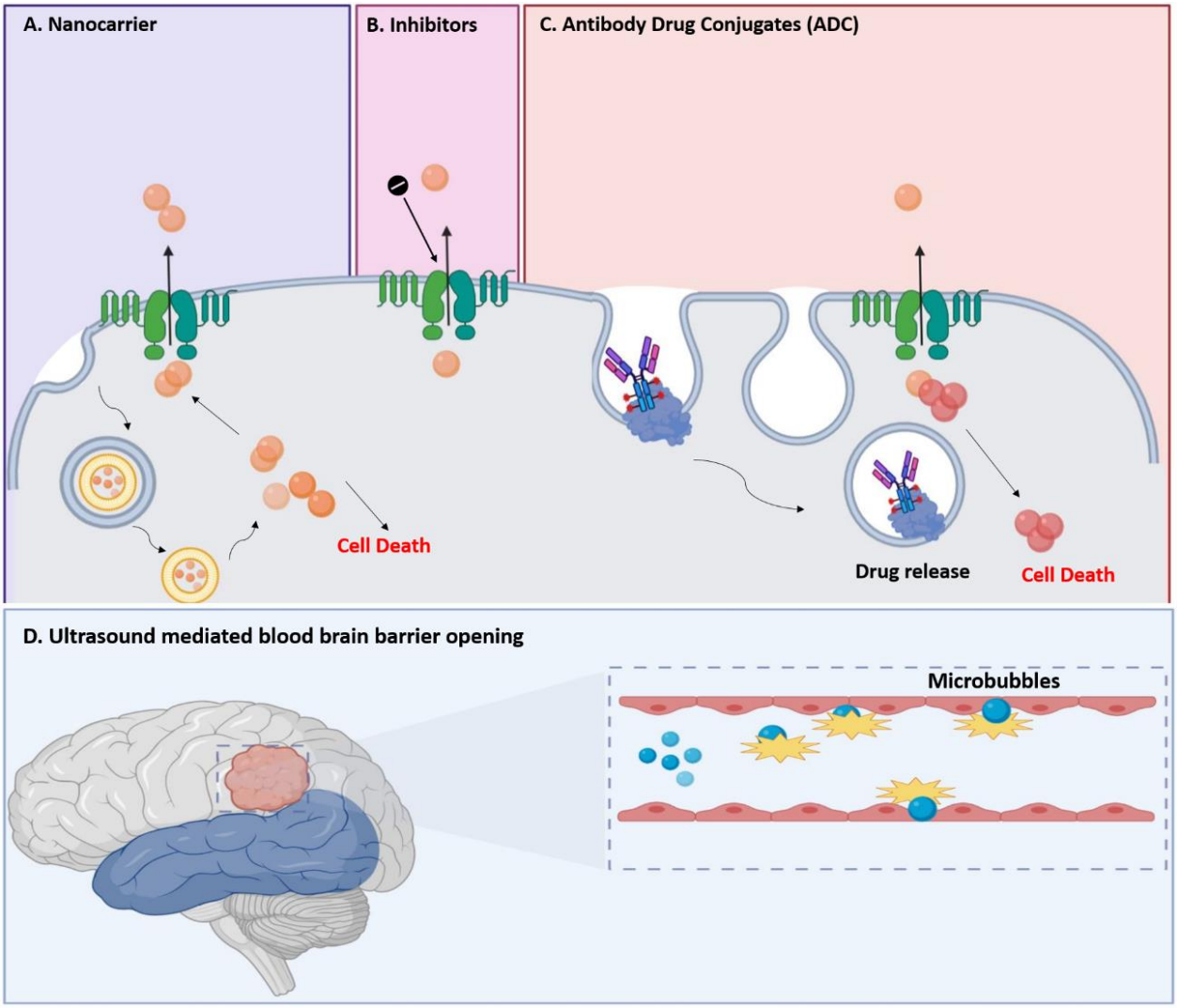

Figure 19: Summary of methods that are being developed to overcome ABC transporters. Panel A: represent the development of nanocarriers that allow the drug to enter via endocytosis. Panel B shows another method by using a partial or complete antagonist that can be administered in combination with the efflux pumps substrates and as a result enhance the activity of the substrates. Panel C shows the antibody drug conjugates approach that relies on an antibody to carry the substrates when binding to its ligand. Panel D represents the combined effect of using microbubbles and low intensity ultrasound to open the BBB. These four methods have been used in vitro and in vivo to develop strategies to overcome ABC efflux pumps (Li et al., 2016).

`

CD80 and CD86: expression and prognostic value in newly diagnosed glioblastoma

Mohammed Ahmed[1,2], Isaias Hernández-Verdin[1,2], Franck Bielle[3], Maite Verreault[1], Julie Lerond[1], Agusti Alentorn[4], Marc Sanson[4], Ahmed Idbaih[4]

[1]Sorbonne Université, Institut du Cerveau - Paris Brain Institute - ICM, Inserm, CNRS, APHP, Hôpital de la Pitié Salpêtrière, Paris, France

[2]Faculté de Médecine Paris-Sud - Université Paris-Saclay, 91190, Saint-Aubin, France.

[3]Sorbonne Université, Inserm, CNRS, UMR S 1127, Institut du Cerveau, ICM, AP-HP, Hôpitaux Universitaires La Pitié Salpêtrière - Charles Foix, Service de Neuropathologie-Escourolle, Paris France

[4]Sorbonne Université, Institut du Cerveau - Paris Brain Institute - ICM, Inserm, CNRS, AP-HP, Hôpital de la Pitié Salpêtrière, DMU Neurosciences, Service de Neurologie 2-Mazarin, F-75013, Paris, France

Corresponding author

Ahmed Idbaih. Sorbonne Université, Institut du Cerveau - Paris Brain Institute - ICM, Inserm, CNRS, AP-HP, Hôpital de la Pitié Salpêtrière, DMU Neurosciences, Service de Neurologie 2-Mazarin, F-75013, Paris, France. Tel: 01-42-16-03-85. Fax: 01-42-16-04-18. Email: ahmed.idbaih@aphp.fr

`

Abstract

Purpose: Strategies to modulate the tumor microenvironment's (TME) including the vascular and immune components, has opened new therapeutic avenues with dramatic yet heterogeneous intertumor efficacy in multiple cancers, including brain malignancies. Therefore, investigating molecular actors of TME may help understand the interactions between tumor cells and TME cells. Immune checkpoint proteins such as a Cluster of Differentiation 80 (CD80) and CD86 are expressed on the surface of tumor cells and infiltrative tumor lymphocytes. However, their expression and prognostic value in glioblastoma (GBM) is still unclear. **Methods**: In this study, we have investigated, in a retrospective local discovery cohort and a validation TCGA dataset, expression of CD80 and CD86 at mRNA level and their prognostic significance in response to standard of care. CD80 and CD86 at the protein level were also investigated in the discovery cohort. **Results**. Both CD80 and CD86 are expressed heterogeneously in GBM at mRNA and protein levels. In a univariate analysis, the mRNA expression of CD80 and CD86 was not correlated with overall survival in both local and TCGA datasets. On the other hand, CD80 and CD86 mRNA high expression was significantly associated with shorter progression free survival (PFS; $p<0.05$). These findings were validated using the TCGA cohort; higher CD80 and CD86 expressions were correlated with shorter PFS ($p<0.05$). In multivariate analysis, CD80 mRNA expression did not provide additional prognostic information to *MGMT* promoter methylation in the local cohort. Interestingly, multivariate analysis of CD86 mRNA expression was an independent prognostic factor for PFS in the TCGA dataset only ($p<0.05$). **Conclusion**: Additional studies are warranted to validate our findings and to explore the expression of CD80 and CD86 in GBM patients treated with immunotherapy and, more specifically, with CTLA-4 inhibitors.

Keywords: Glioblastoma, immune system, microenvironment, immune checkpoint proteins

`

Introduction

Glioblastoma (GBM) is the most common and aggressive glioma in adults. The latest World Health Organization (WHO) guideline classifies GBM as grade IV glioma (Louis et al., 2016). Over the last years, massive efforts have led to a better understanding of the pathology and the genetic of GBM (deSouza et al., 2016). To date, the most effective and approved standard therapeutic regimen is maximum surgical resection of the tumor followed by concurrent chemoradiation and adjuvant chemotherapy with temozolomide (Louis et al., 2016). Despite this very intensive therapeutic regimen, newly diagnosed GBM patients have a dismal outcome with a median overall survival (OS) below 18 months (Marenco-Hillembrand et al., 2020). The main known prognostic factors are: (i) age, (ii) Karnofsky performance status -KPS-, (iii) *MGMT* promoter methylation status, and (iv) *IDH* mutational status (Stupp et al., 2005).

Immunotherapies have dramatically improved the prognosis of melanoma (Leven et al., 2019) and other non-neurological solid tumors (Leven et al., 2019). In the setting of primary brain cancer, results from clinical trials are still disappointing (Muftuoglu and Liau, 2020). Nonetheless, specific GBM patients responded, supporting the identification of biomarkers to stratify patients in the prescription of immunotherapies. Immune checkpoint proteins such as Cluster of differentiation 80 (CD80; known as B7-1) and CD86 (known as B7-2) are expressed on the surface of tumor cells (Ville et al., 2015). Furthermore, CD80 protein expression was observed in infiltrative tumor lymphocytes in melanoma (Hersey et al., 1994). Cytotoxic T-lymphocyte-associated antigen–4 (CTLA-4) and CD28 are located on T-lymphocytes. Both CD28 and CTLA-4 proteins bind to their ligands on the antigen presenting cells and major histocompatibility complex (MHC) (Wei et al., 2018). CTLA-4 has a higher affinity to CD80 and CD86, and when bound to its ligands, T-lymphocytes remain inactive and exhausted (Rowshanravan et al., 2018).

`

Antibodies targeting CTLA-4 were used in both preclinical studies in multiple solid tumors, resulting in many ongoing clinical trials (Letendre et al., 2017). Ipilimumab (anti-CTLA-4) has also shown responses in patients with brain metastases, highlighting efficacy within the central nervous system (Savoia et al., 2016). Expression of the most extensively studied immune checkpoint protein, programmed death-ligand (PD-L1), was inversely correlated with OS in GBM patients (Nduom et al., 2016). However, the expression of CD80 and CD86 in GBM tissues and their prognostic significance have not been reported yet. This study investigated the mRNA and protein expression of CD80 and CD86 in newly diagnosed GBM patients, aged below 70 and with KPS above 70 treated with the standard of care. In addition, we have investigated possible correlations with prognosis.

`

Materials and methods

Patient samples

OncoNeuroTek (ONT) is a local brain tumor tissue bank collecting samples from patients operated at the University Hospital La Pitié-Salpêtrière. All samples were collected with informed consent from patients. The inclusion criteria of the discovery local cohort (47 patients) were as follow: (i) newly diagnosed and histologically verified GBM, (ii) age at diagnosis is below 70 years, (iii) KPS above 70%, (v) known *MGMT* promoter methylation status, (vi) known IDH status, (vii) treated with the standard first-line therapeutic regimen including chemoradiation and adjuvant temozolomide and, (viii) a documented clinical follow-up. The validation cohort (121 patients, the cancer genome atlas, TCGA cohort) clinical information and RNA-seq data (read counts) were downloaded from the National Cancer Institute's Genomic Data commons (GDC) Data portal and from the NCBI GEO GSE62944, respectively.

IHC staining

Paraffin-embedded tissue blocks (5–7 µm) from biopsies of newly diagnosed GBM patients were received from the ONT biobank. Tissue sections were deparaffinized using xylene and rehydrated. For antigen retrieval, each slide was embedded in citrate buffer at pH 4.0 and heated for 15 min in the microwave at 800w. 10% goat serum with 5% fetal bovine serum in 0.2% triton phosphate buffer saline was used as a blocking buffer. 3% hydrogen peroxide was used to block tissue peroxidation. Anti-human CD80 antibody (A16039; Abclonal) and anti-human CD86 antibody (A2353; Abclonal) were used at 1:500 dilution in blocking solution and incubated on the tissue slides overnight at room temperature. Avidin-Biotin Complex (ABC) kit was used as a signal enhancer before the incubation in DAB (3,3′-Diaminobenzidine). Slides were embedded in hematoxylin dye and rinsed with tap water for nuclear staining; gradual alcohol and xylene baths were used for

`

dehydration and mounted with a hydrophobic mounting medium (Eukitt). All stained tissues were scanned via ZEISS Axio Scan 40x for bright field imaging.

Quantification of IHC staining

Following all slides' imaging, three regions of interest with known dimensions (528*528 µm) were randomly selected for each tissue section and quantified using an in-house quantification Fiji code. Shortly, each image was imported to the Fiji program (Schindelin et al., 2012). Using the color deconvolution tool, the area positive for DAB staining was isolated and quantified using a semi-automated in-house generated code. The percentage of DAB positive areaswas calculated, and the mean value from the three images was calculated and used in the survival analysis.

Quantitative Reverse Transcriptase Polymerase Chain Reaction (RT PCR)

RNA samples were obtained from ONT bank and used to synthesize cDNA. Reverse transcription of RNA samples was performed using the Maxima First Strand cDNA Synthesis Kit (Thermo Scientific, K1442) according to the manufacturer's recommendations with 100-250 ng of RNA. qPCR was used to quantify the expression levels of CD80 and CD86 in patients. PPIA gene was used as a house keeping reference gene for normalization. Primer's sequences are listed in **(Figure 25)**. cDNA samples were analyzed using the Light Cycler Probe Master mix 2× (Roche, 04887301001) and the UPL detection system (Roche, 04483433001) in a Light Cycler 96 (Roche). For each qPCR, two independent experiments were completed with duplicate samples in each experiment. The mean of $2^{-(CT^{gene\ of\ interest}-CT^{PPIA})}$ from the two different experiments was used in all analyses.

Statistical analysis

A Violin plot was used to visualize our data's full distribution (GraphPad Prism). Spearman correlation between the expression values (RNA or protein) and age was evaluated to discard age bias. Survival analysis was performed by finding a supervised cut-off value for the CD80 expression or the CD86 expression independently using the

`

`survminer::surv_cutpoint` function, which determines the cut point based on the highest/lowest value of the log-rank statistics (low or high expression values). Then these categories were used for Kaplan-Meier analysis or Cox proportional hazard regression modeling testing for each variable independently or to adjust for multiple variables including CD80/CD86 expressions and *MGMT* promoter methylation status. P-values lower than 0.05 were considered significant (Greenbaum et al., 2003, van Nieuwenhuijze and Liston, 2015)

`

Results

Patients and tumors characteristics

Forty-seven patients with a confirmed GBM diagnosis fulfilled the inclusion criteria: 14 men and 33 women (sex ratio m/w = 0.42). The patients' median age at diagnosis was 55.9 years (range: 24.3-69.5 years). KPS was 70 and above in all patients. The median OS is 559 days (range 31 – 2539) and the median PFS is 266 days (range 26-1355). The IDH status was evaluated as mutant for two patients (4.3%) while wildtype for 45 (95.7%). Furthermore, *MGMT* promoter was methylated in 16 patients (34%) and unmethylated in 31 (66%). All patients received the standard of care first-line treatment regimen.

CD80 and CD86 expression at mRNA and protein level

At the mRNA level, CD86 expression was quantitatively higher than CD80 expression **(Figure 20-A).** In agreement with mRNA expression, IHC analysis showed that the expression of CD86 is higher than CD80 in our discovery cohort **(Figure 20-B).** Based on the IHC staining, CD80 and CD86 are observed in the cell membrane and/or cytoplasm (**Figure 21**). Following protein quantification, we observed a positive correlation between mRNA and protein expression of CD86 (spearman coefficient of correlation Rho=0.28; p=0.08; **Figure 22-A**). However, we observed a weaker correlation between mRNA and protein expression for CD80 (p=0.108; Rho= 0.25; **Figure 22-B**).

Prognostic value of CD80 and CD86 expression

Our patient's cohort was used as a discovery cohort (ONT cohort), while the TCGA dataset was used as a validation cohort. In a univariate analysis, mRNA expression of CD80 and CD86 was not correlated with OS in both ONT cohort and TCGA dataset **(Table 11)**. On the other hand, CD80 and CD86 mRNA high expression was significantly associated with shorter PFS (p=0.04 and p=0.005, respectively; **Figure 23, A, B**). Next, these findings were validated using TCGA cohort; higher CD80 and CD86 expressions were correlated with shorter PFS (p-value=0.04 and p=0.002 respectively; **Figure 23, C and D**). Interestingly, higher CD86 protein expression was associated with shorter PFS in the ONT

`

cohort ($p<0.005$; **Table 12**). CD80 and CD86 protein expressions were not available in the TCGA dataset for validation purpose.

As expected, *MGMT* promoter methylation was associated with longer PFS and longer OS in ONT cohort ($p<0.05$ and $p<0.05$ respectively) and TCGA dataset ($p<0.05$ and $p<0.05$ respectively) (**Table 11** and **Table 12**). Furthermore, *IDH* mutations were also associated with better OS and PFS in the TCGA database ($p<0.05$ and $p<0.05$ respectively); however, in ONT cohort, the limited number of IDH-mutant GBM did not allow a robust analysis ($n=2$). In multivariate analysis, CD80 mRNA expression did not provide additional prognostic information to *MGMT* promoter methylation in ONT cohort. On the other hand, multivariate analysis of CD86 mRNA expression was an independent prognostic factor for PFS in the TCGA dataset only ($p<0.05$; **Figure 24**). We have observed a similar trend ($p=0.27$; **Figure 24**) in the ONT cohort, yet the trend was not significant, which could be related to the lower patient numbers ($n=47$) in the ONT cohort compared to ($n=121$) in TCGA dataset.

`

Discussion

CD80 and CD86 molecules play an essential role in influencing the immune recognition of GBM cells. They bind to the CD28 molecule with a costimulatory signal for T-lymphocytes activation. On the other hand, they bind to CTLA-4, resulting in an immunosuppressive effect. CTLA-4 has a higher affinity to CD80 and CD86, making these molecules' role in immunosuppressive effect higher than their stimulatory effect (van Nieuwenhuijze and Liston, 2015). The current study has linked CD80 and CD86 expression on GBM tumor microenvironment to PFS.

We observed a low correlation between mRNA and protein expression of CD80. However, a better correlation was observed between CD86 protein and mRNA expression. Low correlation between the mRNA and protein expression might be due to post-transcriptional mechanisms involved in turning mRNA into protein. Another reason could be related to the stability of both mRNA and protein in our patient's samples. Finally, there is a possible error and noise in protein quantification and mRNA extraction that could influence mRNA stability and protein expression (Greenbaum et al., 2003).

The number of patients (n=47) in ONT cohort is lower than the number of patients in the TCGA dataset (n=121). The higher number of TCGA GBM samples could be one reason that affected the statistical analysis and provided a better prognostic value in the TCGA dataset compared to the ONT cohort. Indeed, the availability of GBM samples with comprehensive clinical and biological annotations and fulfilling the inclusion criteria is a limitation for ONT cohort. Larger patient cohort is needed to evaluate the prognostic value of CD80 and CD86 expression in GBM samples. In our protein analysis, co-staining of CD80 and CD86 is needed to determine these proteins' expression in different immune cell populations. Furthermore, other immune checkpoint proteins could be evaluated in future studies.

`

The expression of 50 immune checkpoint molecules was investigated in breast cancer. The study showed that high expression of co-stimulatory immune checkpoint molecules was associated with better PFS. However, no significant effect on prognosis was associated with CD80 and CD86 expression in the selected cohort (Fang et al., 2020). Feng et al. reported that low expression of CD80 is a predictive biomarker for poor prognosis in adenocarcinoma (Feng et al., 2019). Furthermore, CD80 and CD86 were found to be potential biomarkers for better prognosis survival in nasopharyngeal carcinoma. (Chang et al., 2007). Additionally, the molecular characterization of PD-L1 expression was correlated with other checkpoint proteins, *i.e.*, CD80, highlighting that higher level of immunosuppression are associated with GBM compared to lower grade gliomas (LGG) (Wang et al., 2016). In myeloma cell lines, silencing the CD28-CD86 pathway resulted in significant cell death of myeloma cells (Gavile et al., 2017). A recent study constructed a more robust model, using GBM and LGG data from the TCGA and CGGA (Chinese glioma genomic atlas), and identified that low expression of CD86 molecules is a good prognostic indicator for OS. PFS analysis were not applied in this study (Qiu et al., 2020).

In 2017, Berghoff et al. described a specific signature to predict the success of TMZ in *MGMT*-methylated patients. They showed that the TME signature could be used to indicate an individual's TMZ sensitivity. The TME was identified to be different between IDH-mutant and IDH-wildtype tumors. A richer tumor infiltrative lymphocyte (TIL) and a higher expression of PD-L1 were observed in IDH-wildtype tumors (Berghoff et al., 2017). However, to date, no studies have linked *MGMT* promoter methylation status with the TME. A recent research article has studied the expression of immune checkpoint inhibitor Tim3 and *MGMT* promoter methylation status. They identified that a high expression of Tim3 in *MGMT*-unmethylated patients is linked to poor prognosis (Zhang et al., 2020b). Pratt et al. have reported that the expression of PD-L1 is a negative prognostic biomarker in recurrent IDH-wildtype GBM (Pratt et al., 2019). In line with these findings, our study

`

supports that the expression of immune checkpoint inhibitors may inhibit T-lymphocytes and anti-tumor reaction.

CD86 expression could be used as potential biomarkers predicting the efficacy of ipilimumab in GBM patients. Furthermore, it could be used as a biomarker for patients' stratification for future clinical trials. Our study suffers from limitation of retrospective studies with limited number of patients. Nonetheless, our results were validated in an independent dataset and support investigations of immune checkpoint molecules as potential prognostic biomarkers and potential predictive biomarkers of response to immunotherapies in GBM.

`

Acknowledgments

This work was supported by the European Union's Horizon 2020 research and innovation program under the Marie Skłodowska-Curie grant agreement #766069 (GLIO-TRAIN). The research leading to these results has received funding from the program Investissements d'avenir" ANR-10-IAIHU-06. Institut Universitaire de Cancérologie. INCA-DGOS-Inserm_12560 (SiRIC CURAMUS) benefits from support from Institut National du Cancer, ministère des Solidarités et de la Santé and Inserm. OncoNeuroTek biobank

Conflicts of interest

No potential conflicts of interest were disclosed.

Author's contribution

MA, MV designed the primers, obtained the tissues. MA performed the experiments. MA, AI designed the experiments, wrote the manuscript, and approved the final version of the manuscript. IHV performed the statistical analysis and revised the manuscript. All authors reviewed the manuscript.

`

Tables, figures, and legends to figures

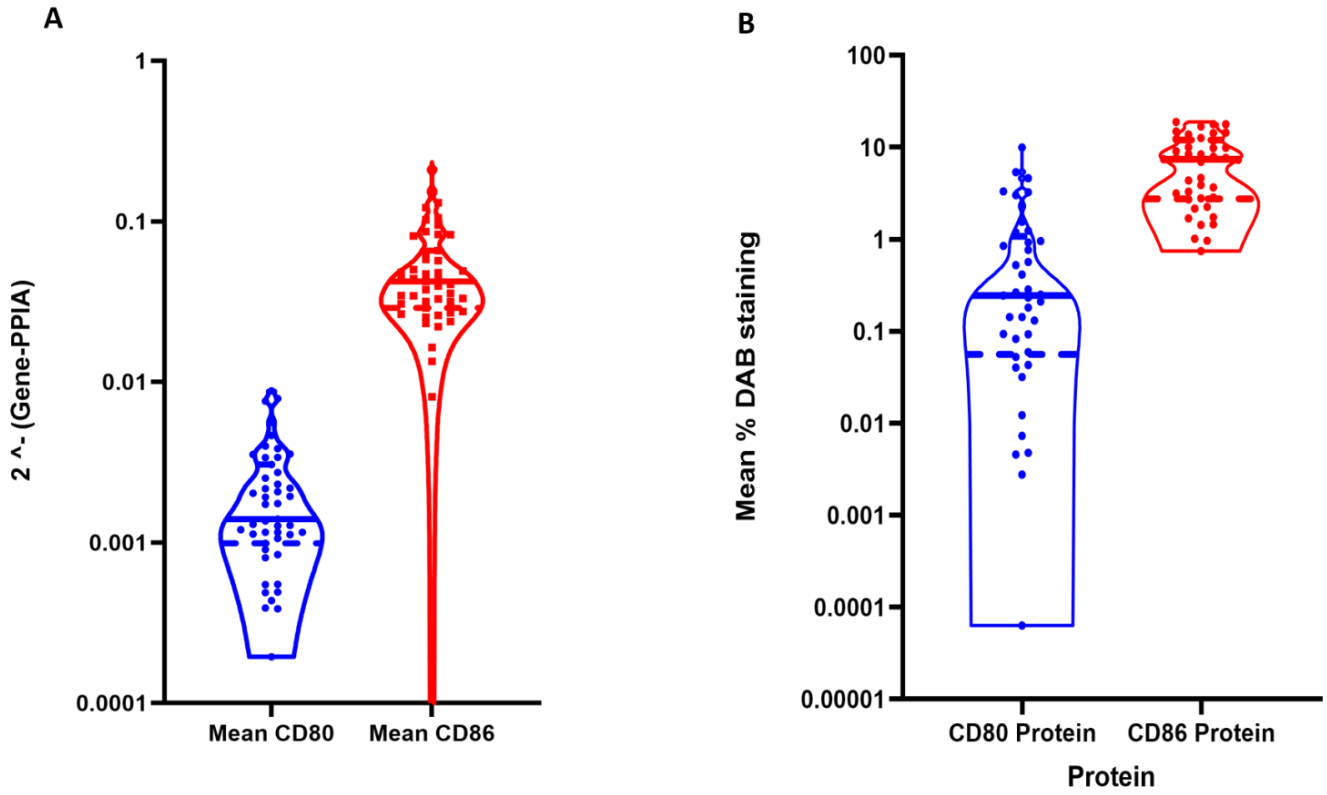

Figure 20: Panel A Violin plot to visualize the data distribution of CD80 and CD86 mRNA expression in ONT cohort Panel B shows CD80 and CD86 protein expression in ONT cohort.

`

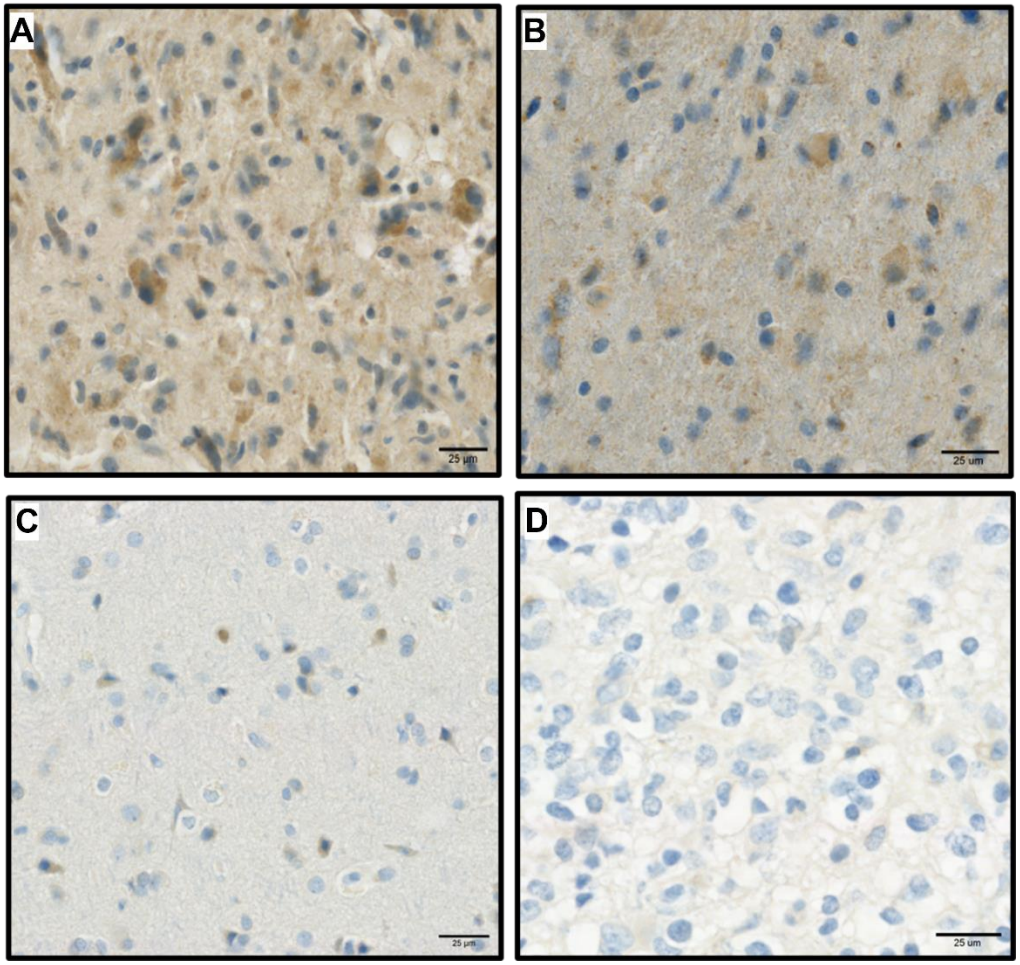

Figure 21: Represent the expression of CD86 and CD80 proteins in paraffin sectioned GBM samples. Panel A: high expression of CD86. Panel B: low expression of CD86. Panel C: High expression of CD80. Panel D: low expression of CD80.

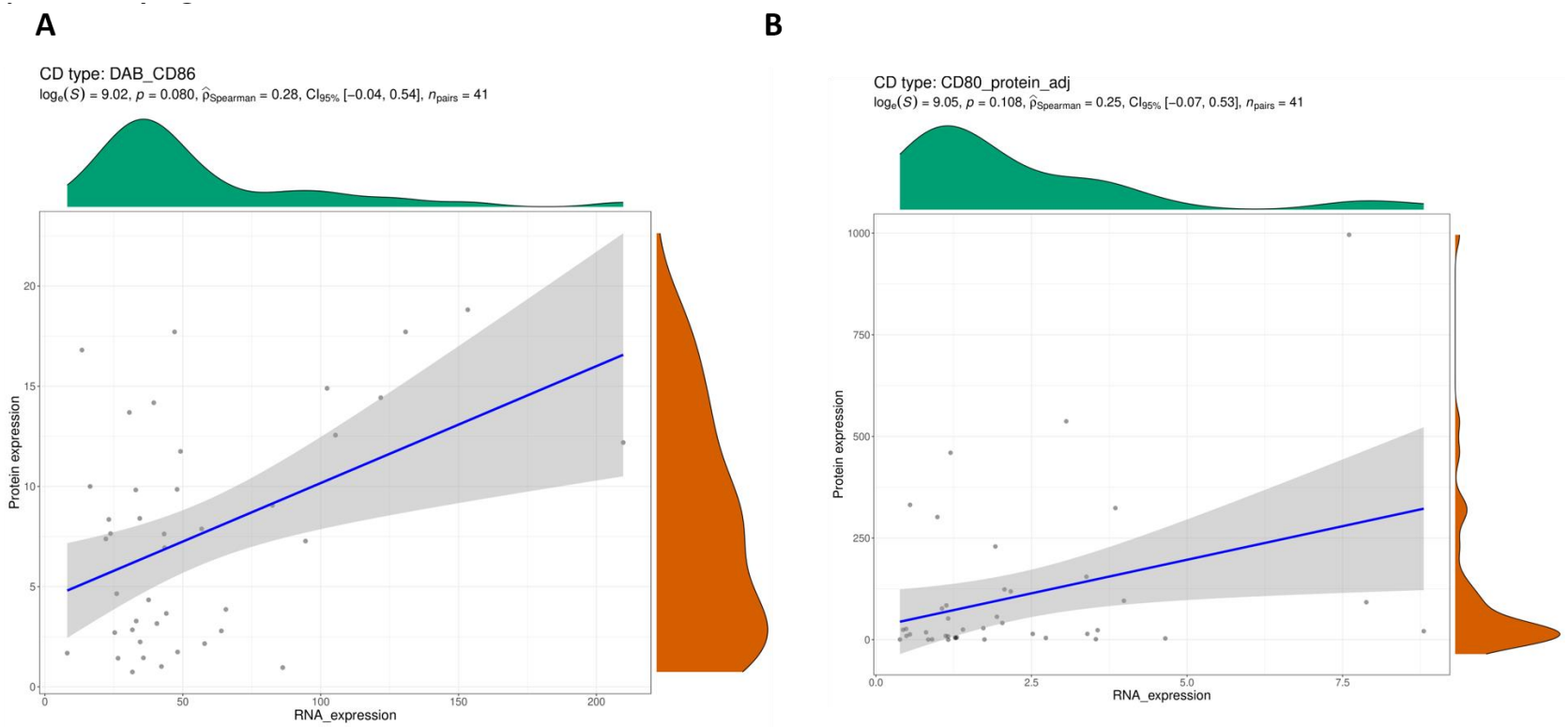

Figure 22: Panel A-B Spearman correlations between the mRNA expression and protein expression in CD86 (Panel A) and CD80 (Panel B). X-axis indicated mRNA expression values while Y-axis indicates protein expression value as percentage of positive IHC signals (CD86 in Panel A and CD80 in Panel B).

`

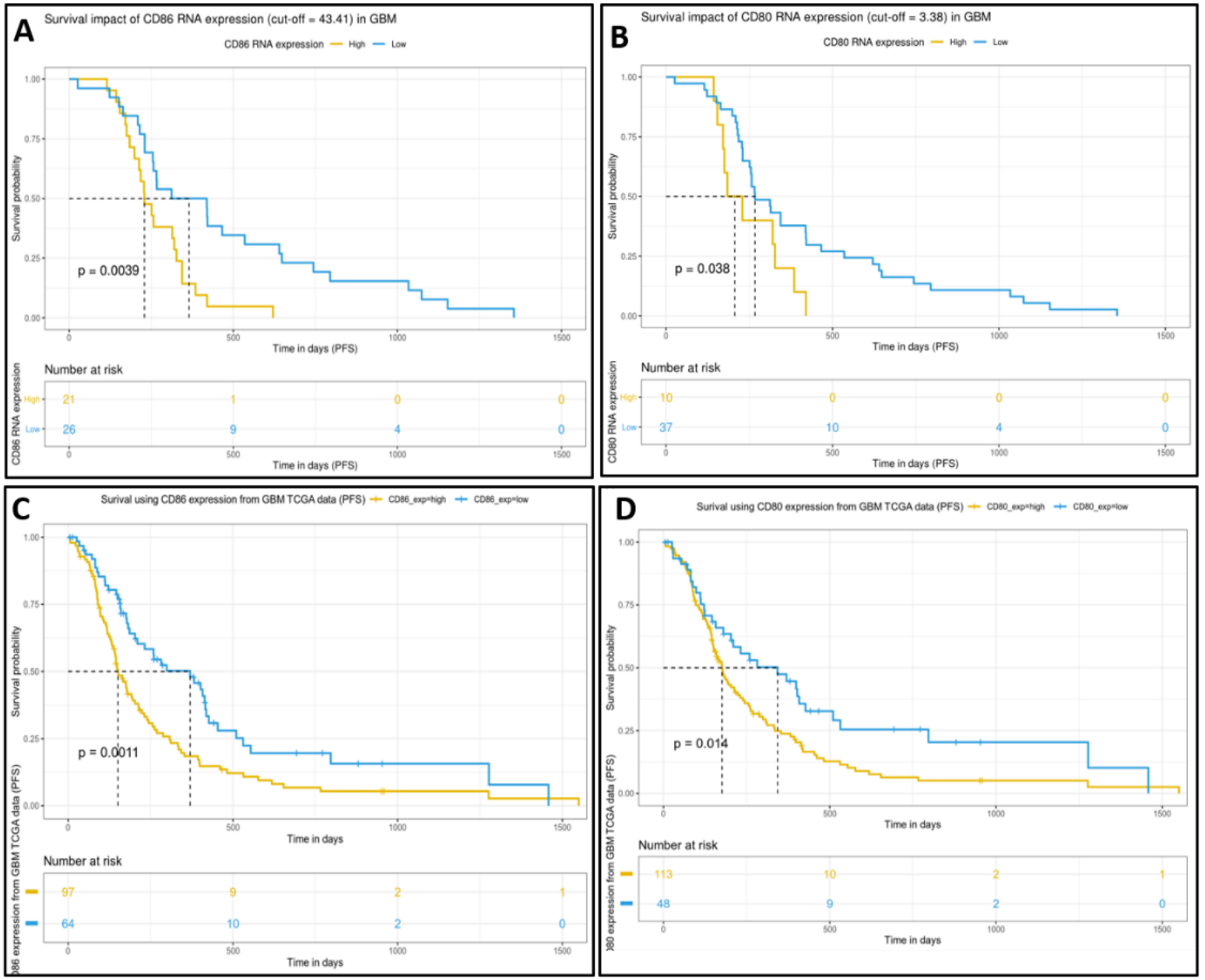
A
Survival impact of CD86 RNA expression (cut-off = 43.41) in GBM
CD86 RNA expression High Low
Survival probability
p = 0.0039
Time in days (PFS)
Number at risk
CD86 RNA expression
High 21 1 0 0
Low 26 9 4 0
B
Survival impact of CD80 RNA expression (cut-off = 3.38) in GBM
CD80 RNA expression High Low
Survival probability
p = 0.038
Time in days (PFS)
Number at risk
CD80 RNA expression
High 10 0 0 0
Low 37 10 4 0
C
Surival using CD86 expression from GBM TCGA data (PFS) CD86_exp=high CD86_exp=low
Survival probability
p = 0.0011
Time in days
Number at risk
97 9 2 1
64 10 2 0
D
Surival using CD80 expression from GBM TCGA data (PFS) CD80_exp=high CD80_exp=low
Survival probability
p = 0.014
Time in days
Number at risk
113 10 2 1
48 9 2 0

115

`

Figure 23 CD80 and CD86 mRNA expression and outcome in GBM in both ONT cohort and TCGA dataset. Panel A: Kaplan-Meier PFS estimates in GBM patients in relation to CD86 (ONT database) Panel B: Kaplan-Meier PFS estimates in GBM patients in relation to CD80 (ONT cohort). C: Kaplan-Meier PFS estimates in GBM patients in relation to CD86 (TCGA dataset). D: Kaplan-Meier PFS estimates in GBM patients in relation to CD80 (TCGA dataset)

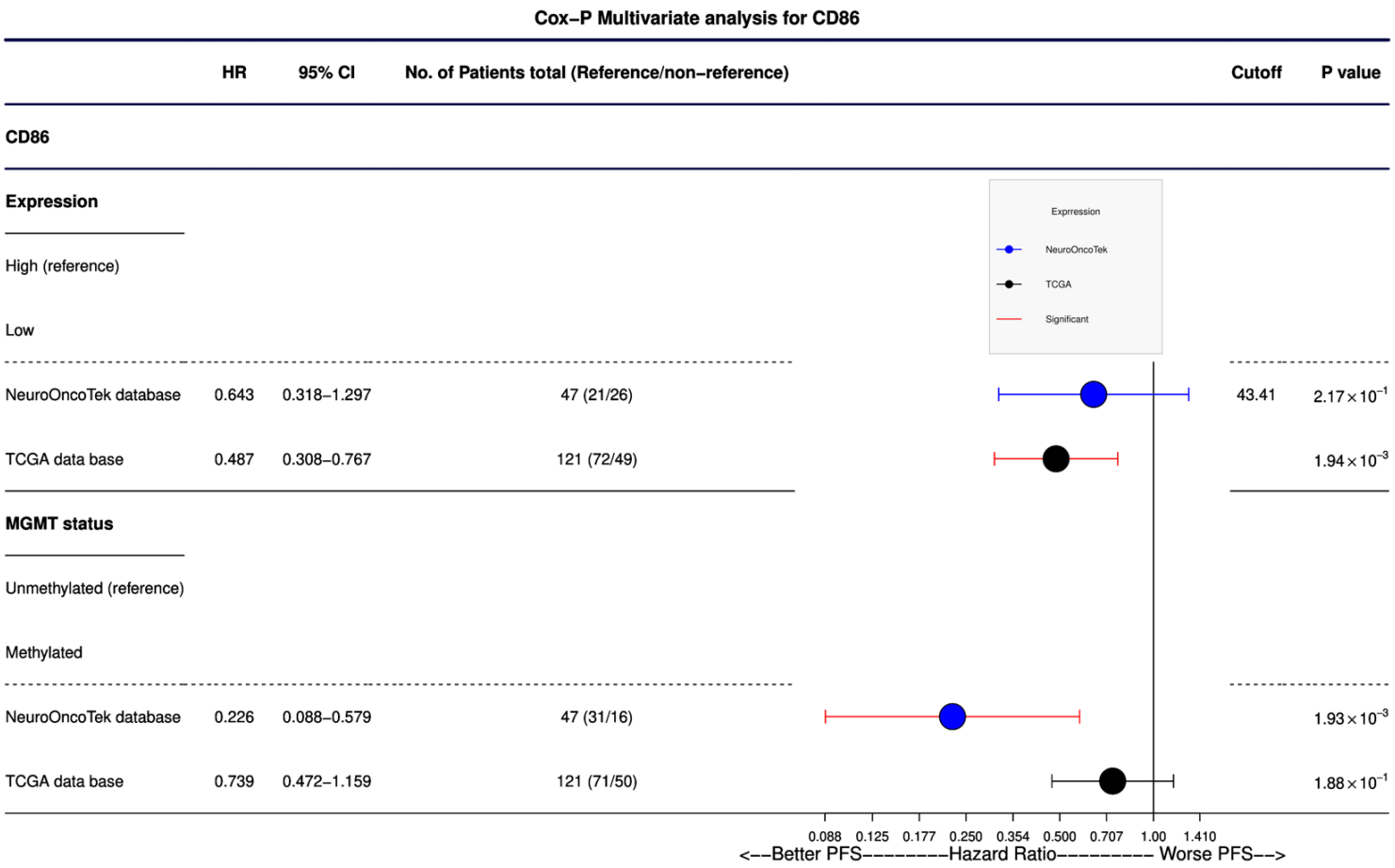

Figure 24: Cox-P (proportional hazards) multivariate analysis of CD86 protein expression and mRNA expression. CD86 was found to be an independent prognostic factor in TCGA database (P=0.0019); mRNA expression of CD86 is a more predictive prognostic factor than *MGMT* methylation. A non-significant trend was observed in our ONT cohort.

`

Target	Forward Primer	Reverse primer	UPL probe
CD86	Cagaagcagccaaaatggat	Gaatcttcagaggagcagcac	15
CD80	Gaagcaaggggctgaaaag	Ggaagttcccagaagaggtca	10
PPIA	Atgctggacccaacacaaat	tctttcactttgccaaacacc	48

Figure 25: Sequences of the forward and reverse primers for CD80, CD86 and PPIA. Universal Probe Library numbers that were used in our RT-PCR.

`

Table 11: Univariate analysis for OS in both ONT cohort and TCGA dataset.

Characteristics		ONT					TCGA				
		N=47	**Percentage %**	**median OS (days)**	**P-value**	**HR [95 % CI]**	**N=121**	**Percentage %**	**median OS (days)**	**P-value**	**HR [95 % CI]**
MGMT	Methylated	16	34.04	986.5	**0.00032**	0.266 [0.129-0.547]	50	41.32	457	**0.0066**	0.544 [0.350-0.844]
	Unmethylated	31	65.95	441			71	58.67	273		
IDH	Wildtype	45	95.74	502	0.321	2.062 [0.493-8.623]	113	93.38	333	**0.0045**	5.39 [1.69-17.22]
	Mutant	2	4.25	1220			8	6.61	845		
CD80 mRNA	High	5	10.63	488	0.192	0.525 [0.200-1.382]	104	85.95	306	0.07	0.573 [0.314-1.046]
	Low	42	89.36	585			17	14.04	485		
CD86 mRNA	High	31	65.95	568	**0.09**	0.55 [0.27-1.11]	36	29.75	421	0.376	1.223 [0.783-1.911]
	Low	16	34.04	500			85	70.24	333		
		N=41	**Percentage %**	**median OS (days)**	**P-value**	**HR [95 % CI]**					
CD80 protein	High	8	19.51	950	**0.011**	3.53 [1.34-9.33]					
	Low	33	80.48	470							
CD86 protein	High	24	58.53	486	0.202	1.537 [0.794-2.972]					
	Low	17	41.46	568							

`

Table 12: Univariate analysis for PFS in both ONT cohort and TCGA dataset

Characteristics		ONT					TCGA				
		N=47	**Percentage %**	**Median PFS (Days)**	**P-value**	**HR [95 % CI]**	**N=121**	**%**	**Median PFS (Days)**	**P-value**	**HR [95 % CI]**
MGMT	Methylated	16	34	587.5	**0.00013**	5.12 [2.22-11.8]	50	41.32	194	**0.0095**	1.788 [1.15-2.77]
	Unmethylated	31	66	251			71	58.67	157		
IDH	Wildtype	45	95.7	266	0.407	0.54 [0.128-2.30]	113	93.38	158	**0.0117**	4.467 [1.40-14.3]
	Mutant	2	4.3	242.5			8	6.61	488		
CD80 mRNA	High	10	21.27	206.5	**0.0426**	0.464 [0.221-0.975]	80	66.11	156	**0.0428**	0.621 [0.392-0.985]
	Low	37	78.72	267			41	33.88	203		
CD86 mRNA	High	21	44.68	229	**0.0049**	0.38 [0.199-0.75]	72	59.50	145	**0.00283**	0.509 [0.327-0.793]
	Low	26	55.31	365.5			49	49	210		
		N=41	**Percentage %**	**Median PFS (Days)**	**P-value**	**HR [95 % CI]**					
CD80 Protein	High	25	60.97	229	0.0841	0.565 [0.296-1.08]					
	Low	16	39.02	402							
CD86 Protein	High	13	31.70	218	**0.0429**	0.48 [0.244-0.977]					
	Low	28	68.29	329							

`

Increased brain delivery of anti-programmed death-ligand 1 using low-intensity pulsed ultrasound-mediated blood-brain barrier opening is associated with increased anti-tumor efficacy and microglia activation in glioblastoma mouse models

Mohammed Ahmed[1,2*], Nolwenn Lemaire[1], Emie Quissac[1], Rana Salam[1], Isaias Hernández-Verdin[1], Coralie L Guerin[3], Lea Guyonnet[3], Noël Zahr[4], Laura Mouton[5], Mathieu Santin[5], Alexandra Petiet[5], Charlotte, Schmidt[6], Guillaume Bouchoux[6], Marc Sanson[7], Maite Verreault[1], Alexandre Carpentier[6,7], Ahmed Idbaih[7*]

[1]Sorbonne Université, Institut du Cerveau - Paris Brain Institute - ICM, Inserm, CNRS, APHP, Hôpital de la Pitié Salpêtrière, Paris, France

[2]Faculté de Médecine Paris-Sud - Université Paris-Saclay, 91190, Saint-Aubin, France.

[3]Curie Institute, Cytometry Department, F-75006, Paris, France.

[4]Pharmacokinetics and Therapeutic Drug Monitoring unit, INSERM, CIC-1901, UMR ICAN 1166, Pitié-Salpêtrière Hospital, Sorbonne Université, AP-HP, F-75013 Paris, France.

[5]Centre de Neuroimagerie de Recherche, Institut du Cerveau - Paris Brain Institute - ICM, Inserm, CNRS, APHP, Hôpital de la Pitié Salpêtrière, Paris, France

[6]CarThera, Institut du Cerveau et de la Moelle épinière (ICM), F-75013, Paris, France

[7]Sorbonne Université, Institut du Cerveau - Paris Brain Institute - ICM, Inserm, CNRS, AP-HP, Hôpital de la Pitié Salpêtrière, DMU Neurosciences, Service de Neurologie 2-Mazarin, F-75013, Paris, France

`

*To whom correspondence should be addressed

Mohammed Ahmed, Pharm.D, Ph.D.

Institut du Cerveau - Paris Brain Institute-ICM,

Inserm, CNRS, APHP, Hôpital de la Pitié Salpêtrière

Paris, France

Tel: + 33 1 57 27 4485

Fax: +33 1 57 27 40 27

Email : mohammed.ahmed.icm@gmail.com

Ahmed Idbaih, M.D, Ph.D.

Sorbonne Université,

Institut du Cerveau-Paris Brain Institute - ICM, Inserm,

CNRS, AP-HP, Hôpital de la Pitié Salpêtrière, DMU Neurosciences,

Service de Neurologie 2-Mazarin, F-75013,

Paris, France.

Tel: 01-42-16-03-85.

Fax: 01-42-16-04-18.

Email : ahmed.idbaih@aphp.fr

`

Abstract

Therapeutic antibodies targeting immune checkpoints have limited efficacy in the overall population of glioblastoma (GBM) patients. Limited penetration of these large molecules within the normal and the tumor brain may explain at least partly these disappointing results. We hypothesized that increasing brain penetration of immune checkpoint inhibitors using low intensity pulsed ultrasound-mediated blood-brain barrier opening (UMBO) may increase their tumor bioavailability and their efficacy against GBM. In syngeneic GBM-bearing immunocompetent mice, we show that UMBO is able to open safely and repeatedly the blood-brain barrier using Evans's blue dye imaging, immunofluorescence, and MRI. UMBO is associated with (i) increased penetration of immune checkpoint inhibitor within the brain when delivered intravenously and (ii) increased circulation of tumor DNA within the bloodstream. Finally, we report here that the combination of UMBO and anti-PD-L1 therapeutic antibody increases dramatically the survival of GBM-bearing mice compared to their counterparts treated with anti-PD-L1 alone. Our study highlights the blood-brain barrier as a limitation to overcome to increase efficacy of immune checkpoint inhibitors in GBM and supports clinical trial combining UMBO and anti-PD-L1 in GBM patients.

Keywords: Sonocloud, GL261 mouse model, BBB opening, antibody delivery

`

Introduction

Glioblastoma (GBM) is the most malignant primary brain tumor in adults, with a median overall survival below 18 months after initial diagnosis (Ostrom et al., 2014). Despite remarkable efforts in the neuro-oncology field to develop new therapeutic alternatives, temozolomide (TMZ) remains today the standard first-line chemotherapy in GBM treatment (Ostrom et al., 2014, Pace et al., 2017). For over five decades, significant efforts have been put into the development of new anti-cancer therapies for GBM including anti-neoplastic agents (Atiq and Parhar, 2020), molecular targeted drugs (Touat et al., 2017), immunotherapeutic approaches (Weenink et al., 2020), and angiogenesis inhibiting compounds (Wang et al., 2017); however, the prognosis of patients has hardly improved (Lara-Velazquez et al., 2017).

The existence of the blood-brain barrier (BBB) as a specificity of the central nervous system (CNS) blood vessels prevents most systemic therapeutic compounds from reaching the brain parenchyma and GBM cells (Drean et al., 2016). Structural and functional changes of the BBB in GBM are frequent. They lead to changes of the BBB, called the blood-tumor barrier (BTB), allowing some chemotherapies to reach the tumor. Although the BTB enhances the delivery of some chemotherapeutic agents, large therapeutic antibodies have no chance to reach the brain at their therapeutic levels (Ait-Belkacem et al., 2014).

Several innovative strategies are known to enhance the delivery of chemotherapeutic agents and antibodies (Drean et al., 2016). Ultrasound-mediated blood-brain barrier opening (UMBO) using low-intensity pulsed ultrasound (LIPU) is one of the safe and effective methods to enhance the delivery of chemotherapeutic agents in preclinical (Zhang et al., 2020a) and clinical settings (Idbaih et al., 2019). Indeed, UMBO showed adequate safety and efficacy in recurrent GBM patients (Idbaih et al., 2019). LIPU is

`

delivered to the brain simultaneously with an intravenous injection of micron-sized bubbles for a few minutes, allowing the microbubbles to oscillate. Microbubbles oscillation produces a mechanical stretching on vessel walls that allows a transient opening of tight junctions (Sheikov et al., 2004).

The choice of therapeutic agents to deliver after UMBO is crucial and remains a point of discussion among researchers and regulators. Direct stimulation of the immune system with ICBs (*e.g.*, PD-1/PD-L1) showed promising effects alone or with other chemotherapies in multiple cancers. Ipilimumab was the first humanized anti-CTLA-4 approved by the American Federal Drug Administration (FDA) to treat inoperable melanoma (Tarhini, 2013). Five years later, Atezolizumab was the first humanized anti-PD-L1 approved by the FDA to treat advanced or metastatic urothelial carcinoma (Hsu et al., 2017). PD-L1 proteins are expressed as surface molecules by cancerous cells such as GBM cells (Hao et al., 2020) and provide a tumor escape mechanism when bound to PD-1 proteins at the surface of activated T-lymphocytes leading to their exhaustion (Azoury et al., 2015). Nivolumab and ipilimumab have limited or no efficacy in GBM patients and Avelumab monotherapy (anti-PD-L1) showed a minor impact on progression-free survival (NCT03047473).

In the present study, we evaluated the effect of anti-PD-L1 and anti-CTLA-4 alone and in combination with UMBO in GBM mouse models.

`

Materials and Methods

Cell culture and in vivo studies

GL261 cells were cultured in Dulbecco's modified essential medium (DMEM) supplemented with 10% fetal bovine serum and 1% Penicillin/Streptomycin. Cells were passaged twice weekly according to their confluence. Nfpp10-luciferase (*NF1*, *PTEN*, and *TP53* deficient) as described in Friedmann-Morvinski et al. (2012). GBM cells were obtained from Dr Gabriele Bergers' laboratory. Nfpp10-luciferase cells were maintained in culture using DMEM/F12 (Gibco; Life Technologies) culture medium supplemented with 1% penicillin-streptomycin, EGF (20 ng/mL), and FGF (20 ng/mL; Preprotech), Heparin 2 µg/ml (Sigma H33930) and N-2-supplement 1/100 (Gibco 17502-048). The animal ethics committee at the Ministry of Higher Education and Research in Paris, France, approved all protocols involving live mice (protocol #17503 and #26137). C57BL/6 mice were purchased from Charles River and were given a week of acclimation before starting any experiment.

GL261 was transduced with a luciferase/mKate2 vector described before(Plessier et al., 2017). GL261-luciferase and Nfpp10-luciferase cells (1.4 x 10^5 cells /2 µL) were inoculated into the right caudate nucleus-putamen (AP +10 mm, DV +0.25 mm, ML +0.15 mm) of 7-8 weeks old C57BL/6 females using a stereotactic injection frame (David Kopf Instruments Tujunga, CA). Mice were imaged using the IVIS Spectrum (PerkinElmer) 10 minutes following a 2 mg subcutaneous injection of luciferin (Sigma, L9504). The growth of GL261-luciferase and Nfpp10-luciferase cells was confirmed by two IVIS imaging one week apart following intracranial cell injection. During the characterization of tumor growth in our mouse models, we observed that mice with bioluminescence values lower than 5.00+E05 would not develop GBM tumors. Therefore, we have chosen to include only

`

mice with bioluminescence values over 5.00+E05 photon/second. Mice were randomly placed into treatment arms once they passed the bioluminescence cutoff value.

Animals were treated with 200µL of anti-CTLA-4 (Bristol-Myers Squibb, G1-XAS-Ab), anti-PD-L1 (Genentech, 6E11) and IgG1 (BXCELL, BE0083) for four doses. Unless specified otherwise, animals were sacrificed when they showed signs of tumor-associated illness (20% body weight loss or changes in behavior or posture).

Calibration of low-intensity pulsed ultrasound device

The ultrasound transducer (CarThera®) used in this study was calibrated before each experiment. The aim was to map the ultrasound field and to determine the electrical set point that the generator uses during the experiments to obtain the targeted acoustic pressure *in situ*. The calibration was performed using degassed water at room temperature with a 200 µm needle hydrophone (HNC0200, ONDA). A 2D acoustic field was scanned at 5 mm from the transducer surface with a 3-axis computer-controlled motorized positioning system (UMS, Precision Acoustics, U.K.). A transducer velocity pattern of 1.05 MHz was then obtained by acoustic holography. The 3D acoustic field was computed from this pattern with the Rayleigh integral. The hydrophone was positioned at the spatial peak pressure determined from the 3D acoustic field. The ratio between the active electrical power drawn by the transducer measured with an oscilloscope and the square of the spatial peak acoustic pressure was measured. This ratio is used as a calibration coefficient by the generator during subsequent experiments: the active electrical power needed to obtain the targeted pressure is calculated by the generator using this coefficient at the beginning of manipulation, and the generator adjusts its set point to obtain the specified active electrical power measured internally.

`

Ultrasound-mediated blood-brain barrier opening

UMBO was delivered to both UMBO and UMBO plus anti-PD-L1 groups. Anti-PD-L1 (6E11 Genentech) was administered intraperitoneally in all experiments at a dose of 200 µg 1 hour before UMBO application. UMBO device for preclinical studies was manufactured by CarThera®. Mice were maintained under anesthesia with isoflurane (2%, 2L/min O_2). For each UMBO application, 200 µL of SonoVue® per mouse was injected by the retro-orbital route less than 10 seconds before the start of ultrasound application. 1MHz LIPU was delivered to the brain through a transducer at an 0.3 MPa acoustic pressure with a pulse length of 23.8 milliseconds (25,000 cycles) and a frequency of 1Hz for two minutes. For each sonication, UMBO was validated using a control mouse. Each control mouse was injected intravenously (IV) with a solution of 2.7% Evans blue (Sigma, E2129) in phosphate buffer saline (PBS) at a dose of 4 mL/kg 10 minutes post UMBO application. UMBO test mice were sacrificed 15 minutes following Evans' blue injection, and their brain was harvested. The passage of Evans blue was assessed both visually and by ZEISS Axio-Scan fluorescence imaging of cryosectioned brains.

Pharmacokinetic analysis of therapeutic antibodies with and without UMBO

Thirty-six mice were used in the pharmacokinetic experiment. Mice were separated in control and UMBO groups. Six-time points were selected as follows: 0.15, 0.3, 3, 6, 24, 48 and 96 hours. Each mouse received a 200 µg of nivolumab (Bristol-Meyers Squibb, New York, NY, USA) intravenous injection 10 minutes following the BBB opening. 100 µL of blood was collected through cardiac puncture using a pre-heparinized syringe. The serum was collected by centrifugation of the blood at 3500 rpm for 10 minutes.

All samples (plasma and brain) were then analyzed using ultra-performance liquid chromatography (UPLC) system coupled to mass spectrometry (LC-MS/ MS; MS-8060,

`

Shimadzu, Japan). Quantifications were achieved in multiple reaction monitoring (MRM) mode, and electrospray ionization was operated in a positive mode. Peak integration and quantification were performed using LabSolutions Insight LC-MS software. Nivolumab was quantified with signature peptide ASGGITFSNSGMHWVR.

MRI data acquisition

MRI acquisitions were performed using a preclinical 11.7 T MRI scanner (Biospec, Bruker BioSpin, Germany) equipped with a CryoProbe dedicated to mouse brain imaging (Biospec, Bruker BioSpin, Germany). The total MRI experiment time was approximately 80 min per mouse (including MRI settings, acquisitions, and gadolinium injection), during which the animals were anesthetized with 1% isoflurane in O2 (2 L/min). The respiration rate was monitored via a respiration pillow sensor, and the body temperature was maintained using a heated water circuit incorporated into the cradle. The head was placed in a prone position and restrained stereotaxically by a bite bar and ear pins. For each animal, the protocol consisted in : (i) acquiring pre-gadolinium enhancement anatomical T1-weighted (T1w) images using a Multi-Slice Multi Echo (MSME) sequence with the following parameters: T.R. = 400 ms, T.E. = 5 ms (one single echo), four averages, 14 slices, and resolution = 60x60x500 μm^3, (ii) following injection of a total volume of 100 µL of gadolinium (DOTAREM®, Guerbet, Aulnay-sous-Bois, France) at 0.5 mM and at physiological temperature in the tail vein of the mouse outside the MRI scanner, (iii) acquiring post-gadolinium T1w images using the same sequence as used for (i) and, (iv) acquiring post-gadolinium injection T2*-weighted (T*2w) images using a Multi Gradient Echo (MGE) sequence. MGE sequence was acquired with the following parameters: T.R. = 80 ms, ten echoes ranging from T.E. = 2.7 ms to 35.1 ms (echo spacing = 3.6 ms), and isotropic resolution of 60x60x60 μm^3.

`

mRNA sequencing

Twelve mice with a confirmed tumor of comparable sizes (as measured by bioluminescence imaging) were included in this experiment. Mice were divided into four groups. UMBO group, anti-PD-L1 group, UMBO plus anti-PD-L1, and InVivoPure pH 6.5 Dilution Buffer (BXCELL, IP0065) for vehicle groups. Two treatment sessions (day 21 and 24) were administered in this experiment. Mice were sacrificed 24 hours after the last treatment by cervical dislocation, and the right hemisphere was snap-frozen in 2 ml RNALater (Thermofisher AM7020). Lysing Matrix D (MBio, 6913050) was used to homogenize the brain tissues. mRNA was extracted using Maxwell RSC simply RNA automated RNA purification kit (Promega, AS1340). RNA quality was analyzed using high sensitivity RNA chips (TapeStation). For RNA sequencing, NovaSeq 6000 sequencer (200 cycles, 800 million reads) and reagent kit were used. Following data alignment and normalization, we applied the publicly available RSTUDIO package called mMCP (Petitprez et al., 2020) to characterize the tumor microenvironment changes before and after UMBO.

Immunohistochemistry (IHC)

Detection of anti-PD-L1 6E11 mouse antibody by IHC is irrelevant due to the cross-reactivity with mouse antibodies. Instead, A 150 KDa rat IgG2 antibody targeting PD-L1 was used in our IHC staining (BXCELL, #BE0101). Goat anti-rat IgG antibody (BA-9400) was used to detect the anti-PD-L1. CD8+ T-lymphocytes were detected using CD8 alpha antibody (1:1000, BioRad, #MCA48R) while Iba1 protein was detected using 1:1000, Abcam, #ab178846. Mouse brains were fixed overnight in 4% paraformaldehyde (PFA) then immersed in 10% sucrose for cryoprotection, then were cryosectioned. 10 µm cryosections were harvested using Leica CM1950 cryostat. Slides were stored at -80°C until analysis.

`

Quantitative digital droplet polymerase chain reaction (ddPCR)

GL261 tumor-bearing mice four weeks following cell inoculation were used in the ddPCR experiment. A single UMBO treatment was completed, and 30 minutes later, blood (100 µl) was collected in heparinized tubes through cardiac puncture. Whole blood DNA was extracted automatically using Maxwell® Blood DNA Purification Kit (AS1010). QX200 ddPCR EvaGeen® was utilized to detect *mKate2* and *Luciferase* genes in the extracted DNA. Primer3Plus web interface was used to design *mKate2* and *Luciferase* primers and was purchased from Life Technologies. The following forward (FR) and reverse (RV) primers were used: luciferase-FR, TCCACGATGAAGAAGTGCTC; luciferase-RV, AGGCTACAAACGCTCTCATC; mKate2-FR, GGTGAGCGAGCTGATTAAGG; and mKate2-RV, GGGTGTGGTTGATGAAGGTT.

Flow cytometry

Twenty mice with a confirmed tumor of comparable sizes were included in this experiment. Mice were separated into four groups: UMBO group, anti-PD-L1 (Genentech, 6E11) group, UMBO plus anti-PD-L1, and vehicle group as described above. One treatment session was delivered in this experiment. Mice were perfused using cold distilled phosphate buffer saline (DPBS) ~16 hours after treatment. Brains were isolated immediately and stored in 2 mL ice-cold Hanks' balanced salt solution (HBSS). According to the manufacturer's protocol, the right hemisphere was isolated and mixed in the enzyme mix solution from the adult brain dissociation kit (Miltenyi Biotec, #130-107-677). Cells gentleMACS® Octo Dissociator with Heaters (#130-096-427) and gentleMACS C Tubes (#130-093-237) were used to perform mice brain dissociation. The number of dissociated cells was calculated using Scepter® 3.0 Handheld Cell Counter.

`

Samples were acquired on a spectral flow cytometer (Aurora, Cytek) and analyzed by FlowJo software (FlowJo, LLC). Briefly, cells were selected based on their morphology, doublets, and dead cells were excluded using (Biolegend, #423107) while tumor cells were excluded based on their *mKate* expression. Monocytes ($Ly6C^+$ $Ly6G^-$), neutrophils ($Ly6C^+$ $Ly6G^+$) were excluded from non-tumoral live cells using Ly-6C (Biolegend, #128036) and Ly-6G (Biolegend, #127617). Microglia were identified based on their expression of $CD11b^+$ and $CD45^{low}$ using CD45 (Biolegend, #103131) and CD11b (Biolegend, #101255). Activated microglia were identified as $CD68^+$ using (Biolegend, #137003). F4/80 marker (Biolegend, #123117) was used to determine macrophages in the $CD45^{high}$ $CD11b^+$ cell population. CD206 marker (Biolegend, #141729) was used to distinguish between subpopulations of macrophages. Lymphocytes $CD4^+$ (Biolegend, #100541) and $CD8^+$ (Biolegend, #100737) were identified on the $CD45^+$ $CD11b^-$ fraction of non-tumoral live cells. The percentage of each subpopulation was calculated and using in our flow cytometry analyses.

Statistical tests

Statistical analysis was performed using Prism software (GraphPad). Data are shown as mean values plus and minus standard error of the mean (SEM). Statistical significance of differences between groups was verified using appropriate statistical tests. Significance level were denoted with asterisks: * for $p \leq 0.05$; ** for $p \leq 0.01$; *** for $p \leq 0.001$, and **** for $p \leq 0{,}0001$.

`

Results

Anti-PD-L1 increases survival of GL261-bearing mice and Nfpp10 -bearing mice

Pilot studies using both GL261-luciferase and Nfpp10-luciferase mouse models were performed. These two experiments aimed to determine the effect of anti-PD-L1 and anti-CTLA-4 in our GBM mouse model and select the best candidates to combine with UMBO.

Anti-PD-L1 antibody alone has shown a limited effect on survival of GL261-bearing **(Figure 26-B)**, even though a slight regression in tumor growth was seen **(Figure 26-A)**. Anti-CTLA-4 treatment did not affect tumor growth **(Figure 26-A)** or animal survival **(Figure 26-B).** No treatments had an impact on mice's body weight **(Figure 26-C)**.

Interestingly, anti-PD-L1 antibody showed better efficacy in Nfpp10 GBM mouse model compared to GL261-bearing mice **(Figure 26-E).** Anti-PD-L1 treatment reduced tumor growth in some mice **(Figure 26-D)** and increased the number of long-term survivors (3/6) **(Figure 26-E)**.

Blood-brain barrier integrity in GBM bearing mice

We evaluated the BBB integrity in both mouse models. Assessment of BBB disruption was performed using 1.2 mg of Hoechst 33342 (Sigma) diluted in PBS was injected intravenously 20 min prior to sacrifice. Hoechst staining was not detected in normal brain tissue **(Figure 27-A)**, yet higher staining intensity was observed in brain tissue harvested from Nfpp10-bearing mice compared to GL261-bearing mice. Those as mentioned earlier could indicate a higher BBB permeability in the Nfpp10 GBM mouse model. Overall, this makes the anti-PD-L1 antibody the best candidate to be combined with UMBO in the GL261 GBM mouse model.

`

UMBO is safe and effective in immunocompetent mice

UMBO parameters were previously optimized in our setting using athymic nude mice (Dréan et al., 2019). The safety and the efficacy of UMBO were then evaluated in C57BL/6 mice. We have selected 0.3 MPa for a safe and effective UMBO. UMBO was optimized to target the right hemisphere, and BBB opening was confirmed macroscopically (**Figure 27**-B) and by fluorescence microscopy with a BBB opening on the right hemisphere **(Figure 27-C).** Next, we evaluated UMBO parameters and treatment frequency in GL261 GBM mouse models. T1w MRI **(Figure 27-E)** showed a marked gadolinium contrast enhancement within an hour following emission of ultrasound.

We observed tolerability of GL261-bearing mice to repeated biweekly UMBO and UMBO did not affect mice's weight **(Figure 27-A)**. Furthermore, the Kaplan-Meier estimate shows no significant difference in the OS between UMBO and non-treated groups in the GL261 GBM mouse model **(Figure 27-A)**. Overall, the UMBO parameters that are used for repeated UMBO opening are safe and tolerable in GL261-bearing mice.

UMBO dramatically increased the efficacy of anti-PD-L1 in GL261-bearing mice

We attempted to investigate any possible positive outcome from UMBO in combination with anti-PD-L1 in the GL261 GBM mouse model. We initially hypothesized that anti-PD-L1 efficacy was limited because the BBB protects GBM cells from exposure to a therapeutic level of anti-PD-L1.

Mice with comparable bioluminescence values were divided into five groups: (i) UMBO group, (ii) anti-PD-L1 group, (iii) UMBO plus anti-PD-L1 group, (iv) IgG1 group, and (v) IgG1 plus UMBO group. In each treatment protocol, all mice received 200 µl of warm saline injection before anesthesia to prevent any possible hypothermic effect. Intraperitoneal injection of anti-PD-L1 injection was given 60 min before sonication to

`

ensure anti-PD-L1 absorption. We have not observed any toxic effect in UMBO plus anti-PD-L1 treated mice *versus* control mice **(Figure 28-C)**. UMBO and anti-PD-L1 did not show an early impact against tumor growth **(Figure 28-D)**; however, a delayed effect on tumor size was observed two weeks after the last dose of treatment **(Figure 28-F)**.

Interestingly, mice received an anti-PD-L1 antibody with UMBO showed a (13/17) 76 % long-term survivors (over 100 days) compared to (4/15) 26 % in anti-PD-L1 alone and (0/16) 0% in control groups. Kaplan-Meier estimate shows a significant difference ($p<0.05$) in UMBO's overall survival plus anti-PD-L1 treated mice *versus* anti-PD-L1 alone treated mice. Furthermore, a higher significance difference ($p=0.0001$) was observed in UMBO plus anti-PD-L1 treated mice compared to the IgG1 plus UMBO treated mice in the GL261 GBM mouse model.

UMBO increased the penetration of ICBs into brain parenchyma

The BBB can easily block large therapeutic agents as antibodies. With UMBO, we attempted to deliver antibodies to the brain parenchyma. IHC staining of anti-PD-L1 (BXCELL, BE0101) confirms UMBO's ability to deliver anti-PD-L1 to the right hemisphere brain parenchyma **(Figure 29-A)**. Furthermore, an already clinically optimized nSMOL LC-MS (Iwamoto et al., 2018) measurement protocol was used to compare nivolumab's pharmacokinetics with and without UMBO. Three C57BL/6 mice per time point (six-time points) per group were used in the analysis. We observed a comparable serum concentration of nivolumab in control and in UMBO-treated mice.

Interestingly, we detected a neglected concentration (<0.2 µg/200mg brain) of nivolumab in control mice brains **(Figure 29-B)**. Interestingly, higher concentrations of nivolumab were detected in mice' brain treated with nivolumab plus UMBO. The maximum concentration (Cmax) of nivolumab was detected at 24 hours which starts to decline and

`

reaches (<0.2µg/200mg) at 96 hours. An analysis of the fold changes in brain concentration shows that UMBO enhanced the delivery of nivolumab up to 28.8 folds compared to control group.

UMBO increased circulating GL261-DNA to the peripheral blood circulation

Additionally, we aimed to evaluate molecules circulation between tumor brain and blood with and without UMBO. Therefore, we evaluated whether UMBO could enhance the leakage of circulating tumor DNA to the bloodstream. GL261-bearing mice four weeks following GL261 cell grafting were used in the experiment. We have observed a significant elevation ($p<0.01$) in the number of copies for both m-Kate and luciferase in the UMBO treated group compared to the control.

UMBO increased $CD8^+$ T-lymphocytes in the brain and modulate microglia's phonotype.

Microglia staining in anti-PD-L1 plus UMBO treated group shows a phenotype of activated microglia. Double nuclear staining in the UMBO plus anti-PD-L1 treated GL261-bearing mice show a possible induction of microglia's cell division **(Figure 30)**. Therefore, our foreseen flow cytometry analysis of activated microglia would provide additional evidence of UMBO's effect on microglia's activations.

Additionally, we observed an enhanced passage of $CD8^+$ T-lymphocytes in UMBO plus anti-PD-L1 compared to anti-PD-L1 treated GL261-bearing mice. This effect is currently under investigation by flow cytometry analysis of microglia, macrophages, $CD3^+$, $CD8^+$, and $CD4^+$ T-lymphocytes.

`

Discussion

Patients with GBM have a dismal outcome with a median overall survival below 18 months with the current standard of care, including concurrent administration of TMZ and radiotherapy followed by adjuvant TMZ. Since 2005,TMZ has remained the first-line chemotherapy in treating GBM patients. TMZ is an alkylating agent with a small molecular weight (194.15 g/mol) that readily passes BBB. As suggested from TMZ clinical pharmacokinetics studies between 20-30% of TMZ reaches the brain following oral administration(Ostermann et al., 2004) however, large therapeutic agents, *i.e.*, antibodies, do not cross the BBB in physiological conditions. UMBO and several innovative strategies continuously evolve to overcome the BBB by increasing drug delivery(Drean et al., 2016). Immunotherapies, including ICIs and cell therapies, have revolutionized multiple solid tumors' treatments through activating the general antitumor immune response.

CheckMate-143 phase 3 clinical trial was then initiated to evaluate the effect of nivolumab *versus* bevacizumab. Unfortunately, nivolumab did not demonstrate higher efficacy compared to bevacizumab. Several reasons might explain the low efficacy of ICIs in GBM: (i) low tumor mutation load, (ii) lack of predictor of response and lack of selection of patients, (iii) low penetration of ICIs within the brain parenchyma, (iv) low peripheral priming, (v) local immunosuppression and (vi) low penetration of T-lymphocytes(Beccaria et al., 2020).

We explored the BBB as the limitation for antibody and lymphocytes penetration and priming and attempted to evaluate UMBO's effect on the penetrating large therapeutics to the brain and modulating the immune microenvironment in GBM mouse model. Our data confirmed the limited efficacy of ICIs efficacy in the Gl261-bearing and Nfpp10-

`

bearing mouse models. Consistent with our data, preclinical evaluation of anti-PD-L1 and anti-CTLA-4 in GL261-bearing mice model showed comparable limited efficacy of both antibodies in a GL261 GBM mouse model. In this study, they have used a different treatment regimen, yet the efficacy was comparable(Reardon et al., 2016).

To the best of our knowledge, this is the first research article that report a dramatic increase in the overall survival of GL261-bearing mice when treated with UMBO plus anti-PD-L1. Indeed, 76% of GL261-bearing mice treated with anti-PD-L1 plus UMBO survive longer than 100 days compared to 26% for GL261 mice treated with anti-PD-L1 alone. Next, we tried to understand the mechanisms involved in the anti-tumor effect. We initially hypothesized that the BBB was responsible for the limited efficacy by blocking anti-CTLA-4 and anti-PD-L1 from reaching the GBM tumor. This hypothesis is consistent with a recent study that reported an enhanced efficacy of ICIs following their delivery to brain tumors (Guo et al., 2020). Additionally, a recent study, illustrated that focused ultrasound enhanced the delivery of an intrasnal delivery of anti-PD-L1 but not overall survival of GL261-bearning mice. UMBO plus 200 µg of the anti-PD-L1 biweekly treatment regimen was used to maintain the higher concentration of anti-PD-L1 within the brain parenchyma. Immune checkpoint blockade with anti-PD-L1 was performed on day 14 post-inoculation to allow for T-lymphocytes depletion(Aslan et al., 2020).

Using LC-MS/MS and IHC we reported an enhancement of nivolumab and anti-PD-L1 concentrations in the brain parenchyma. In our setting, we reported that UMBO enhanced antibody's concentration up to 28 folds compared to control. UMBO was optimized to disturb one hemisphere; however, in our PK analysis, we have used a whole-brain homogenization method; therefore, local concentrations of nivolumab could have been even higher. Consistent with our data, a study has shown that UMBO enhanced the

`

delivery of bevacizumab ~149 KDa to the brain parenchyma by 5.7 to 56.7 folds compared to non-sonicated brain in a glioma mouse model(Liu et al., 2016).

GBM tumors have low chances of extracranial metastases with negligible risk for GBM spreading after surgical brain biopsies(Lun et al., 2011). UMBO stimulates a detectable peripheral circulation of GL261 DNA. We have observed a significant elevation of *mKate2* and *luciferase* DNA 30-mintues following UMBO. Consistent with our data, a recently published article investigated the possibility of using UMBO for liquid biopsies in GBM models. They have observed a detectable level of green fluorescent protein mRNA 20-mins following UMBO in the GL261 mouse model(Zhu et al., 2018).

Here, we have investigated the effect of peripheral circulation of DNA to extrapolate the possibility of priming effect. The priming effect could activate naïve T-lymphocytes through their exposure to new antigens. As mentioned previously, the BBB is protecting the tumor from T-lymphocytes infiltration and immune activation. Thus, we have shown that the possibility of detecting GL261 tumors in the peripheral circulation might activate the global antitumor effect. Further functional demonstration of lymphocyte activation should be performed to evaluate any priming effect of UMBO.

Our results showing microglia activation in the UMBO plus anti-PD-L1 treated GL261-bearing mice suggest a possible mechanism for the observed enhanced therapeutic efficacy of anti-PD-L1. Our flow cytometry analysis is consistent with a newly published article that observed a high ratio of Iba1 staining in sonicated brain regions compared to the non-sonicated one. However, this observation was not significant(Sinharay et al., 2019). PD-L1 is expressed on the cell surface of both GL261 and microglia(Chen et al., 2019b). A possible effect on microglia phenotype might be related

`

to the combined effect of UMBO and anti-PD-L1 delivery to the brain parenchyma. Activated microglia might have an impact on the cytotoxic effect against GL261 tumor cells(Li et al., 2017).

To date, there is no clear evidence on the effect of UMBO on T-lymphocytes passage to the brain. We have not observed any significant elevation in the percentage of $CD8^+$ and $CD4^+$ T-lymphocytes at one timepoint (~16 hours). This effect might be related to the timing of sample collection. We have not evaluated the effect of our treatment regimen at later time points. We have seen a delayed antitumor effect in UMBO and anti-PD-L1 group which could be related to a delayed effect on T-lymphocytes. Furthermore, we have not analyzed any subpopulations of $CD8^+$ T lymphocytes *i.e.,* PD-1^+ $CD8^+$ T-lymphocytes.

Syngeneic mice models and especially the GL261 mouse model is one limitations of this study. GL261 mouse model has a high mutation load which is not consistent with GBM patients. Not to mention, a heterogeneity of responses in the GL261 mouse model was reported when treated with ICIs *in vivo*(Aslan et al., 2020). Another limitation of our findings is the inability to demonstrate functional analysis of the role of UMBO in priming naïve T-lymphocytes through their exposure to new antigens. Additional functional analysis on the effect of UMBO plus anti-PD-L1 would explain the dramatic effect on OS that was observed in our study.

Conclusions

Our study showed statistically significant increased brain penetration and efficacy of anti-PD-L1 in GL261-bearing mice when delivered by UMBO. We have also provided clear evidence of the possible safe and effective delivery of large therapeutic agents using UMBO. Further investigations are needed to confirm the impact of UMBO on brain

`

penetration and efficacy of chemotherapeutic agents and anti-PD-L1 to overcome the resistance of GBM to the current treatments.

Acknowledgments

This work was supported by the European Union's Horizon 2020 research and innovation program under the Marie Skłodowska-Curie grant agreement #766069 (GLIO-TRAIN), INCA-DGOS-Inserm-12560 (SiRIC CURAMUS), Institut National du Cancer, ministère des solidarités et de la Santé and Inserm.

Conflicts of interest

No potential conflicts of interest were disclosed.

Author's contribution

M.A designed and performed experiments, analyzed data, and wrote the paper. MA, NL, EQ, CG, LG, NZ, LM, AP performed the experiments. IH.; performed bioinformatic analyses of mRNA sequencing data. MV, AI supervised the research.

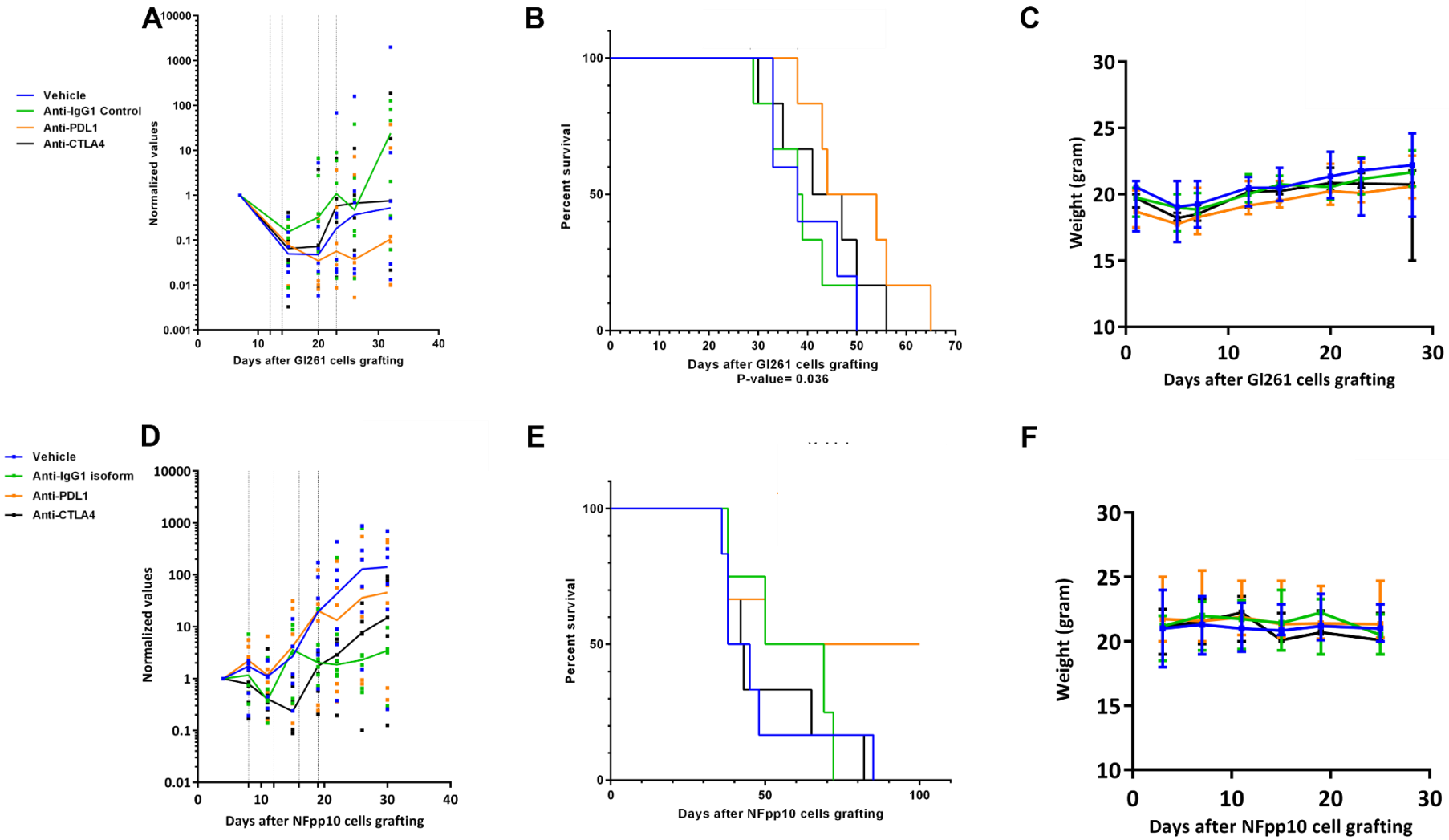
A
Vehicle
Anti-IgG1 Control
Anti-PDL1
Anti-CTLA4
Normalized values
Days after Gl261 cells grafting
B
Percent survival
Days after Gl261 cells grafting
P-value= 0.036
C
Weight (gram)
Days after Gl261 cells grafting
D
Vehicle
Anti-IgG1 isoform
Anti-PDL1
Anti-CTLA4
Normalized values
Days after NFpp10 cells grafting
E
Percent survival
Days after NFpp10 cells grafting
F
Weight (gram)
Days after NFpp10 cell grafting

`

Figure 26: Anti-PD-L1 increased survival of GL261 and Nfpp10 -bearing mice. Animals were treated with anti-PDL-1, IgG1 antibody, anti-CTL-4, and vehicle for four doses. Panel A: bioluminescence measures normalized to the first measured value performed on day 7 after cell inoculation in GL261-bearing mice model. Each dot represents values for one animal and the line represents the mean value for the group. Bioluminescence signal was measured weekly. Dotted lines represent the days of treatments. Panel B: Kaplan Meier curves in GL261-bearing mice. Panel C: mean of animal body weight in each group over time. Panel D: bioluminescence measures normalized to the first measured value performed on day 7 after cell inoculation in Nfpp10 mouse model. Dotted lines represent the days of treatments. Panel E, Kaplan Meier curves in Nfpp10-bearing mice. Panel F: mean of animal body weight in each group over time.

`

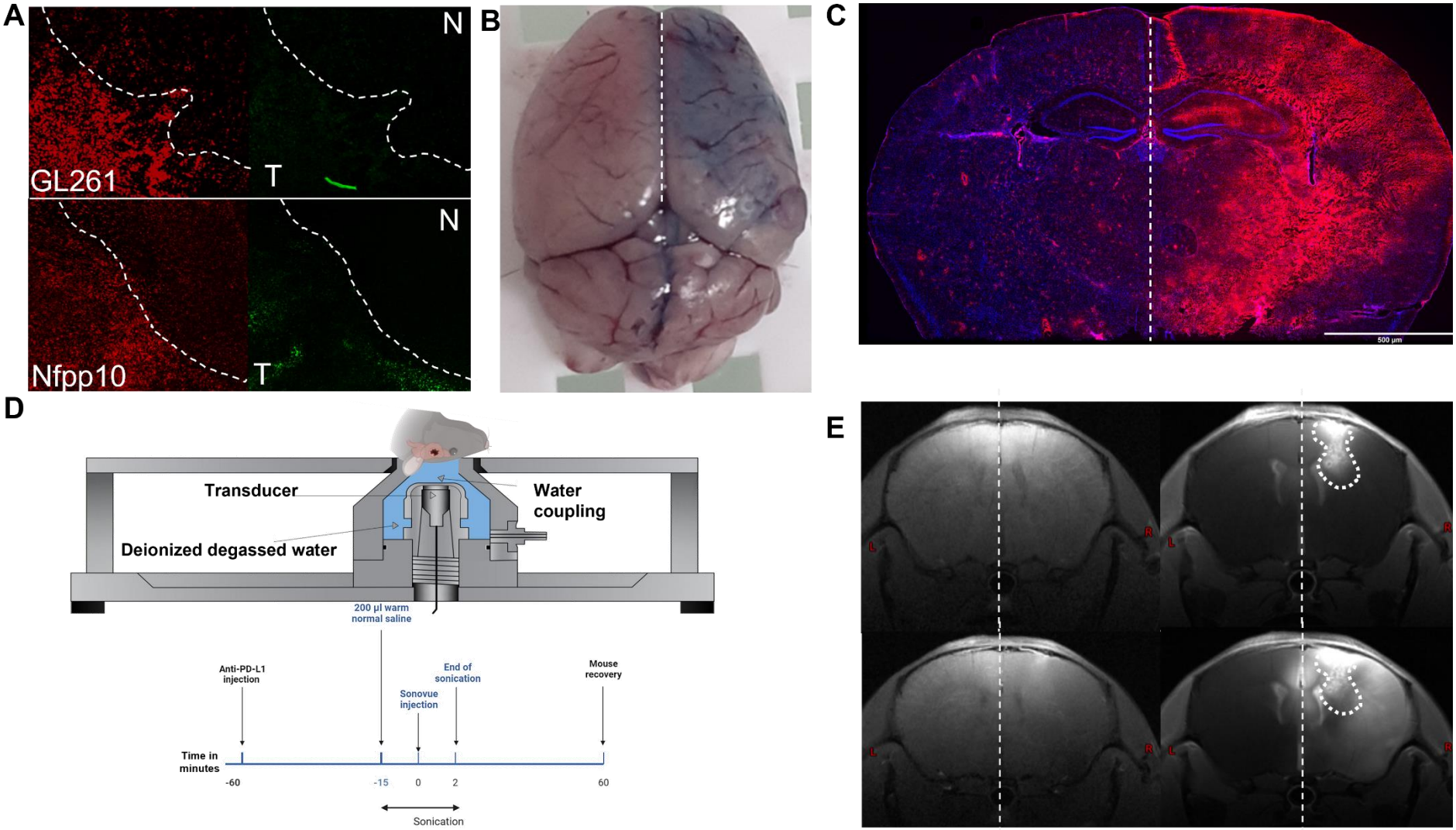
A
N
GL261
T
N
Nfpp10
T
B
C
500 µm
D
Transducer
Water coupling
Deionized degassed water
200 µl warm normal saline
Anti-PD-L1 injection
Sonovue injection
End of sonication
Mouse recovery
Time in minutes
-60
-15
0
2
60
Sonication
E
L
R

`

Figure 27: UMBO is safe and effective in C57BL/6 mice. Panel A: BBB integrity in GL261-bearing and Nfpp10-bearing mice. Hoechst staining (in green) was not detected in normal (N) brain tissue. However, higher staining intensity was observed in the tumor (T) area in Nfpp10 model compared to GL261 model. Panel B-C: Evans blue staining was enhanced in sonicated brain hemisphere compared to the control hemisphere visually (Panel B) and by fluorescence (Panel C; Evans blue in red, DAPI in blue) in a cryo-sectioned mouse brain. Panel D: schematic representation of Sonocloud® device used in our setting and timeline used for UMBO plus anti-PD-L1 treatments. Panel E: T_1W MRI showed a marked gadolinium contrast enhancement within an hour following the ultrasound emission. The lower two T1-MRI images were obtained after UMBO (pre- gadolinium left MRIs; and post gadolinium right MRIs).

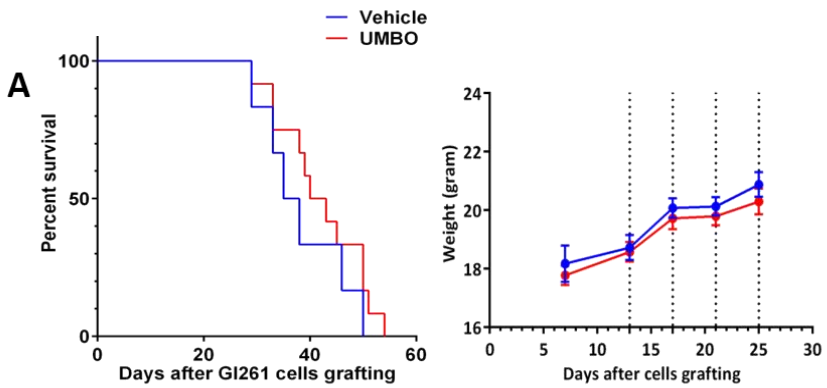
A
Vehicle
UMBO
Percent survival
Days after GI261 cells grafting
Weight (gram)
Days after cells grafting

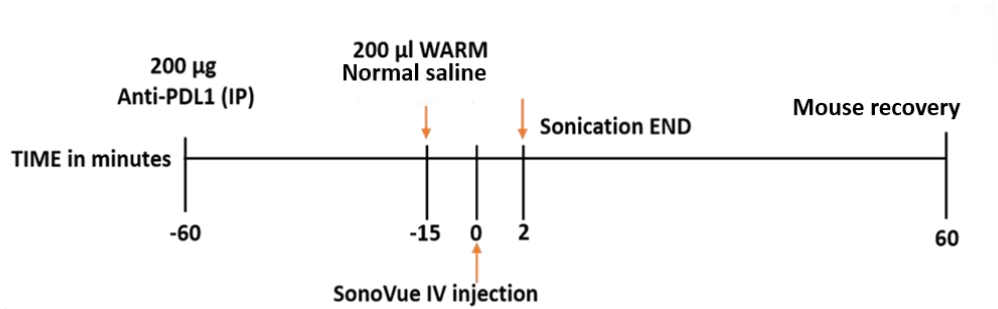
B
200 µg
Anti-PDL1 (IP)
200 µl WARM
Normal saline
Sonication END
Mouse recovery
TIME in minutes
-60
-15
0
2
60
SonoVue IV injection

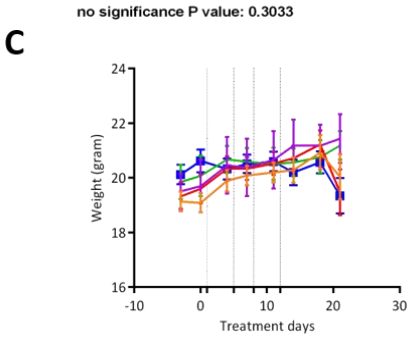
no significance P value: 0.3033
C
Weight (gram)
Treatment days

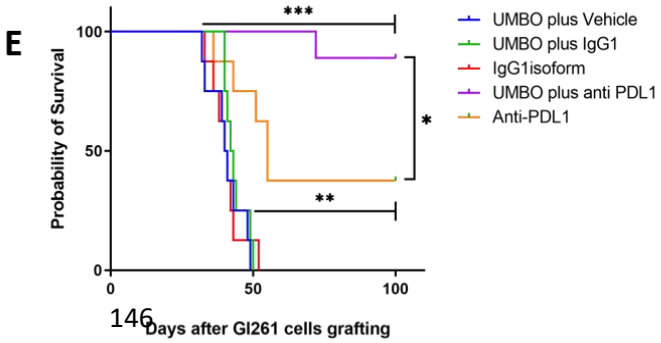
E
***
*
**
Probability of Survival
Days after GI261 cells grafting
UMBO plus Vehicle
UMBO plus IgG1
IgG1isoform
UMBO plus anti PDL1
Anti-PDL1

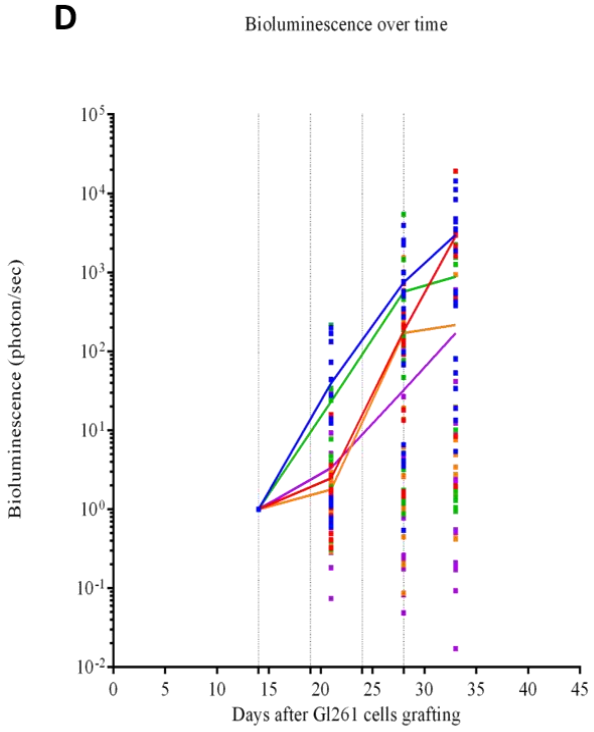
D
Bioluminescence over time
Bioluminescence (photon/sec)
Days after GI261 cells grafting

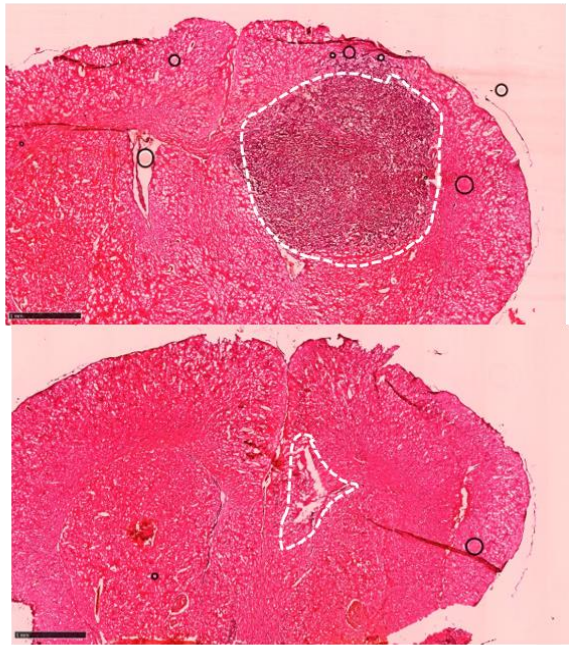
F

`

Figure 28: UMBO dramatically increases the efficacy of anti-PD-L1 in GL261-bearing mice. Panel A: Repeated UMBO application alone does not affect OS and mouse body weight in GL261-bearing mice compared to non-treated mice. Panel B: Schematic representation of the timeline used for UMBO plus anti-PD-L1 treatments. Panel C: All treatments have no impact on mice body weight. Panel D: bioluminescence measures normalized to the first measured value performed on day 7 after cell inoculation in GL261-bearing mice model. Each dot represents values for one animal and the line represents the mean value for the group. Bioluminescence signal was measured weekly. Dotted lines represent the days of treatments. Panel E: UMBO plus anti-PD-L1 increased overall survival: *$p<0.05$ compared to anti-PD-L1 alone and ***$p<0.0001$ compared to vehicle-treated group Panel F: Comparison of tumor size in UMBO plus anti-PD-L1 at day 45 compared to anti-PD-L1 treated mouse in GL261-bearing mice.

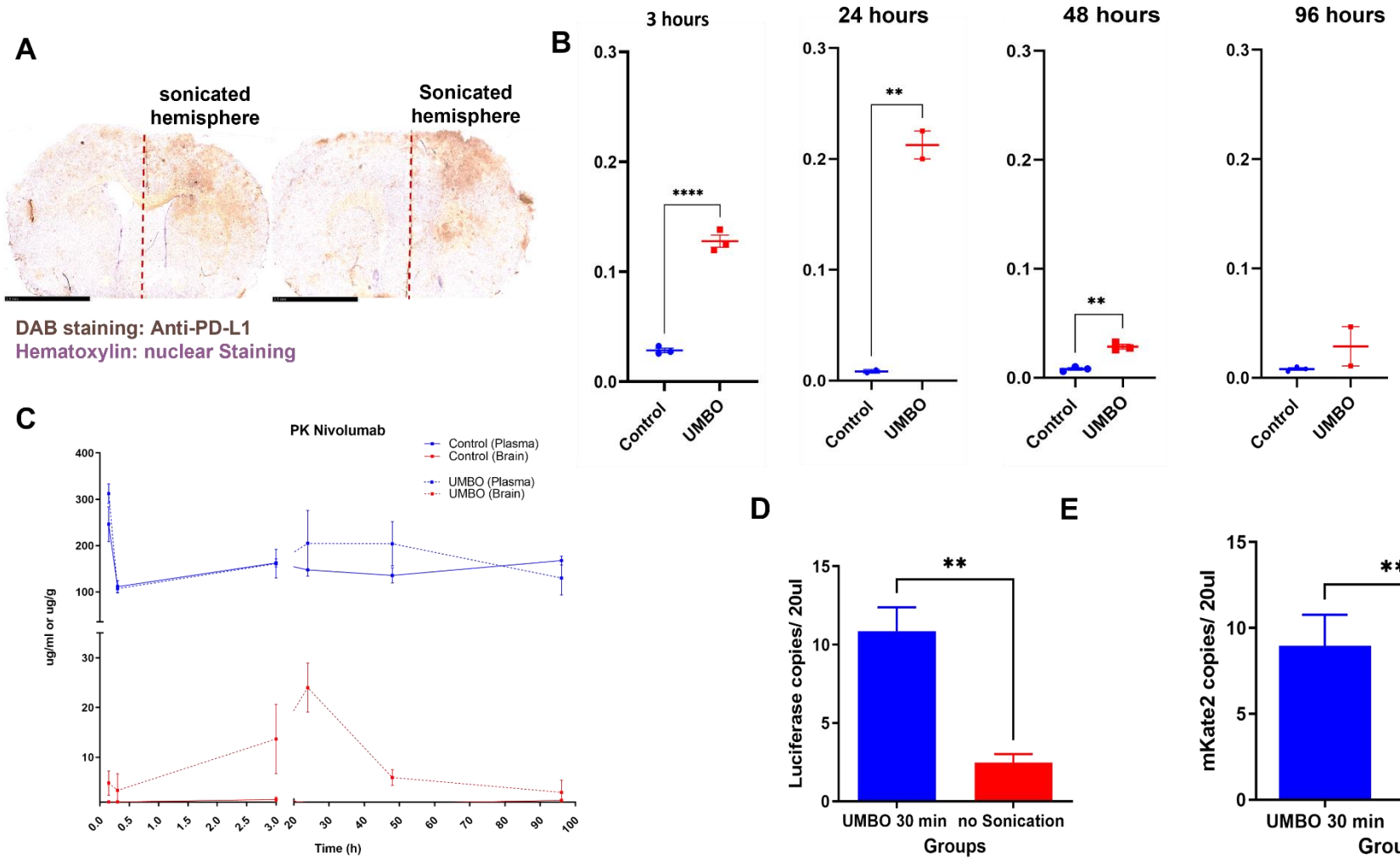
A
sonicated hemisphere
Sonicated hemisphere
DAB staining: Anti-PD-L1
Hematoxylin: nuclear Staining
B
3 hours
24 hours
48 hours
96 hours
Control
UMBO
C
PK Nivolumab
Control (Plasma)
Control (Brain)
UMBO (Plasma)
UMBO (Brain)
ug/ml or ug/g
Time (h)
D
Luciferase copies/ 20ul
UMBO 30 min
no Sonication
Groups
E
mKate2 copies/ 20ul
UMBO 30 min
No sonication
Groups

`

Figure 29: UMBO increased the penetration of ICBs into brain parenchyma. Panel A: IHC staining of anti-PD-L1 (BXCELL, in the brain parenchyma showing greater staining in the UMBO-targeted right hemisphere. Panel B: Pharmacokinetic analysis of Nivolumab concentration in the C57BL/6 mice blood and brain. Panel C: Brain/plasma ratio of nivolumab concentration over time. UMBO enhanced the brain/plasma ratio of nivolumab compared to control mice. Panel D: ddPCR analysis of Luciferase DNA in the blood 30 minutes following UMBO. Panel E: ddPCR analysis of mKate2 DNA in the blood 30 minutes following UMBO.

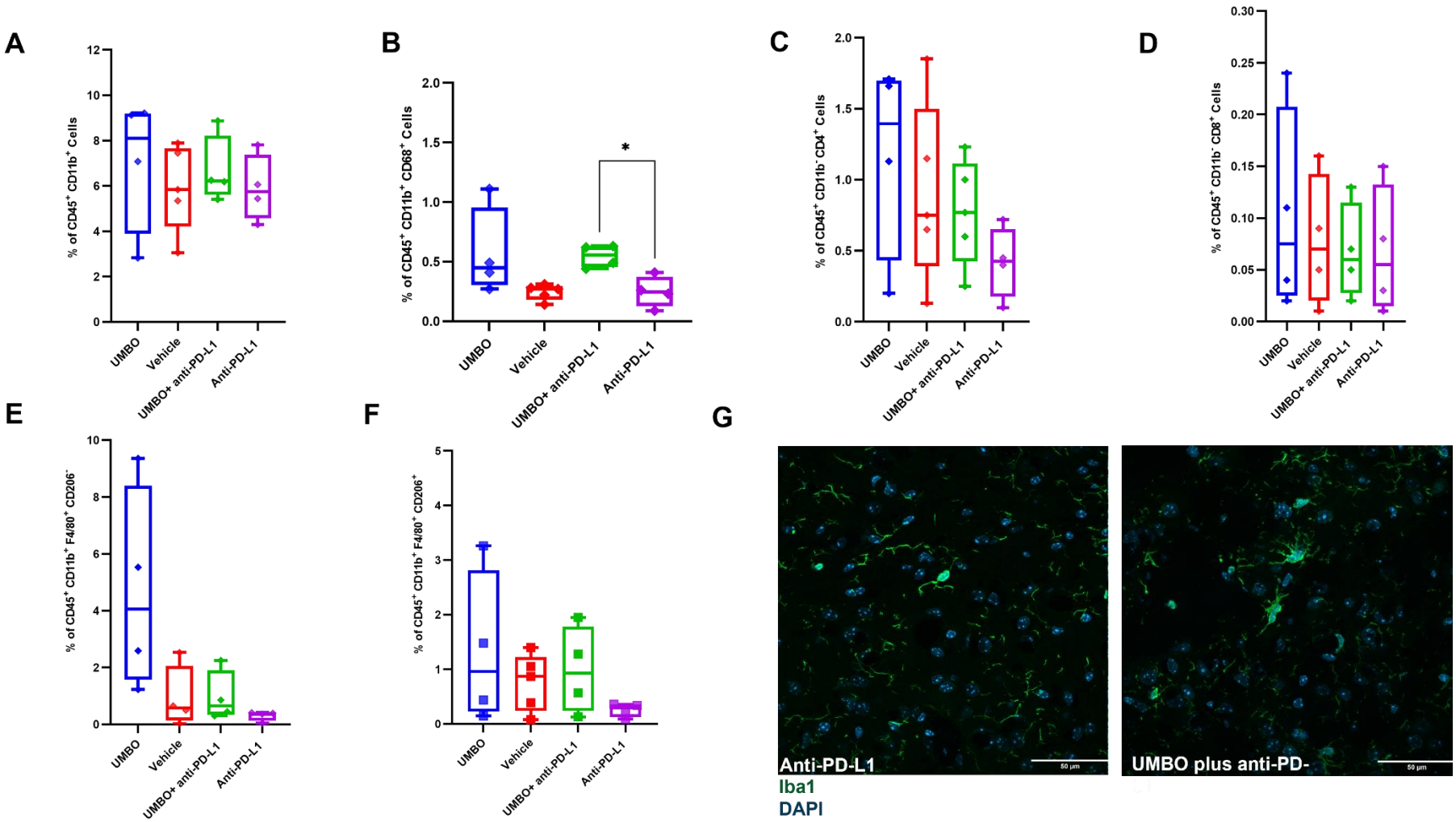
A
% of CD45+ CD11b+ Cells
B
% of CD45+ CD11b+ CD68+ Cells
*
C
% of CD45+ CD11b- CD4+ Cells
D
% of CD45+ CD11b- CD8+ Cells
E
% of CD45+ CD11b+ F4/80+ CD206-
F
% of CD45+ CD11b+ F4/80+ CD206+
UMBO
Vehicle
UMBO+ anti-PD-L1
Anti-PD-L1
G
Anti-PD-L1
UMBO plus anti-PD-
Iba1
DAPI

`

Figure 30: UMBO plus anti-PD-L1 activates microglia and modulates microglial phenotype. Panel A: Flow cytometry analysis of the percentage of total microglia in all different groups (n=4-5). Panel B: UMBO plus anti-PD-L1 significantly enhanced (*$p<0.05$) the percentage of $CD68^+$ cells than anti-PD-L1 alone. Panel C-D: UMBO plus anti-PD-L1 did not influence $CD4^+$ and $CD8^+$ T-lymphocytes percentages compared to other groups. Panel E-F: No significant difference in $CD206^+$ and $CD206^-$ macrophages in all groups. UMBO plus anti-PD-L1 did not modulate macrophages' expression. Panel G: Green: Iba1 microglia/macrophages Blue: DAPI nuclear staining; microglia staining in anti-PD-L1 plus UMBO (right photos) treated group confirm a phenotype of activated microglia. Double nuclear staining in the UMBO plus anti-PD-L1 staining shows a possible induction of microglia cell division.

`

General Discussion

TME is of growing interest in oncology and neuro-oncology. Anti-angiogenic and immune monoclonal antibodies have demonstrated that modulation of TME could be beneficial in anti-tumor therapy in multiple cancer. Cancer cells alone should not be the unique therapeutic target.

TME includes a cellular compartment and an acellular compartment. To elaborate more, the cellular compartment includes (i) vascular cells, (ii) normal tissue-specific cells, (iii) hematopoietic cells (iv) immune cells i.e., lymphocytes, and macrophages. They are involved in various immune responses and inflammatory reactions. The most prominent immune cell type in the TME of solid tumors is macrophages. Macrophages have diverse functions linked to GBM development and progression and can suppress antitumor immune mechanisms and responses. On the other hand, the acellular compartment includes: (i) structural proteins (ii) signaling molecules. All these components have an impact on GBM progression.

TME in GBM is peculiar compared to TME in non-neurological cancers. Indeed, the brain is an immune-privileged organ, glymphatic recently discovered in animal models and is primarily active during sleep and neuropathological disorders. Besides, the BBB protects the brain, limiting the exchange between the normal and tumor brain and the rest of the body. By controlling these exchanges, the BBB reduces endogenous (i.e., host immune system) and exogenous (i.e., medicines) anti-tumor molecular and cellular interventions against brain cancer. This thesis main goal is to investigate how TME modulation such as BBB disruption may overcome the resistance of GBM to anti-tumor treatments.

`

A. ABC transporters as a GBM TME therapeutic target

A few ABC transporters are predominantly expressed in ECs of the BBB (Mahringer and Fricker, 2016). Indeed, ABCB1 and ABCG2 are expressed in ECs of the BBB, while others (ABCC, ABCG2) can be found in other cells such as astrocytes and neurons (Linton and Higgins, 2007, Shen and Zhang, 2010, Mahringer and Fricker, 2016).

We reviewed the effect of ABC transporters in GBM chemoresistance. Furthermore, we summarized all the original research articles that have been published to discuss the role of ABC transporters in GBM chemoresistance, and the strategies that have been developed to overcome their negative effects for therapy purposes.

In the literature review article, we showed that ABCB1, ABCG2, and ABCC1 are the most studied ABC transporters in GBM. Furthermore, we discussed the failure of ABC protein blocking strategy to show significant clinical benefit. Although a limited number of clinical trials were initiated to modulate ABC proteins, the clinical benefit from these studies was hardly met and could be related to a few reasons. Firstly, the study design was not optimal, i.e., in the early clinical trials, the patients were not stratified based on high expression of ABC proteins, and a precise evaluation of the role of ABCB1 and ABCG2 transporters in patients could not be conducted. Secondly, modulators of ABC proteins could change the pharmacokinetics of other drugs reducing their anti-tumor properties. Finally, the dose of inhibitors selected to inhibit the ABC protein was perhaps not sufficient, or a higher dose could not be applied safely in patients.

The selection of cancer cell lines is a crucial step in *in vitro* studies dedicated to GBM. Many commercial human cell lines are available for GBM. Our group showed previously that patient-derived cell lines (PDCL) recapitulated better ABC gene expression patterns

`

of human GBM compared to commercial cell lines and can thus be considered a better model to test the biology of ABC proteins in GBM. Besides, we found that fetal bovine serum that is usually added to the cell culture medium for commercial GBM cell lines modulates resistance to TMZ. Moreover, the high passaging number of commercial GBM cell lines could change the expression level of ABC protein and could lead to conclusions irrelevant to newly diagnosed human tumors.

Finally, we summarized the strategies that are developed to overcome the ABC transporters-induced chemoresistance in GBM. Strategies vary from partial to complete chemical or physical inhibition of ABC transporter to approaches that overcome ABC efflux pumps *i.e.,* (i) nanocarriers technologies, (ii) antibody-drug conjugates and (iii) UMBO. Inhibition of ABC transporters limits the efflux of therapeutic agents from ECs to blood and increase their penetration into the normal and the tumor brain. In addition to chemical or pharmaceutical inhibition of ABC proteins, physical disruption approaches may also by-pass the BBB. Indeed, recently, ultrasound application was shown to inhibit the expression of ABC transporters. UMBO could decrease the expression of ABCB1 protein in cerebral vessels without affecting the integrity of other proteins (Choi et al., 2019). More studies should be performed to evaluate the role of UMBO to bypass the BBB and their role in enhancing the efficacy of chemotherapies in GBM.

`

B. Clinical significance of GBM TME protein

The expression of CD80 and CD86 in GBM tissues and their prognostic significance was not reported before. We have investigated the mRNA and protein expression of CD80 and CD86 in newly diagnosed GBM patients aged below 70 and with KPS above 70 treated with the standard of care. We have observed a link between CD80 and CD86 expression to prognosis and, more specifically, PFS in our local discovery cohort and the TCGA dataset.

CD80 and CD86 are expressed in the GBM tumor bulk. We assumed that CD80 and CD86 are mainly expressed by GBM cells. Nonetheless, additional studies are required to identify cells expressing these proteins considering all tumor bulk cell populations (*i.e.,* tumor cells and TME components). Low expression of CD80 and CD86 are associated with better prognosis in terms of PFS in newly diagnosed GBM. CD80 and CD86 act as T-lymphocytes inhibitors; we hypothesized that CD80-low/CD86-low GBM is more permissive for cytotoxic T-lymphocytes. In the same line, CD80-high/CD86-high GBM should respond better to anti-CTLA-4 immunotherapeutic antibodies.

Although we failed to demonstrate that CD80 and CD86 are independent prognostic factors in newly diagnosed GBM, probably due to the limited statistical power of our local discovery cohort, a trend was observed. This observation supports investigations of GBM TME features as prognostic or predictive factors in GBM. Indeed, composite biomarkers based on patient characteristics, tumor characteristics, and TME characteristics might be more powerful to guide prognostic evaluation and drug prescription (Russell et al., 2018)

`

C. UMBO enhances delivery and efficacy of ICBs through modulation of the GBM immune TME

Immunotherapies, including ICBs and cell therapies, have revolutionized the treatment of multiple solid tumors through activating the general antitumor immune response. In GBM, the earliest clinical trials evaluating the effect of nivolumab monotherapy or in combination with ipilimumab showed a limited efficacy with multiples toxicities. CheckMate-143 phase 3 clinical trial was then initiated to evaluate the effect of nivolumab versus bevacizumab. Unfortunately, nivolumab did not demonstrate higher efficacy over bevacizumab. A few reasons might explain the low efficacy of ICBs in GBM: (i) low tumor mutation load within GBM cells, (ii) lack of predictor of response to guide prescription, (iii) low penetration of ICBs within the brain parenchyma, (iv) low peripheral immune priming in lymph nodes, (v) local TME immunosuppression, (vi) low penetration of lymphocytes within the normal and the tumor brain (Hodges et al., 2017, Galstyan et al., 2019, Beccaria et al., 2020).

Our first data confirmed the limitation of ICBs efficacy in GL261 and Nfpp10 GBM mouse model. Consistent with our data, preclinical evaluation of anti-PD-L1 and anti-CTLA-4 in GL261 showed comparable limited efficacy of both antibodies in GL261 GBM mouse model. Their study has used a different treatment regimen, yet the efficacy was comparable (Reardon et al., 2016). Therefore, we have investigated ICBs combined with UMBO in murine preclinical models of GBM to overcome some of these limitations.

UMBO parameters, i.e., acoustic pressure, time, microbubbles dose, and ultrasound waves frequency, influence UMBO's safety and efficacy. The safety and the efficacy of UMBO were evaluated in C57BL/6 mice bearing GL261 tumor cells. UMBO was optimized to target the right hemisphere where the GBM cells are grafted. Additionally, each mouse

`

model should be subjected to an in-depth evaluation of the UMBO parameters. Here, I evaluated UMBO parameters and treatment frequency in GL261 GBM mouse models. T1-weighted MRI results described previously showed a marked gadolinium contrast enhancement within an hour following UMBO. The large area of UMBO opening in animal models suggest a larger delivery of the therapeutic antibodies to the normal and tumor brain, a larger penetration of T-lymphocytes within the normal and tumor brain, and a larger circulation of tumor antigen from the brain to blood for better priming.

Antibody sequence is crucial in the nano-surface and molecular-orientation limited (nSMOL) proteolysis method to measure the antibody through mass spectroscopy (LC-MS). nSMOL method identify a signature peptide *i.e.,* nivolumab signature peptide was identified as ASGGITFSNSGMHWVR. To identity the signature peptide antibody sequencing should be performed. We have obtained our murine anti-PD-L1 antibody from Genentech, USA through material transfer agreement. This agreement did not allow any sequencing of the antibody. Therefore, we have used nivolumab for this purpose. On the other hand, we have optimized our in-house ELISA analysis to study the pharmacokinetics of anti-PD-L1. This experiment is currently under analysis.

Nivolumab concentration in the brain parenchyma was enhanced up to 28 folds following UMBO. In our setting, UMBO was optimized to distributing one hemisphere. In our pharmacokinetics analysis, we have used a whole-brain homogenization method instead of one hemisphere homogenization. Consequently, local concentrations of nivolumab within the sonicated hemisphere are probably higher. Consistent with our data, a study has shown that UMBO enhanced the delivery of bevacizumab ~149 KDa to the brain parenchyma by 5.7- to 56.7-fold compared to non-sonicated brain in a glioma

`

mouse model (Liu et al., 2016). An already planned experiment with optimized ELISA analysis is going to be done in the foreseen weeks to identify the pharmacokinetics of anti-PD-L1 (Genentech, 6E11) with and without UMBO.

In the other direction, we have investigated the passage of tumor molecules from the tumor bulk to blood flow stream. Significant number of GL261 copies were identified in the blood stream of mice treated with UMBO 30 min prior to blood collection. We can demonstrate that tumor DNA in whole blood is higher in GL261-bearing mice treated with UMBO compared to their counterparts without UMBO. We hypothesized that this increase of tumor DNA passage may increase T-lymphocytes priming. However, this hypothesis remains to be tested. Furthermore, additional experiments to study the effect of UMBO at different time point to follow the fate of GL261 DNA in the blood stream overtime.

We initially hypothesized that the BBB was responsible for the limited efficacy by mainly blocking anti-CTLA-4 and anti-PD-L1 from reaching the GBM tumor. This hypothesis is consistent with two recent studies that reported an enhanced efficacy of ICBs following their brain tumor . Interestingly we have observed an enhanced efficacy of anti-PD-L1 when delivered after UMBO. 76 % long-term survival (over 100 days) compared to (4/15) 26 % in anti-PD-L1 alone in GL261-bearing mice.

A possible effect on microglia's phenotype might be observed as an effect and anti-PD-L1 delivery plus UMBO to the brain parenchyma. Therefore, our foreseen flow cytometry analysis of immune cell populations is inevitable to support this observation.

`

General Conclusion

The clinical role of ABC proteins is still under investigation, and the failure of previous clinical trials raised several questions regarding the strategies to overcome MDR in GBM A wide range of *in vitro* and *in vivo* models could allow precise testing of the novel drugs. One of the most important models is the utilization of low passaging of PDCLs which carry the molecular features of ABC efflux pumps. Furthermore, dual ABC inhibitors with a high specificity could be developed for more effective treatment strategies.

There are multiple immune pathways involved in antitumor immunity. Because of the complexity and evolution of tumor immune responses, it is impossible to rely on blockade of one or two inhibitory pathways to elicit long-lasting or curative antitumor effects for many patients. Combination therapies are being developed *i.e.,* between (i) chemotherapies and ICBs, (ii) ICBs and vaccines, (iii) block multiple immune inhibitory pathways or provide agonists to activate the immune stimulatory pathways. It is reasonable to develop markers to guide future combination therapy strategies and for patient stratifications to hopefully increase response rates in clinical trials.

Finally, my thesis opens new avenues for the efficacy of UMBO to deliver antibodies and in the treatment of GBM. Indeed, further studies should be warranted before the translation of this work to clinical trials. ICBs plus chemotherapies are currently being evaluated in clinical trials. Combinational therapies of UMBO plus TMZ and ICBs could be evaluated as a next step. Furthermore, UMBO was able to deliver both chemotherapies and antibodies to the brain. Additional treatments as cellular therapy or vaccinations could be delivered using UMBO *in vivo* studies.

`

References

(11C)dLop as a Marker of P-Glycoprotein Function in Patients With Gliomas [Online]. Available: https://clinicaltrials.gov/ct2/show/NCT01281982?id=NCT01281982&draw=2&rank=1&load=cart [Accessed].

Raymond GV, Moser AB, Fatemi A. X-Linked Adrenoleukodystrophy. 1999 Mar 26 [Updated 2018 Feb 15]. In: Adam MP, Ardinger HH, Pagon RA, et al., editors. GeneReviews® [Internet]. Seattle (WA): University of Washington, Seattle; 1993-2020. Bookshelf URL: https://www.ncbi.nlm.nih.gov/books/.

AGARWAL, S., MITTAPALLI, R. K., ZELLMER, D. M., GALLARDO, J. L., DONELSON, R., SEILER, C., DECKER, S. A., SANTACRUZ, K. S., POKORNY, J. L., SARKARIA, J. N., ELMQUIST, W. F. & OHLFEST, J. R. 2012. Active efflux of Dasatinib from the brain limits efficacy against murine glioblastoma: broad implications for the clinical use of molecularly targeted agents. *Mol Cancer Ther,* 11**,** 2183-92.

AIT-BELKACEM, R., BERENGUER, C., VILLARD, C., OUAFIK, L., FIGARELLA-BRANGER, D., BECK, A., CHINOT, O. & LAFITTE, D. 2014. Monitoring therapeutic monoclonal antibodies in brain tumor. *MAbs,* 6**,** 1385-93.

AL RIHANI, S. B., DARAKJIAN, L. I., DEODHAR, M., DOW, P., TURGEON, J. & MICHAUD, V. 2021. Disease-Induced Modulation of Drug Transporters at the Blood-Brain Barrier Level. *Int J Mol Sci,* 22.

ALECOU, T., GIANNAKOU, M. & DAMIANOU, C. 2017. Amyloid β Plaque Reduction With Antibodies Crossing the Blood-Brain Barrier, Which Was Opened in 3 Sessions of Focused Ultrasound in a Rabbit Model. *J Ultrasound Med,* 36**,** 2257-2270.

AMARAL, T., KIECKER, F., SCHAEFER, S., STEGE, H., KAEHLER, K., TERHEYDEN, P., GESIERICH, A., GUTZMER, R., HAFERKAMP, S., UTTIKAL, J., BERKING, C., RAFEI-SHAMSABADI, D., REINHARDT, L., MEIER, F., KAROGLAN, A., POSCH, C., GAMBICHLER, T., PFOEHLER, C., THOMS, K., TIETZE, J., DEBUS, D., HERBST, R., EMMERT, S., LOQUAI, C., HASSEL, J. C., MEISS, F., TUETING, T., HEINRICH, V., EIGENTLER, T., GARBE, C. & ZIMMER, L. 2020. Combined immunotherapy with nivolumab and ipilimumab with and without local therapy in patients with melanoma brain metastasis: a DeCOG* study in 380 patients. *J Immunother Cancer,* 8.

ASHBY, L. S., SMITH, K. A. & STEA, B. 2016. Gliadel wafer implantation combined with standard radiotherapy and concurrent followed by adjuvant temozolomide for treatment of newly diagnosed high-grade glioma: a systematic literature review. *World J Surg Oncol,* 14**,** 225.

ASLAN, K., TURCO, V., BLOBNER, J., SONNER, J. K., LIUZZI, A. R., NÚÑEZ, N. G., DE FEO, D., KICKINGEREDER, P., FISCHER, M., GREEN, E., SADIK, A., FRIEDRICH, M., SANGHVI, K., KILIAN, M., CICHON, F., WOLF, L., JÄHNE, K., VON LANDENBERG, A., BUNSE, L., SAHM, F., SCHRIMPF, D., MEYER, J., ALEXANDER, A., BRUGNARA, G.,

RÖTH, R., PFLEIDERER, K., NIESLER, B., VON DEIMLING, A., OPITZ, C., BRECKWOLDT, M. O., HEILAND, S., BENDSZUS, M., WICK, W., BECHER, B. & PLATTEN, M. 2020. Heterogeneity of response to immune checkpoint blockade in hypermutated experimental gliomas. *Nature Communications,* 11**,** 931.

ATIQ, A. & PARHAR, I. 2020. Anti-neoplastic Potential of Flavonoids and Polysaccharide Phytochemicals in Glioblastoma. *Molecules,* 25.

ATLAS, H. P. *ABCG2 Human protein expression* [Online]. Available: https://www.proteinatlas.org/ENSG00000118777-ABCG2/tissue [Accessed].

ATLAS, T. H. P. 2020. Available: https://www.proteinatlas.org/ENSG00000085563-ABCB1/tissue [Accessed].

AZOURY, S. C., STRAUGHAN, D. M. & SHUKLA, V. 2015. Immune Checkpoint Inhibitors for Cancer Therapy: Clinical Efficacy and Safety. *Curr Cancer Drug Targets,* 15**,** 452-62.

BALAYSSAC, D., CAYRE, A., AUTHIER, N., BOURDU, S., PENAULT-LLORCA, F., GILLET, J. P., MAUBLANT, J., ESCHALIER, A. & COUDORE, F. 2005. Patterns of P-glycoprotein activity in the nervous system during vincristine-induced neuropathy in rats. *J Peripher Nerv Syst,* 10**,** 301-10.

BALKWILL, F. & MANTOVANI, A. 2001. Inflammation and cancer: back to Virchow? *Lancet,* 357**,** 539-45.

BARUA, N. U., HOPKINS, K., WOOLLEY, M., O'SULLIVAN, S., HARRISON, R., EDWARDS, R. J., BIENEMANN, A. S., WYATT, M. J., ARSHAD, A. & GILL, S. S. 2016. A novel implantable catheter system with transcutaneous port for intermittent convection-enhanced delivery of carboplatin for recurrent glioblastoma. *Drug Deliv,* 23**,** 167-73.

BAUER, M., ROMERMANN, K., KARCH, R., WULKERSDORFER, B., STANEK, J., PHILIPPE, C., MAIER-SALAMON, A., HASLACHER, H., JUNGBAUER, C., WADSAK, W., JAGER, W., LOSCHER, W., HACKER, M., ZEITLINGER, M. & LANGER, O. 2016. Pilot PET Study to Assess the Functional Interplay Between ABCB1 and ABCG2 at the Human Blood-Brain Barrier. *Clin Pharmacol Ther,* 100**,** 131-41.

BECCARIA, K., CANNEY, M., BOUCHOUX, G., DESSEAUX, C., GRILL, J., HEIMBERGER, A. B. & CARPENTIER, A. 2020. Ultrasound-induced blood-brain barrier disruption for the treatment of gliomas and other primary CNS tumors. *Cancer Lett,* 479**,** 13-22.

BECCARIA, K., CANNEY, M., GOLDWIRT, L., FERNANDEZ, C., PIQUET, J., PERIER, M. C., LAFON, C., CHAPELON, J. Y. & CARPENTIER, A. 2016. Ultrasound-induced opening of the blood-brain barrier to enhance temozolomide and irinotecan delivery: an experimental study in rabbits. *J Neurosurg,* 124**,** 1602-10.

BEIER, C. P., SCHMID, C., GORLIA, T., KLEINLETZENBERGER, C., BEIER, D., GRAUER, O., STEINBRECHER, A., HIRSCHMANN, B., BRAWANSKI, A., DIETMAIER, C., JAUCH-WORLEY, T., KÖLBL, O., PIETSCH, T., PROESCHOLDT, M., RÜMMELE, P., MUIGG, A., STOCKHAMMER, G., HEGI, M., BOGDAHN, U. & HAU, P. 2009. RNOP-09: pegylated liposomal doxorubicine and prolonged temozolomide in addition to radiotherapy in newly diagnosed glioblastoma--a phase II study. *BMC Cancer,* 9**,** 308.

BERGHOFF, A. S., KIESEL, B., WIDHALM, G., WILHELM, D., RAJKY, O., KURSCHEID, S., KRESL, P., WÖHRER, A., MAROSI, C., HEGI, M. E. & PREUSSER, M. 2017. Correlation of immune phenotype with IDH mutation in diffuse glioma. *Neuro-Oncology,* 19**,** 1460-1468.

BORST, P. & SCHINKEL, A. H. 2013. P-glycoprotein ABCB1: a major player in drug handling by mammals. *J Clin Invest,* 123**,** 4131-3.

BRAT, D. J., ALDAPE, K., COLMAN, H., FIGRARELLA-BRANGER, D., FULLER, G. N., GIANNINI, C., HOLLAND, E. C., JENKINS, R. B., KLEINSCHMIDT-DEMASTERS, B., KOMORI, T., KROS, J. M., LOUIS, D. N., MCLEAN, C., PERRY, A., REIFENBERGER, G., SARKAR, C., STUPP, R., VAN DEN BENT, M. J., VON DEIMLING, A. & WELLER, M. 2020. cIMPACT-NOW update 5: recommended grading criteria and terminologies for IDH-mutant astrocytomas. *Acta Neuropathol,* 139**,** 603-608.

BREM, S. 1976. The role of vascular proliferation in the growth of brain tumors. *Clin Neurosurg,* 23**,** 440-53.

BROEKMAN, M. L., MAAS, S. L. N., ABELS, E. R., MEMPEL, T. R., KRICHEVSKY, A. M. & BREAKEFIELD, X. O. 2018. Multidimensional communication in the microenvirons of glioblastoma. *Nat Rev Neurol,* 14**,** 482-495.

CAO, Y., LI, X., KONG, S., SHANG, S. & QI, Y. 2020. CDK4/6 inhibition suppresses tumour growth and enhances the effect of temozolomide in glioma cells. *J Cell Mol Med,* 24**,** 5135-5145.

CARLSON, R. D., FLICKINGER, J. C., JR. & SNOOK, A. E. 2020. Talkin' Toxins: From Coley's to Modern Cancer Immunotherapy. *Toxins,* 12**,** 241.

CARPENTIER, A., CANNEY, M., VIGNOT, A., REINA, V., BECCARIA, K., HORODYCKID, C., KARACHI, C., LECLERCQ, D., LAFON, C., CHAPELON, J. Y., CAPELLE, L., CORNU, P., SANSON, M., HOANG-XUAN, K., DELATTRE, J. Y. & IDBAIH, A. 2016. Clinical trial of blood-brain barrier disruption by pulsed ultrasound. *Sci Transl Med,* 8.

CHANG, C. S., CHANG, J. H., HSU, N. C., LIN, H. Y. & CHUNG, C. Y. 2007. Expression of CD80 and CD86 costimulatory molecules are potential markers for better survival in nasopharyngeal carcinoma. *BMC Cancer,* 7**,** 88.

`

CHAVES, C., SHAWAHNA, R., JACOB, A., SCHERRMANN, J. M. & DECLEVES, X. 2014. Human ABC transporters at blood-CNS interfaces as determinants of CNS drug penetration. *Curr Pharm Des,* 20**,** 1450-62.

CHEN, D. S. & MELLMAN, I. 2013. Oncology meets immunology: the cancer-immunity cycle. *Immunity,* 39**,** 1-10.

CHEN, J., MCKAY, R. M. & PARADA, L. F. 2012. Malignant glioma: lessons from genomics, mouse models, and stem cells. *Cell,* 149**,** 36-47.

CHEN, K.-T., WEI, K.-C. & LIU, H.-L. 2019a. Theranostic Strategy of Focused Ultrasound Induced Blood-Brain Barrier Opening for CNS Disease Treatment. 10.

CHEN, Q., XU, L., DU, T., HOU, Y., FAN, W., WU, Q. & YAN, H. 2019b. Enhanced Expression of PD-L1 on Microglia After Surgical Brain Injury Exerts Self-Protection from Inflammation and Promotes Neurological Repair. *Neurochem Res,* 44**,** 2470-2481.

CHO, E. E., DRAZIC, J., GANGULY, M., STEFANOVIC, B. & HYNYNEN, K. 2011. Two-photon fluorescence microscopy study of cerebrovascular dynamics in ultrasound-induced blood-brain barrier opening. *J Cereb Blood Flow Metab,* 31**,** 1852-62.

CHOI, H., LEE, E. H., HAN, M., AN, S. H. & PARK, J. 2019. Diminished Expression of P-glycoprotein Using Focused Ultrasound Is Associated With JNK-Dependent Signaling Pathway in Cerebral Blood Vessels. *Front Neurosci,* 13**,** 1350.

CHUA, C., ZAIDEN, N., CHONG, K. H., SEE, S. J., WONG, M. C., ANG, B. T. & TANG, C. 2008. Characterization of a side population of astrocytoma cells in response to temozolomide. *J Neurosurg,* 109**,** 856-66.

CLARKE, J. L., MOLINARO, A. M., DESILVA, A. A., RABBITT, J. E., DRUMMOND, D. C., CHANG, S. M., BUTOWSKI, N. A. & PRADOS, M. 2015. A phase I trial of intravenous liposomal irinotecan in patients with recurrent high-grade gliomas. *Journal of Clinical Oncology,* 33**,** 2029-2029.

COLE, S. P., BHARDWAJ, G., GERLACH, J. H., MACKIE, J. E., GRANT, C. E., ALMQUIST, K. C., STEWART, A. J., KURZ, E. U., DUNCAN, A. M. & DEELEY, R. G. 1992. Overexpression of a transporter gene in a multidrug-resistant human lung cancer cell line. *Science,* 258**,** 1650-4.

CRESPO, I., VITAL, A. L., GONZALEZ-TABLAS, M., PATINO MDEL, C., OTERO, A., LOPES, M. C., DE OLIVEIRA, C., DOMINGUES, P., ORFAO, A. & TABERNERO, M. D. 2015. Molecular and Genomic Alterations in Glioblastoma Multiforme. *Am J Pathol,* 185**,** 1820-33.

`

DAUBA, A., DELALANDE, A., KAMIMURA, H. A. S., CONTI, A., LARRAT, B., TSAPIS, N. & NOVELL, A. 2020. Recent Advances on Ultrasound Contrast Agents for Blood-Brain Barrier Opening with Focused Ultrasound. *Pharmaceutics,* 12.

DE GOOIJER, M. C., BUIL, L. C. M., CITIRIKKAYA, C. H., HERMANS, J., BEIJNEN, J. H. & VAN TELLINGEN, O. 2018a. ABCB1 Attenuates the Brain Penetration of the PARP Inhibitor AZD2461. *Mol Pharm,* 15**,** 5236-5243.

DE GOOIJER, M. C., DE VRIES, N. A., BUCKLE, T., BUIL, L. C. M., BEIJNEN, J. H., BOOGERD, W. & VAN TELLINGEN, O. 2018b. Improved Brain Penetration and Antitumor Efficacy of Temozolomide by Inhibition of ABCB1 and ABCG2. *Neoplasia,* 20**,** 710-720.

DE LEO, A., UGOLINI, A. & VEGLIA, F. 2020. Myeloid Cells in Glioblastoma Microenvironment. *Cells,* 10.

DEELEY, R. G., WESTLAKE, C. & COLE, S. P. 2006. Transmembrane transport of endo- and xenobiotics by mammalian ATP-binding cassette multidrug resistance proteins. *Physiol Rev,* 86**,** 849-99.

DESLAND, F. A. & HORMIGO, A. 2020. The CNS and the Brain Tumor Microenvironment: Implications for Glioblastoma Immunotherapy. *Int J Mol Sci,* 21.

DESOUZA, R. M., SHAWEIS, H., HAN, C., SIVASUBRAMANIAM, V., BRAZIL, L., BEANEY, R., SADLER, G., AL-SARRAJ, S., HAMPTON, T., LOGAN, J., HURWITZ, V., BHANGOO, R., GULLAN, R. & ASHKAN, K. 2016. Has the survival of patients with glioblastoma changed over the years? *Br J Cancer,* 114**,** 146-50.

DOYLE, L. A., YANG, W., ABRUZZO, L. V., KROGMANN, T., GAO, Y., RISHI, A. K. & ROSS, D. D. 1998. A multidrug resistance transporter from human MCF-7 breast cancer cells. *Proc Natl Acad Sci U S A,* 95**,** 15665-70.

DREAN, A., GOLDWIRT, L., VERREAULT, M., CANNEY, M., SCHMITT, C., GUEHENNEC, J., DELATTRE, J. Y., CARPENTIER, A. & IDBAIH, A. 2016. Blood-brain barrier, cytotoxic chemotherapies and glioblastoma. *Expert Rev Neurother,* 16**,** 1285-1300.

DRÉAN, A., LEMAIRE, N., BOUCHOUX, G., GOLDWIRT, L., CANNEY, M., GOLI, L., BOUZIDI, A., SCHMITT, C., GUEHENNEC, J., VERREAULT, M., SANSON, M., DELATTRE, J. Y., MOKHTARI, K., SOTTILINI, F., CARPENTIER, A. & IDBAIH, A. 2019. Temporary blood-brain barrier disruption by low intensity pulsed ultrasound increases carboplatin delivery and efficacy in preclinical models of glioblastoma. *J Neurooncol,* 144**,** 33-41.

DREAN, A., ROSENBERG, S., LEJEUNE, F. X., GOLI, L., NADARADJANE, A. A., GUEHENNEC, J., SCHMITT, C., VERREAULT, M., BIELLE, F., MOKHTARI, K., SANSON, M., CARPENTIER, A., DELATTRE, J. Y. & IDBAIH, A. 2018a. ATP binding cassette (ABC) transporters: expression and clinical value in glioblastoma. *J Neurooncol,* 138**,** 479-486.

`

DREAN, A., ROSENBERG, S., LEJEUNE, F. X., GOLI, L., NADARADJANE, A. A., GUEHENNEC, J., SCHMITT, C., VERREAULT, M., BIELLE, F., MOKHTARI, K., SANSON, M., CARPENTIER, A., DELATTRE, J. Y. & IDBAIH, A. 2018b. Correction to: ATP binding cassette (ABC) transporters: expression and clinical value in glioblastoma. *J Neurooncol,* 138**,** 487.

DURMAZ, R., DELIORMAN, S., UYAR, R., ISIKSOY, S., EROL, K. & TEL, E. 1999. The effects of anticancer drugs in combination with nimodipine and verapamil on cultured cells of glioblastoma multiforme. *Clin Neurol Neurosurg,* 101**,** 238-44.

ELHAM, H., NOOSHIN, B. & HASSAN ALI, N. 2017. Cancer and Treatment Modalities. *Current Cancer Therapy Reviews,* 13**,** 17-27.

EMERY, I. F., GOPALAN, A., WOOD, S., CHOW, K. H., BATTELLI, C., GEORGE, J., BLASZYK, H., FLORMAN, J. & YUN, K. 2017. Expression and function of ABCG2 and XIAP in glioblastomas. *J Neurooncol,* 133**,** 47-57.

FAN, C. H., TING, C. Y., LIU, H. L., HUANG, C. Y., HSIEH, H. Y., YEN, T. C., WEI, K. C. & YEH, C. K. 2013. Antiangiogenic-targeting drug-loaded microbubbles combined with focused ultrasound for glioma treatment. *Biomaterials,* 34**,** 2142-55.

FAN, T. Y., WANG, H., XIANG, P., LIU, Y. W., LI, H. Z., LEI, B. X., YU, M. & QI, S. T. 2014. Inhibition of EZH2 reverses chemotherapeutic drug TMZ chemosensitivity in glioblastoma. *Int J Clin Exp Pathol,* 7**,** 6662-70.

FANG, J., CHEN, F., LIU, D., GU, F., CHEN, Z. & WANG, Y. 2020. Prognostic value of immune checkpoint molecules in breast cancer. *Biosci Rep,* 40.

FELLNER, S., BAUER, B., MILLER, D. S., SCHAFFRIK, M., FANKHANEL, M., SPRUSS, T., BERNHARDT, G., GRAEFF, C., FARBER, L., GSCHAIDMEIER, H., BUSCHAUER, A. & FRICKER, G. 2002. Transport of paclitaxel (Taxol) across the blood-brain barrier in vitro and in vivo. *J Clin Invest,* 110**,** 1309-18.

FENG, X. Y., LU, L., WANG, K. F., ZHU, B. Y., WEN, X. Z., PENG, R. Q., DING, Y., LI, D. D., LI, J. J., LI, Y. & ZHANG, X. S. 2019. Low expression of CD80 predicts for poor prognosis in patients with gastric adenocarcinoma. *Future Oncol,* 15**,** 473-483.

FINCH, A., SOLOMOU, G., WYKES, V., POHL, U., BARDELLA, C. & WATTS, C. 2021. Advances in Research of Adult Gliomas. *Int J Mol Sci,* 22.

FOMICHOV, V., BROHOLM, H., GRUNNET, K., POULSEN, H. S., BRATTHALL, C., STRANDEUS, M., PAPAGIANNOPOULOU, A., STENMARK-ASKMALM, M., GREEN, H. & SODERKVIST, P. *Pharmacogenomics J.*

`

FRANCESCHI, E., LAMBERTI, G., VISANI, M., PACCAPELO, A., MURA, A., TALLINI, G., PESSION, A., DE BIASE, D., MINICHILLO, S., TOSONI, A., DI BATTISTA, M., CUBEDDU, A., BARTOLINI, S. & BRANDES, A. A. 2018. Temozolomide rechallenge in recurrent glioblastoma: when is it useful? *Future Oncol,* 14**,** 1063-1069.

FRIEDMAN, H. S., KERBY, T. & CALVERT, H. 2000. Temozolomide and Treatment of Malignant Glioma. 6**,** 2585-2597.

FRIEDMANN-MORVINSKI, D., BUSHONG, E. A., KE, E., SODA, Y., MARUMOTO, T., SINGER, O., ELLISMAN, M. H. & VERMA, I. M. 2012. Dedifferentiation of Neurons and Astrocytes by Oncogenes Can Induce Gliomas in Mice. 338**,** 1080-1084.

FRUEHAUF, J. P., BREM, H., BREM, S., SLOAN, A., BARGER, G., HUANG, W. & PARKER, R. 2006. In vitro drug response and molecular markers associated with drug resistance in malignant gliomas. *Clin Cancer Res,* 12**,** 4523-32.

GALSTYAN, A., MARKMAN, J. L., SHATALOVA, E. S., CHIECHI, A., KORMAN, A. J., PATIL, R., KLYMYSHYN, D., TOURTELLOTTE, W. G., ISRAEL, L. L., BRAUBACH, O., LJUBIMOV, V. A., MASHOUF, L. A., RAMESH, A., GRODZINSKI, Z. B., PENICHET, M. L., BLACK, K. L., HOLLER, E., SUN, T., DING, H., LJUBIMOV, A. V. & LJUBIMOVA, J. Y. 2019. Blood-brain barrier permeable nano immunoconjugates induce local immune responses for glioma therapy. *Nat Commun,* 10**,** 3850.

GAN, H. K., VAN DEN BENT, M., LASSMAN, A. B., REARDON, D. A. & SCOTT, A. M. 2017. Antibody-drug conjugates in glioblastoma therapy: the right drugs to the right cells. *Nat Rev Clin Oncol,* 14**,** 695-707.

GAVILE, C. M., BARWICK, B. G., NEWMAN, S., NERI, P., NOOKA, A. K., LONIAL, S., LEE, K. P. & BOISE, L. H. 2017. CD86 regulates myeloma cell survival. *Blood Adv,* 1**,** 2307-2319.

GILLET, J. P. & GOTTESMAN, M. M. 2010. Mechanisms of multidrug resistance in cancer. *Methods Mol Biol,* 596**,** 47-76.

GOLDWIRT, L., BECCARIA, K., CARPENTIER, A., FARINOTTI, R. & FERNANDEZ, C. 2014. Irinotecan and temozolomide brain distribution: a focus on ABCB1. *Cancer Chemother Pharmacol,* 74**,** 185-93.

GOLDWIRT, L., CANNEY, M., HORODYCKID, C., POUPON, J., MOURAH, S., VIGNOT, A., CHAPELON, J. Y. & CARPENTIER, A. 2016. Enhanced brain distribution of carboplatin in a primate model after blood-brain barrier disruption using an implantable ultrasound device. *Cancer Chemother Pharmacol,* 77**,** 211-6.

GONZÁLEZ-TABLAS PIMENTA, M., OTERO, Á., ARANDIA GUZMAN, D. A., PASCUAL-ARGENTE, D., RUÍZ MARTÍN, L., SOUSA-CASASNOVAS, P., GARCÍA-MARTIN, A., ROA MONTES DE OCA, J. C., VILLASEÑOR-LEDEZMA, J., TORRES CARRETERO, L., ALMEIDA, M., ORTIZ, J., NIETO, A., ORFAO, A. & TABERNERO, M. D.

2021. Tumor cell and immune cell profiles in primary human glioblastoma: Impact on patient outcome. *Brain Pathol,* 31**,** 365-380.

GREENBAUM, D., COLANGELO, C., WILLIAMS, K. & GERSTEIN, M. 2003. Comparing protein abundance and mRNA expression levels on a genomic scale. *Genome Biology,* 4**,** 117.

GRÉGOIRE, H., RONCALI, L., ROUSSEAU, A., CHÉREL, M., DELNESTE, Y., JEANNIN, P., HINDRÉ, F. & GARCION, E. 2020. Targeting Tumor Associated Macrophages to Overcome Conventional Treatment Resistance in Glioblastoma. *Front Pharmacol,* 11**,** 368.

GUO, H., WANG, R., WANG, D., WANG, S., ZHOU, J., CHAI, Z., YAO, S., LI, J., LU, L., LIU, Y., XIE, C. & LU, W. 2020. Deliver anti-PD-L1 into brain by p-hydroxybenzoic acid to enhance immunotherapeutic effect for glioblastoma. *J Control Release,* 320**,** 63-72.

HAMBARDZUMYAN, D. & BERGERS, G. 2015. Glioblastoma: Defining Tumor Niches. *Trends Cancer,* 1**,** 252-265.

HAO, C., CHEN, G., ZHAO, H., LI, Y., CHEN, J., ZHANG, H., LI, S., ZHAO, Y., CHEN, F., LI, W. & JIANG, W. G. 2020. PD-L1 Expression in Glioblastoma, the Clinical and Prognostic Significance: A Systematic Literature Review and Meta-Analysis. *Front Oncol,* 10**,** 1015.

HARDEE, M. E. & ZAGZAG, D. 2012. Mechanisms of glioma-associated neovascularization. *Am J Pathol,* 181**,** 1126-41.

HASSENBUSCH, S. J., NARDONE, E. M., LEVIN, V. A., LEEDS, N. & PIETRONIGRO, D. 2003. Stereotactic injection of DTI-015 into recurrent malignant gliomas: phase I/II trial. *Neoplasia,* 5**,** 9-16.

HEGI, M. E., DISERENS, A.-C., GORLIA, T., HAMOU, M.-F., DE TRIBOLET, N., WELLER, M., KROS, J. M., HAINFELLNER, J. A., MASON, W., MARIANI, L., BROMBERG, J. E. C., HAU, P., MIRIMANOFF, R. O., CAIRNCROSS, J. G., JANZER, R. C. & STUPP, R. 2005. MGMT Gene Silencing and Benefit from Temozolomide in Glioblastoma. 352**,** 997-1003.

HERSEY, P., SI, Z., SMITH, M. J. & THOMAS, W. D. 1994. Expression of the co-stimulatory molecule B7 on melanoma cells. *Int J Cancer,* 58**,** 527-32.

HIRA, D. & TERADA, T. 2018. BCRP/ABCG2 and high-alert medications: Biochemical, pharmacokinetic, pharmacogenetic, and clinical implications. *Biochem Pharmacol,* 147**,** 201-210.

`

HODGES, T. R., OTT, M., XIU, J., GATALICA, Z., SWENSEN, J., ZHOU, S., HUSE, J. T., DE GROOT, J., LI, S., OVERWIJK, W. W., SPETZLER, D. & HEIMBERGER, A. B. 2017. Mutational burden, immune checkpoint expression, and mismatch repair in glioma: implications for immune checkpoint immunotherapy. *Neuro Oncol,* 19**,** 1047-1057.

HOLASH, J., MAISONPIERRE, P. C., COMPTON, D., BOLAND, P., ALEXANDER, C. R., ZAGZAG, D., YANCOPOULOS, G. D. & WIEGAND, S. J. 1999. Vessel cooption, regression, and growth in tumors mediated by angiopoietins and VEGF. *Science,* 284**,** 1994-8.

HSU, F. S., SU, C. H. & HUANG, K. H. 2017. A Comprehensive Review of US FDA-Approved Immune Checkpoint Inhibitors in Urothelial Carcinoma. *J Immunol Res,* 2017**,** 6940546.

HUANG, B., LI, X., LI, Y., ZHANG, J., ZONG, Z. & ZHANG, H. 2020. Current Immunotherapies for Glioblastoma Multiforme. *Front Immunol,* 11**,** 603911.

HUANG, P. W. & CHANG, J. W. 2019. Immune checkpoint inhibitors win the 2018 Nobel Prize. *Biomed J,* 42**,** 299-306.

HYNYNEN, K., MCDANNOLD, N., VYKHODTSEVA, N. & JOLESZ, F. A. 2001. Noninvasive MR imaging-guided focal opening of the blood-brain barrier in rabbits. *Radiology,* 220**,** 640-6.

IDBAIH, A., CANNEY, M., BELIN, L., DESSEAUX, C., VIGNOT, A., BOUCHOUX, G., ASQUIER, N., LAW-YE, B., LECLERCQ, D., BISSERY, A., DE RYCKE, Y., TROSCH, C., CAPELLE, L., SANSON, M., HOANG-XUAN, K., DEHAIS, C., HOUILLIER, C., LAIGLE-DONADEY, F., MATHON, B., ANDRÉ, A., LAFON, C., CHAPELON, J.-Y., DELATTRE, J.-Y. & CARPENTIER, A. 2019. Safety and Feasibility of Repeated and Transient Blood–Brain Barrier Disruption by Pulsed Ultrasound in Patients with Recurrent Glioblastoma. 25**,** 3793-3801.

INFORMATION, N. C. F. B. 2020. *Temozolomide* [Online]. PubChem Database. Available: https://pubchem.ncbi.nlm.nih.gov/compound/Temozolomide [Accessed Feb. 6 2020].

ISHIDA, Y. 2020. PD-1: Its Discovery, Involvement in Cancer Immunotherapy, and Beyond. *Cells,* 9.

IWAMOTO, N., YOKOYAMA, K., TAKANASHI, M., YONEZAWA, A., MATSUBARA, K. & SHIMADA, T. 2018. Application of nSMOL coupled with LC-MS bioanalysis for monitoring the Fc-fusion biopharmaceuticals Etanercept and Abatacept in human serum. *Pharmacol Res Perspect,* 6**,** e00422.

JAKOBSEN, J. N., URUP, T., GRUNNET, K., TOFT, A., JOHANSEN, M. D., POULSEN, S. H., CHRISTENSEN, I. J., MUHIC, A. & POULSEN, H. S. 2018. Toxicity and efficacy of lomustine and bevacizumab in recurrent glioblastoma patients. *J Neurooncol,* 137**,** 439-446.

`

JANOWICZ, P. W., LEINENGA, G., GÖTZ, J. & NISBET, R. M. 2019. Ultrasound-mediated blood-brain barrier opening enhances delivery of therapeutically relevant formats of a tau-specific antibody. *Sci Rep,* 9**,** 9255.

JOHNSTONE, R. W., RUEFLI, A. A. & SMYTH, M. J. 2000. Multiple physiological functions for multidrug transporter P-glycoprotein? *Trends Biochem Sci,* 25**,** 1-6.

JULIANO, R. L. & LING, V. 1976. A surface glycoprotein modulating drug permeability in Chinese hamster ovary cell mutants. *Biochim Biophys Acta,* 455**,** 152-62.

KADRY, H., NOORANI, B. & CUCULLO, L. 2020. A blood–brain barrier overview on structure, function, impairment, and biomarkers of integrity. *Fluids and Barriers of the CNS,* 17**,** 69.

KERNOHAN, J. W., MABON, R. F. & ET AL. 1949. A simplified classification of the gliomas. *Proc Staff Meet Mayo Clin,* 24**,** 71-5.

KINOSHITA, M., MCDANNOLD, N., JOLESZ, F. A. & HYNYNEN, K. 2006a. Noninvasive localized delivery of Herceptin to the mouse brain by MRI-guided focused ultrasound-induced blood-brain barrier disruption. *Proc Natl Acad Sci U S A,* 103**,** 11719-23.

KINOSHITA, M., MCDANNOLD, N., JOLESZ, F. A. & HYNYNEN, K. 2006b. Targeted delivery of antibodies through the blood-brain barrier by MRI-guided focused ultrasound. *Biochem Biophys Res Commun,* 340**,** 1085-90.

KOBUS, T., ZERVANTONAKIS, I. K., ZHANG, Y. & MCDANNOLD, N. J. 2016. Growth inhibition in a brain metastasis model by antibody delivery using focused ultrasound-mediated blood-brain barrier disruption. *J Control Release,* 238**,** 281-288.

KUDULAITI, N., ZHOU, Z., LUO, C., ZHANG, J., ZHU, F. & WU, J. 2021. A nomogram for individualized prediction of overall survival in patients with newly diagnosed glioblastoma: a real-world retrospective cohort study. *BMC Surg,* 21**,** 238.

LAMBORN, K. R., CHANG, S. M. & PRADOS, M. D. 2004. Prognostic factors for survival of patients with glioblastoma: recursive partitioning analysis. *Neuro Oncol,* 6**,** 227-35.

LARA-VELAZQUEZ, M., AL-KHARBOOSH, R., JEANNERET, S., VAZQUEZ-RAMOS, C., MAHATO, D., TAVANAIEPOUR, D., RAHMATHULLA, G. & QUINONES-HINOJOSA, A. 2017. Advances in Brain Tumor Surgery for Glioblastoma in Adults. *Brain Sci,* 7.

`

LATHIA, J. D., MACK, S. C., MULKEARNS-HUBERT, E. E., VALENTIM, C. L. & RICH, J. N. 2015. Cancer stem cells in glioblastoma. *Genes Dev,* 29**,** 1203-17.

LEONARD, G. D., FOJO, T. & BATES, S. E. 2003. The role of ABC transporters in clinical practice. *Oncologist,* 8**,** 411-24.

LETENDRE, P., MONGA, V., MILHEM, M. & ZAKHARIA, Y. 2017. Ipilimumab: from preclinical development to future clinical perspectives in melanoma. *Future Oncol,* 13**,** 625-636.

LEVEN, C., PADELLI, M., CARRÉ, J. L., BELLISSANT, E. & MISERY, L. 2019. Immune Checkpoint Inhibitors in Melanoma: A Review of Pharmacokinetics and Exposure-Response Relationships. *Clin Pharmacokinet,* 58**,** 1393-1405.

LI, B., HE, H., TAO, B. B., ZHAO, Z. Y., HU, G. H., LUO, C., CHEN, J. X., DING, X. H., SHENG, P., DONG, Y., ZHANG, L. & LU, Y. C. 2012. Knockdown of CDK6 enhances glioma sensitivity to chemotherapy. *Oncol Rep,* 28**,** 909-14.

LI, F., XU, J. & LIU, S. 2021a. Cancer Stem Cells and Neovascularization. *Cells,* 10.

LI, M., REN, X., DONG, G., WANG, J., JIANG, H., YANG, C., ZHAO, X., ZHU, Q., CUI, Y., YU, K. & LIN, S. 2021b. Distinguishing Pseudoprogression From True Early Progression in Isocitrate Dehydrogenase Wild-Type Glioblastoma by Interrogating Clinical, Radiological, and Molecular Features. *Front Oncol,* 11**,** 627325.

LI, S. W., QIU, X. G., CHEN, B. S., ZHANG, W., REN, H., WANG, Z. C. & JIANG, T. 2009. Prognostic factors influencing clinical outcomes of glioblastoma multiforme. *Chin Med J (Engl),* 122**,** 1245-9.

LI, W., ZHANG, H., ASSARAF, Y. G., ZHAO, K., XU, X., XIE, J., YANG, D. H. & CHEN, Z. S. 2016. Overcoming ABC transporter-mediated multidrug resistance: Molecular mechanisms and novel therapeutic drug strategies. *Drug Resist Updat,* 27**,** 14-29.

LI, Y., ZHANG, R., HOU, X., ZHANG, Y., DING, F., LI, F., YAO, Y. & WANG, Y. 2017. Microglia activation triggers oligodendrocyte precursor cells apoptosis via HSP60. *Mol Med Rep,* 16**,** 603-608.

LIANG, F., WANG, B., BAO, L., ZHAO, Y. S., ZHANG, S. M. & ZHANG, S. Q. 2017. Overexpression of ILK promotes temozolomide resistance in glioma cells. *Mol Med Rep,* 15**,** 1297-1304.

LIN, F., DE GOOIJER, M. C., ROIG, E. M., BUIL, L. C., CHRISTNER, S. M., BEUMER, J. H., WURDINGER, T., BEIJNEN, J. H. & VAN TELLINGEN, O. 2014. ABCB1, ABCG2, and PTEN determine the response of glioblastoma to temozolomide and ABT-888 therapy. *Clin Cancer Res,* 20**,** 2703-13.

`

LINTON, K. J. & HIGGINS, C. F. 2007. Structure and function of ABC transporters: the ATP switch provides flexible control. *Pflugers Arch,* 453**,** 555-67.

LIU, B., GUO, Z., DONG, H., DAOFENG, T., CAI, Q., JI, B., ZHANG, S., WU, L., WANG, J., WANG, L., ZHU, X., LIU, Y. & CHEN, Q. 2015a. LRIG1, human EGFR inhibitor, reverses multidrug resistance through modulation of ABCB1 and ABCG2. *Brain Res,* 1611**,** 93-100.

LIU, H. L., HSU, P. H., LIN, C. Y., HUANG, C. W., CHAI, W. Y., CHU, P. C., HUANG, C. Y., CHEN, P. Y., YANG, L. Y., KUO, J. S. & WEI, K. C. 2016. Focused Ultrasound Enhances Central Nervous System Delivery of Bevacizumab for Malignant Glioma Treatment. *Radiology,* 281**,** 99-108.

LIU, Y., GUO, Q., ZHANG, H., LI, G. H., FENG, S., YU, X. Z., KONG, L. S., ZHAO, L. & JIN, F. 2015b. Effect of siRNA-Livin on drug resistance to chemotherapy in glioma U251 cells and CD133(+) stem cells. *Exp Ther Med,* 10**,** 1317-1323.

LOCKHART, A. C., TIRONA, R. G. & KIM, R. B. 2003. Pharmacogenetics of ATP-binding cassette transporters in cancer and chemotherapy. *Mol Cancer Ther,* 2**,** 685-98.

LOUIS, D. N., PERRY, A., REIFENBERGER, G., VON DEIMLING, A., FIGARELLA-BRANGER, D., CAVENEE, W. K., OHGAKI, H., WIESTLER, O. D., KLEIHUES, P. & ELLISON, D. W. 2016. The 2016 World Health Organization Classification of Tumors of the Central Nervous System: a summary. *Acta Neuropathol,* 131**,** 803-20.

LOUIS, D. N., WESSELING, P., ALDAPE, K., BRAT, D. J., CAPPER, D., CREE, I. A., EBERHART, C., FIGARELLA-BRANGER, D., FOULADI, M., FULLER, G. N., GIANNINI, C., HABERLER, C., HAWKINS, C., KOMORI, T., KROS, J. M., NG, H. K., ORR, B. A., PARK, S. H., PAULUS, W., PERRY, A., PIETSCH, T., REIFENBERGER, G., ROSENBLUM, M., ROUS, B., SAHM, F., SARKAR, C., SOLOMON, D. A., TABORI, U., VAN DEN BENT, M. J., VON DEIMLING, A., WELLER, M., WHITE, V. A. & ELLISON, D. W. 2020. cIMPACT-NOW update 6: new entity and diagnostic principle recommendations of the cIMPACT-Utrecht meeting on future CNS tumor classification and grading. *Brain Pathol,* 30**,** 844-856.

LUM, B. L., KAUBISCH, S., YAHANDA, A. M., ADLER, K. M., JEW, L., EHSAN, M. N., BROPHY, N. A., HALSEY, J., GOSLAND, M. P. & SIKIC, B. I. 1992. Alteration of etoposide pharmacokinetics and pharmacodynamics by cyclosporine in a phase I trial to modulate multidrug resistance. *J Clin Oncol,* 10**,** 1635-42.

LUN, M., LOK, E., GAUTAM, S., WU, E. & WONG, E. T. 2011. The natural history of extracranial metastasis from glioblastoma multiforme. *J Neurooncol,* 105**,** 261-73.

LUNDY, P., DOMINO, J., RYKEN, T., FOUKE, S., MCCRACKEN, D. J., ORMOND, D. R. & OLSON, J. J. 2020. The role of imaging for the management of newly diagnosed glioblastoma in adults: a systematic review and evidence-based clinical practice guideline update. *J Neurooncol,* 150**,** 95-120.

`

MAHRINGER, A. & FRICKER, G. 2016. ABC transporters at the blood-brain barrier. *Expert Opin Drug Metab Toxicol,* 12**,** 499-508.

MALMSTROM, A. & LYSIAK, M. 2019. ABCB1 single-nucleotide variants and survival in patients with glioblastoma treated with radiotherapy concomitant with temozolomide.

MALMSTRÖM, A., ŁYSIAK, M., KRISTENSEN, B. W., HOVEY, E., HENRIKSSON, R. & SÖDERKVIST, P. 2020. Do we really know who has an MGMT methylated glioma? Results of an international survey regarding use of MGMT analyses for glioma. *Neurooncol Pract,* 7**,** 68-76.

MAO, Q. & UNADKAT, J. D. 2015. Role of the breast cancer resistance protein (BCRP/ABCG2) in drug transport--an update. *Aaps j,* 17**,** 65-82.

MARENCO-HILLEMBRAND, L., WIJESEKERA, O., SUAREZ-MEADE, P., MAMPRE, D., JACKSON, C., PETERSON, J., TRIFILETTI, D., HAMMACK, J., ORTIZ, K., LESSER, E., SPIEGEL, M., PREVATT, C., HAWAYEK, M., QUINONES-HINOJOSA, A. & CHAICHANA, K. L. 2020. Trends in glioblastoma: outcomes over time and type of intervention: a systematic evidence based analysis. *Journal of Neuro-Oncology,* 147**,** 297-307.

MARTIN, V., SANCHEZ-SANCHEZ, A. M., HERRERA, F., GOMEZ-MANZANO, C., FUEYO, J., ALVAREZ-VEGA, M. A., ANTOLIN, I. & RODRIGUEZ, C. 2013. Melatonin-induced methylation of the ABCG2/BCRP promoter as a novel mechanism to overcome multidrug resistance in brain tumour stem cells. *Br J Cancer,* 108**,** 2005-12.

MUFTUOGLU, Y. & LIAU, L. M. 2020. Results From the CheckMate 143 Clinical Trial: Stalemate or New Game Strategy for Glioblastoma Immunotherapy? *JAMA Oncology,* 6**,** 987-989.

MUNOZ, J. L., RODRIGUEZ-CRUZ, V., GRECO, S. J., NAGULA, V., SCOTTO, K. W. & RAMESHWAR, P. 2014. Temozolomide induces the production of epidermal growth factor to regulate MDR1 expression in glioblastoma cells. *Mol Cancer Ther,* 13**,** 2399-411.

MUNOZ, J. L., RODRIGUEZ-CRUZ, V., RAMKISSOON, S. H., LIGON, K. L., GRECO, S. J. & RAMESHWAR, P. 2015a. Temozolomide resistance in glioblastoma occurs by miRNA-9-targeted PTCH1, independent of sonic hedgehog level. *Oncotarget,* 6**,** 1190-201.

MUNOZ, J. L., WALKER, N. D., SCOTTO, K. W. & RAMESHWAR, P. 2015b. Temozolomide competes for P-glycoprotein and contributes to chemoresistance in glioblastoma cells. *Cancer Lett,* 367**,** 69-75.

NAIR, N., CALLE, A. S., ZAHRA, M. H., PRIETO-VILA, M., OO, A. K. K., HURLEY, L., VAIDYANATH, A., SENO, A., MASUDA, J., IWASAKI, Y., TANAKA, H., KASAI, T. & SENO, M. 2017. A cancer stem cell model as the point of origin of cancer-associated fibroblasts in tumor microenvironment. *Sci Rep,* 7**,** 6838.

`

NAKAI, E., PARK, K., YAWATA, T., CHIHARA, T., KUMAZAWA, A., NAKABAYASHI, H. & SHIMIZU, K. 2009. Enhanced MDR1 expression and chemoresistance of cancer stem cells derived from glioblastoma. *Cancer Invest,* 27**,** 901-8.

NDUOM, E. K., WEI, J., YAGHI, N. K., HUANG, N., KONG, L. Y., GABRUSIEWICZ, K., LING, X., ZHOU, S., IVAN, C., CHEN, J. Q., BURKS, J. K., FULLER, G. N., CALIN, G. A., CONRAD, C. A., CREASY, C., RITTHIPICHAI, K., RADVANYI, L. & HEIMBERGER, A. B. 2016. PD-L1 expression and prognostic impact in glioblastoma. *Neuro Oncol,* 18**,** 195-205.

NOWELL, P. C. 1976. The clonal evolution of tumor cell populations. *Science,* 194**,** 23-8.

OBEROI, R. K., MITTAPALLI, R. K. & ELMQUIST, W. F. 2013. Pharmacokinetic assessment of efflux transport in sunitinib distribution to the brain. *J Pharmacol Exp Ther,* 347**,** 755-64.

OSTERMANN, S., CSAJKA, C., BUCLIN, T., LEYVRAZ, S., LEJEUNE, F., DECOSTERD, L. A. & STUPP, R. 2004. Plasma and cerebrospinal fluid population pharmacokinetics of temozolomide in malignant glioma patients. *Clin Cancer Res,* 10**,** 3728-36.

OSTROM, Q. T., BAUCHET, L., DAVIS, F. G., DELTOUR, I., FISHER, J. L., LANGER, C. E., PEKMEZCI, M., SCHWARTZBAUM, J. A., TURNER, M. C., WALSH, K. M., WRENSCH, M. R. & BARNHOLTZ-SLOAN, J. S. 2014. The epidemiology of glioma in adults: a "state of the science" review. *Neuro Oncol,* 16**,** 896-913.

OSTROM, Q. T., GITTLEMAN, H., LIAO, P., VECCHIONE-KOVAL, T., WOLINSKY, Y., KRUCHKO, C. & BARNHOLTZ-SLOAN, J. S. 2017. CBTRUS Statistical Report: Primary brain and other central nervous system tumors diagnosed in the United States in 2010-2014. *Neuro Oncol,* 19**,** v1-v88.

PACE, A., DIRVEN, L., KOEKKOEK, J. A. F., GOLLA, H., FLEMING, J., RUDA, R., MAROSI, C., RHUN, E. L., GRANT, R., OLIVER, K., OBERG, I., BULBECK, H. J., ROONEY, A. G., HENRIKSSON, R., PASMAN, H. R. W., OBERNDORFER, S., WELLER, M. & TAPHOORN, M. J. B. 2017. European Association for Neuro-Oncology (EANO) guidelines for palliative care in adults with glioma. *Lancet Oncol,* 18**,** e330-e340.

PARRISH, K. E., CEN, L., MURRAY, J., CALLIGARIS, D., KIZILBASH, S., MITTAPALLI, R. K., CARLSON, B. L., SCHROEDER, M. A., SLUDDEN, J., BODDY, A. V., AGAR, N. Y., CURTIN, N. J., ELMQUIST, W. F. & SARKARIA, J. N. 2015. Efficacy of PARP Inhibitor Rucaparib in Orthotopic Glioblastoma Xenografts Is Limited by Ineffective Drug Penetration into the Central Nervous System. *Mol Cancer Ther,* 14**,** 2735-43.

PEARSON, J. R. D., CUZZUBBO, S., MCARTHUR, S., DURRANT, L. G., ADHIKAREE, J., TINSLEY, C. J., POCKLEY, A. G. & MCARDLE, S. E. B. 2020. Immune Escape in Glioblastoma Multiforme and the Adaptation of Immunotherapies for Treatment. *Front Immunol,* 11**,** 582106.

PEDROTE, M. M., MOTTA, M. F., FERRETTI, G. D. S., NORBERTO, D. R., SPOHR, T. C. L. S., LIMA, F. R. S., GRATTON, E., SILVA, J. L. & DE OLIVEIRA, G. A. P. 2020. Oncogenic Gain of Function in Glioblastoma Is Linked to Mutant p53 Amyloid Oligomers. *iScience,* 23**,** 100820.

PEIGNAN, L., GARRIDO, W., SEGURA, R., MELO, R., ROJAS, D., CARCAMO, J. G., SAN MARTIN, R. & QUEZADA, C. 2011. Combined use of anticancer drugs and an inhibitor of multiple drug resistance-associated protein-1 increases sensitivity and decreases survival of glioblastoma multiforme cells in vitro. *Neurochem Res,* 36**,** 1397-406.

PERSICO, P., LORENZI, E., DIPASQUALE, A., PESSINA, F., NAVARRIA, P., POLITI, L. S., SANTORO, A. & SIMONELLI, M. 2021. Checkpoint Inhibitors as High-Grade Gliomas Treatment: State of the Art and Future Perspectives. *J Clin Med,* 10.

PESSINA, S., CANTINI, G., KAPETIS, D., CAZZATO, E., DI IANNI, N., FINOCCHIARO, G. & PELLEGATTA, S. 2016. The multidrug-resistance transporter Abcc3 protects NK cells from chemotherapy in a murine model of malignant glioma. *Oncoimmunology,* 5**,** e1108513.

PETITPREZ, F., LEVY, S., SUN, C.-M., MEYLAN, M., LINHARD, C., BECHT, E., ELAROUCI, N., TAVEL, D., ROUMENINA, L. T., AYADI, M., SAUTÈS-FRIDMAN, C., FRIDMAN, W. H. & DE REYNIÈS, A. 2020. The murine Microenvironment Cell Population counter method to estimate abundance of tissue-infiltrating immune and stromal cell populations in murine samples using gene expression. *Genome Medicine,* 12**,** 86.

PIO, R., AJONA, D., ORTIZ-ESPINOSA, S., MANTOVANI, A. & LAMBRIS, J. D. 2019. Complementing the Cancer-Immunity Cycle. 10.

PLESSIER, A., LE DRET, L., VARLET, P., BECCARIA, K., LACOMBE, J., MÉRIAUX, S., GEFFROY, F., FIETTE, L., FLAMANT, P., CHRÉTIEN, F., BLAUWBLOMME, T., PUGET, S., GRILL, J., DEBILY, M. A. & CASTEL, D. 2017. New in vivo avatars of diffuse intrinsic pontine gliomas (DIPG) from stereotactic biopsies performed at diagnosis. *Oncotarget,* 8**,** 52543-52559.

PRATT, D., DOMINAH, G., LOBEL, G., OBUNGU, A., LYNES, J., SANCHEZ, V., ADAMSTEIN, N., WANG, X., EDWARDS, N. A., WU, T., MARIC, D., GILES, A. J., GILBERT, M. R., QUEZADO, M. & NDUOM, E. K. 2019. Programmed Death Ligand 1 Is a Negative Prognostic Marker in Recurrent Isocitrate Dehydrogenase-Wildtype Glioblastoma. *Neurosurgery,* 85**,** 280-289.

PULGAR, V. M. 2018. Transcytosis to Cross the Blood Brain Barrier, New Advancements and Challenges. *Front Neurosci,* 12**,** 1019.

QIU, H., LI, Y., CHENG, S., LI, J., HE, C. & LI, J. 2020. A Prognostic Microenvironment-Related Immune Signature via ESTIMATE (PROMISE Model) Predicts Overall Survival of Patients With Glioma. *Front Oncol,* 10**,** 580263.

`

RAJARATNAM, V., ISLAM, M. M., YANG, M., SLABY, R., RAMIREZ, H. M. & MIRZA, S. P. 2020. Glioblastoma: Pathogenesis and Current Status of Chemotherapy and Other Novel Treatments. *Cancers (Basel),* 12.

RAMIREZ, Y. P., WEATHERBEE, J. L., WHEELHOUSE, R. T. & ROSS, A. H. 2013. Glioblastoma multiforme therapy and mechanisms of resistance. *Pharmaceuticals (Basel),* 6**,** 1475-506.

RAO, V. K., WANGSA, D., ROBEY, R. W., HUFF, L., HONJO, Y., HUNG, J., KNUTSEN, T., RIED, T. & BATES, S. E. 2005. Characterization of ABCG2 gene amplification manifesting as extrachromosomal DNA in mitoxantrone-selected SF295 human glioblastoma cells. *Cancer Genet Cytogenet,* 160**,** 126-33.

RATNAM, N. M., GILBERT, M. R. & GILES, A. J. 2019. Immunotherapy in CNS cancers: the role of immune cell trafficking. *Neuro Oncol,* 21**,** 37-46.

RAZAVI, S. M., LEE, K. E., JIN, B. E., AUJLA, P. S., GHOLAMIN, S. & LI, G. 2016. Immune Evasion Strategies of Glioblastoma. *Front Surg,* 3**,** 11.

REARDON, D. A., GOKHALE, P. C., KLEIN, S. R., LIGON, K. L., RODIG, S. J., RAMKISSOON, S. H., JONES, K. L., CONWAY, A. S., LIAO, X., ZHOU, J., WEN, P. Y., VAN DEN ABBEELE, A. D., HODI, F. S., QIN, L., KOHL, N. E., SHARPE, A. H., DRANOFF, G. & FREEMAN, G. J. 2016. Glioblastoma Eradication Following Immune Checkpoint Blockade in an Orthotopic, Immunocompetent Model. *Cancer Immunol Res,* 4**,** 124-35.

REARDON, D. A., LASSMAN, A. B., VAN DEN BENT, M., KUMTHEKAR, P., MERRELL, R., SCOTT, A. M., FICHTEL, L., SULMAN, E. P., GOMEZ, E., FISCHER, J., LEE, H. J., MUNASINGHE, W., XIONG, H., MANDICH, H., ROBERTS-RAPP, L., ANSELL, P., HOLEN, K. D. & GAN, H. K. 2017. Efficacy and safety results of ABT-414 in combination with radiation and temozolomide in newly diagnosed glioblastoma. *Neuro Oncol,* 19**,** 965-975.

RIGANTI, C., SALAROGLIO, I. C., CALDERA, V., CAMPIA, I., KOPECKA, J., MELLAI, M., ANNOVAZZI, L., BOSIA, A., GHIGO, D. & SCHIFFER, D. 2013. Temozolomide downregulates P-glycoprotein expression in glioblastoma stem cells by interfering with the Wnt3a/glycogen synthase-3 kinase/beta-catenin pathway. *Neuro Oncol,* 15**,** 1502-17.

ROWSHANRAVAN, B., HALLIDAY, N. & SANSOM, D. M. 2018. CTLA-4: a moving target in immunotherapy. *Blood,* 131**,** 58-67.

RUSSELL, M., HUANG, X., VUZMAN, D., LVOVA, M., PANTAZI, A., LYLE, S. & TSE, J. Y. 2018. Characterization of biomarkers to immune checkpoint blockade therapy across solid tumors. 36**,** 26-26.

SAHA, D., MARTUZA, R. L. & RABKIN, S. D. 2017. Macrophage Polarization Contributes to Glioblastoma Eradication by Combination Immunovirotherapy and Immune Checkpoint Blockade. *Cancer Cell,* 32**,** 253-267.e5.

`

SALAROGLIO, I. C., MUJUMDAR, P., ANNOVAZZI, L., KOPECKA, J., MELLAI, M., SCHIFFER, D., POULSEN, S. A. & RIGANTI, C. 2018. Carbonic Anhydrase XII Inhibitors Overcome P-Glycoprotein-Mediated Resistance to Temozolomide in Glioblastoma. *Mol Cancer Ther,* 17**,** 2598-2609.

SAUNDERS, N. R., DREIFUSS, J. J., DZIEGIELEWSKA, K. M., JOHANSSON, P. A., HABGOOD, M. D., MØLLGÅRD, K. & BAUER, H. C. 2014. The rights and wrongs of blood-brain barrier permeability studies: a walk through 100 years of history. *Front Neurosci,* 8**,** 404.

SAVOIA, P., ASTRUA, C. & FAVA, P. 2016. Ipilimumab (Anti-Ctla-4 Mab) in the treatment of metastatic melanoma: Effectiveness and toxicity management. *Hum Vaccin Immunother,* 12**,** 1092-101.

SCHAICH, M., KESTEL, L., PFIRRMANN, M., ROBEL, K., ILLMER, T., KRAMER, M., DILL, C., EHNINGER, G., SCHACKERT, G. & KREX, D. 2009. A MDR1 (ABCB1) gene single nucleotide polymorphism predicts outcome of temozolomide treatment in glioblastoma patients. *Ann Oncol,* 20**,** 175-81.

SCHEFFEL, T. B., GRAVE, N., VARGAS, P., DIZ, F. M., ROCKENBACH, L. & MORRONE, F. B. 2020. Immunosuppression in Gliomas via PD-1/PD-L1 Axis and Adenosine Pathway. *Front Oncol,* 10**,** 617385.

SCHINDELIN, J., ARGANDA-CARRERAS, I., FRISE, E., KAYNIG, V., LONGAIR, M., PIETZSCH, T., PREIBISCH, S., RUEDEN, C., SAALFELD, S., SCHMID, B., TINEVEZ, J. Y., WHITE, D. J., HARTENSTEIN, V., ELICEIRI, K., TOMANCAK, P. & CARDONA, A. 2012. Fiji: an open-source platform for biological-image analysis. *Nat Methods,* 9**,** 676-82.

SCHINKEL, A. H. & JONKER, J. W. 2003. Mammalian drug efflux transporters of the ATP binding cassette (ABC) family: an overview. *Adv Drug Deliv Rev,* 55**,** 3-29.

SCHINKEL, A. H., SMIT, J. J., VAN TELLINGEN, O., BEIJNEN, J. H., WAGENAAR, E., VAN DEEMTER, L., MOL, C. A., VAN DER VALK, M. A., ROBANUS-MAANDAG, E. C., TE RIELE, H. P. & ET AL. 1994. Disruption of the mouse mdr1a P-glycoprotein gene leads to a deficiency in the blood-brain barrier and to increased sensitivity to drugs. *Cell,* 77**,** 491-502.

SHAWAHNA, R., UCHIDA, Y., DECLÈVES, X., OHTSUKI, S., YOUSIF, S., DAUCHY, S., JACOB, A., CHASSOUX, F., DAUMAS-DUPORT, C., COURAUD, P. O., TERASAKI, T. & SCHERRMANN, J. M. 2011. Transcriptomic and quantitative proteomic analysis of transporters and drug metabolizing enzymes in freshly isolated human brain microvessels. *Mol Pharm,* 8**,** 1332-41.

SHEIKOV, N., MCDANNOLD, N., VYKHODTSEVA, N., JOLESZ, F. & HYNYNEN, K. 2004. Cellular mechanisms of the blood-brain barrier opening induced by ultrasound in presence of microbubbles. *Ultrasound Med Biol,* 30**,** 979-89.

SHEN, S. & ZHANG, W. 2010. ABC transporters and drug efflux at the blood-brain barrier. *Rev Neurosci,* 21**,** 29-53.

SHIN, J., KONG, C., CHO, J. S., LEE, J., KOH, C. S., YOON, M. S., NA, Y. C., CHANG, W. S. & CHANG, J. W. 2018. Focused ultrasound-mediated noninvasive blood-brain barrier modulation: preclinical examination of efficacy and safety in various sonication parameters. *Neurosurg Focus,* 44**,** E15.

SIA, J., SZMYD, R., HAU, E. & GEE, H. E. 2020. Molecular Mechanisms of Radiation-Induced Cancer Cell Death: A Primer. 8.

SINHARAY, S., TU, T.-W., KOVACS, Z. I., SCHREIBER-STAINTHORP, W., SUNDBY, M., ZHANG, X., PAPADAKIS, G. Z., REID, W. C., FRANK, J. A. & HAMMOUD, D. A. 2019. In vivo imaging of sterile microglial activation in rat brain after disrupting the blood-brain barrier with pulsed focused ultrasound: [18F]DPA-714 PET study. *Journal of Neuroinflammation,* 16**,** 155.

SMRDEL, U., VIDMAR, M. S. & SMRDEL, A. 2018. Glioblastoma in Patients over 70 Years of Age. *Radiol Oncol,* 52**,** 167-172.

SOTTORIVA, A., KANG, H., MA, Z., GRAHAM, T. A., SALOMON, M. P., ZHAO, J., MARJORAM, P., SIEGMUND, K., PRESS, M. F., SHIBATA, D. & CURTIS, C. 2015. A Big Bang model of human colorectal tumor growth. *Nature Genetics,* 47**,** 209-216.

STOYANOV, G. S. & DZHENKOV, D. L. 2018. On the Concepts and History of Glioblastoma Multiforme - Morphology, Genetics and Epigenetics. *Folia Med (Plovdiv),* 60**,** 48-66.

STUPP, R., MASON, W. P., VAN DEN BENT, M. J., WELLER, M., FISHER, B., TAPHOORN, M. J., BELANGER, K., BRANDES, A. A., MAROSI, C., BOGDAHN, U., CURSCHMANN, J., JANZER, R. C., LUDWIN, S. K., GORLIA, T., ALLGEIER, A., LACOMBE, D., CAIRNCROSS, J. G., EISENHAUER, E. & MIRIMANOFF, R. O. 2005. Radiotherapy plus concomitant and adjuvant temozolomide for glioblastoma. *N Engl J Med,* 352**,** 987-96.

STUPP, R., TAILLIBERT, S., KANNER, A., READ, W., STEINBERG, D., LHERMITTE, B., TOMS, S., IDBAIH, A., AHLUWALIA, M. S., FINK, K., DI MECO, F., LIEBERMAN, F., ZHU, J. J., STRAGLIOTTO, G., TRAN, D., BREM, S., HOTTINGER, A., KIRSON, E. D., LAVY-SHAHAF, G., WEINBERG, U., KIM, C. Y., PAEK, S. H., NICHOLAS, G., BRUNA, J., HIRTE, H., WELLER, M., PALTI, Y., HEGI, M. E. & RAM, Z. 2017. Effect of Tumor-Treating Fields Plus Maintenance Temozolomide vs Maintenance Temozolomide Alone on Survival in Patients With Glioblastoma: A Randomized Clinical Trial. *Jama,* 318**,** 2306-2316.

SUN, C., DAI, X., ZHAO, D., WANG, H., RONG, X., HUANG, Q. & LAN, Q. 2019. Mesenchymal stem cells promote glioma neovascularization in vivo by fusing with cancer stem cells. *BMC Cancer,* 19**,** 1240.

`

SUN, R., HU, Z. & CURTIS, C. 2018. Big Bang Tumor Growth and Clonal Evolution. *Cold Spring Harb Perspect Med,* 8.

TAMAKI, A., IERANO, C., SZAKACS, G., ROBEY, R. W. & BATES, S. E. 2011. The controversial role of ABC transporters in clinical oncology. *Essays Biochem,* 50**,** 209-32.

TARHINI, A. A. 2013. Tremelimumab: a review of development to date in solid tumors. *Immunotherapy,* 5**,** 215-29.

TIVNAN, A., ZAKARIA, Z., O'LEARY, C., KOGEL, D., POKORNY, J. L., SARKARIA, J. N. & PREHN, J. H. 2015. Inhibition of multidrug resistance protein 1 (MRP1) improves chemotherapy drug response in primary and recurrent glioblastoma multiforme. *Front Neurosci,* 9**,** 218.

TOMASZOWSKI, K. H., SCHIRRMACHER, R. & KAINA, B. 2015. Multidrug Efflux Pumps Attenuate the Effect of MGMT Inhibitors. *Mol Pharm,* 12**,** 3924-34.

TOUAT, M., IDBAIH, A., SANSON, M. & LIGON, K. L. 2017. Glioblastoma targeted therapy: updated approaches from recent biological insights. *Ann Oncol,* 28**,** 1457-1472.

TSO, J. L., YANG, S., MENJIVAR, J. C., YAMADA, K., ZHANG, Y., HONG, I., BUI, Y., STREAM, A., MCBRIDE, W. H., LIAU, L. M., NELSON, S. F., CLOUGHESY, T. F., YONG, W. H., LAI, A. & TSO, C. L. 2015. Bone morphogenetic protein 7 sensitizes O6-methylguanine methyltransferase expressing-glioblastoma stem cells to clinically relevant dose of temozolomide. *Mol Cancer,* 14**,** 189.

TURK, D., HALL, M. D., CHU, B. F., LUDWIG, J. A., FALES, H. M., GOTTESMAN, M. M. & SZAKACS, G. 2009. Identification of compounds selectively killing multidrug-resistant cancer cells. *Cancer Res,* 69**,** 8293-301.

UHLEN, M., FAGERBERG, L., HALLSTROM, B. M., LINDSKOG, C., OKSVOLD, P., MARDINOGLU, A., SIVERTSSON, A., KAMPF, C., SJOSTEDT, E., ASPLUND, A., OLSSON, I., EDLUND, K., LUNDBERG, E., NAVANI, S., SZIGYARTO, C. A., ODEBERG, J., DJUREINOVIC, D., TAKANEN, J. O., HOBER, S., ALM, T., EDQVIST, P. H., BERLING, H., TEGEL, H., MULDER, J., ROCKBERG, J., NILSSON, P., SCHWENK, J. M., HAMSTEN, M., VON FEILITZEN, K., FORSBERG, M., PERSSON, L., JOHANSSON, F., ZWAHLEN, M., VON HEIJNE, G., NIELSEN, J. & PONTEN, F. 2015. Proteomics. Tissue-based map of the human proteome. *Science,* 347**,** 1260419.

VALDEZ, M. A., FERNANDEZ, E., MATSUNAGA, T., ERICKSON, R. P. & TROUARD, T. P. 2020. Distribution and Diffusion of Macromolecule Delivery to the Brain via Focused Ultrasound using Magnetic Resonance and Multispectral Fluorescence Imaging. *Ultrasound Med Biol,* 46**,** 122-136.

VAN NIEUWENHUIJZE, A. & LISTON, A. 2015. The Molecular Control of Regulatory T Cell Induction. *Prog Mol Biol Transl Sci,* 136**,** 69-97.

VASILIOU, V., VASILIOU, K. & NEBERT, D. W. 2009. Human ATP-binding cassette (ABC) transporter family. *Hum Genomics,* 3**,** 281-90.

VELDHUIJZEN VAN ZANTEN, S. E. M., DE WITT HAMER, P. C. & VAN DONGEN, G. A. M. S. 2019. Brain Access of Monoclonal Antibodies as Imaged and Quantified by ⁸⁹Zr-Antibody PET: Perspectives for Treatment of Brain Diseases. 60**,** 615-616.

VENTOLA, C. L. 2017. Cancer Immunotherapy, Part 1: Current Strategies and Agents. *P & T : a peer-reviewed journal for formulary management,* 42**,** 375-383.

VERHAAK, R. G., HOADLEY, K. A., PURDOM, E., WANG, V., QI, Y., WILKERSON, M. D., MILLER, C. R., DING, L., GOLUB, T., MESIROV, J. P., ALEXE, G., LAWRENCE, M., O'KELLY, M., TAMAYO, P., WEIR, B. A., GABRIEL, S., WINCKLER, W., GUPTA, S., JAKKULA, L., FEILER, H. S., HODGSON, J. G., JAMES, C. D., SARKARIA, J. N., BRENNAN, C., KAHN, A., SPELLMAN, P. T., WILSON, R. K., SPEED, T. P., GRAY, J. W., MEYERSON, M., GETZ, G., PEROU, C. M. & HAYES, D. N. 2010. Integrated genomic analysis identifies clinically relevant subtypes of glioblastoma characterized by abnormalities in PDGFRA, IDH1, EGFR, and NF1. *Cancer Cell,* 17**,** 98-110.

VESELY, M. D., KERSHAW, M. H., SCHREIBER, R. D. & SMYTH, M. J. 2011. Natural innate and adaptive immunity to cancer. *Annu Rev Immunol,* 29**,** 235-71.

VILLE, S., POIRIER, N., BLANCHO, G. & VANHOVE, B. 2015. Co-Stimulatory Blockade of the CD28/CD80-86/CTLA-4 Balance in Transplantation: Impact on Memory T Cells? 6.

WAGER, T. T., HOU, X., VERHOEST, P. R. & VILLALOBOS, A. 2016. Central Nervous System Multiparameter Optimization Desirability: Application in Drug Discovery. *ACS Chemical Neuroscience,* 7**,** 767-775.

WANG, N., JAIN, R. K. & BATCHELOR, T. T. 2017. New Directions in Anti-Angiogenic Therapy for Glioblastoma. *Neurotherapeutics,* 14**,** 321-332.

WANG, Z., ZHANG, C., LIU, X., WANG, Z., SUN, L., LI, G., LIANG, J., HU, H., LIU, Y., ZHANG, W. & JIANG, T. 2016. Molecular and clinical characterization of PD-L1 expression at transcriptional level via 976 samples of brain glioma. *Oncoimmunology,* 5**,** e1196310.

WEENINK, B., FRENCH, P. J., SILLEVIS SMITT, P. A. E., DEBETS, R. & GEURTS, M. 2020. Immunotherapy in Glioblastoma: Current Shortcomings and Future Perspectives. *Cancers (Basel),* 12.

WEI, S. C., DUFFY, C. R. & ALLISON, J. P. 2018. Fundamental Mechanisms of Immune Checkpoint Blockade Therapy. 8**,** 1069-1086.

`

WICK, W., GORLIA, T., BENDSZUS, M., TAPHOORN, M., SAHM, F., HARTING, I., BRANDES, A. A., TAAL, W., DOMONT, J., IDBAIH, A., CAMPONE, M., CLEMENT, P. M., STUPP, R., FABBRO, M., LE RHUN, E., DUBOIS, F., WELLER, M., VON DEIMLING, A., GOLFINOPOULOS, V., BROMBERG, J. C., PLATTEN, M., KLEIN, M. & VAN DEN BENT, M. J. 2017. Lomustine and Bevacizumab in Progressive Glioblastoma. *N Engl J Med,* 377**,** 1954-1963.

WINKLER, F., KIENAST, Y., FUHRMANN, M., VON BAUMGARTEN, L., BURGOLD, S., MITTEREGGER, G., KRETZSCHMAR, H. & HERMS, J. 2009. Imaging glioma cell invasion in vivo reveals mechanisms of dissemination and peritumoral angiogenesis. *Glia,* 57**,** 1306-15.

WOLF, S. J., BACHTIAR, M., WANG, J., SIM, T. S., CHONG, S. S. & LEE, C. G. 2011. An update on ABCB1 pharmacogenetics: insights from a 3D model into the location and evolutionary conservation of residues corresponding to SNPs associated with drug pharmacokinetics. *Pharmacogenomics J,* 11**,** 315-25.

XIAO, Z.-Z., WANG, Z.-F., LAN, T., HUANG, W.-H., ZHAO, Y.-H., MA, C. & LI, Z.-Q. 2020. Carmustine as a Supplementary Therapeutic Option for Glioblastoma: A Systematic Review and Meta-Analysis. 11.

XUE, W., DU, X., WU, H., LIU, H., XIE, T., TONG, H., CHEN, X., GUO, Y. & ZHANG, W. 2017. Aberrant glioblastoma neovascularization patterns and their correlation with DCE-MRI-derived parameters following temozolomide and bevacizumab treatment. *Scientific Reports,* 7**,** 13894.

YAO, L., XUE, X., YU, P., NI, Y. & CHEN, F. 2018. Evans Blue Dye: A Revisit of Its Applications in Biomedicine. *Contrast Media & Molecular Imaging,* 2018**,** 7628037.

YIN, J. & ZHANG, J. 2011. Multidrug resistance-associated protein 1 (MRP1/ABCC1) polymorphism: from discovery to clinical application. *Zhong Nan Da Xue Xue Bao Yi Xue Ban,* 36**,** 927-38.

ZAHAVI, D. & WEINER, L. 2020. Monoclonal Antibodies in Cancer Therapy. *Antibodies (Basel),* 9.

ZHANG, D. Y., DMELLO, C., CHEN, L., ARRIETA, V. A., GONZALEZ-BUENDIA, E., KANE, J. R., MAGNUSSON, L. P., BARAN, A., JAMES, C. D., HORBINSKI, C., CARPENTIER, A., DESSEAUX, C., CANNEY, M., MUZZIO, M., STUPP, R. & SONABEND, A. M. 2020a. Ultrasound-mediated Delivery of Paclitaxel for Glioma: A Comparative Study of Distribution, Toxicity, and Efficacy of Albumin-bound Versus Cremophor Formulations. *Clin Cancer Res,* 26**,** 477-486.

ZHANG, J., SAI, K., WANG, X. L., YE, S. Q., LIANG, L. J., ZHOU, Y., CHEN, Z. J., HU, W.-M. & LIU, J. M. 2020b. Tim-3 Expression and MGMT Methylation Status Association With Survival in Glioblastoma. 11.

ZHANG, P. & CHEN, X. B. 2018. Down-regulation of ABCE1 inhibits temozolomide resistance in glioma through the PI3K/Akt/NF-kappaB signaling pathway. 38.

`

ZHANG, Y., WANG, S. X., MA, J. W., LI, H. Y., YE, J. C., XIE, S. M., DU, B. & ZHONG, X. Y. 2015. EGCG inhibits properties of glioma stem-like cells and synergizes with temozolomide through downregulation of P-glycoprotein inhibition. *J Neurooncol,* 121**,** 41-52.

ZHAO, M., VAN STRATEN, D., BROEKMAN, M. L. D., PRÉAT, V. & SCHIFFELERS, R. M. 2020. Nanocarrier-based drug combination therapy for glioblastoma. *Theranostics,* 10**,** 1355-1372.

ZHU, L., CHENG, G., YE, D., NAZERI, A., YUE, Y., LIU, W., WANG, X., DUNN, G. P., PETTI, A. A., LEUTHARDT, E. C. & CHEN, H. 2018. Focused Ultrasound-enabled Brain Tumor Liquid Biopsy. *Scientific Reports,* 8**,** 6553.

ZOLNERCIKS, J. K., ANDRESS, E. J., NICOLAOU, M. & LINTON, K. J. 2011. Structure of ABC transporters. *Essays Biochem,* 50**,** 43-61.

Titre : Modulation du microenvironnement tumoral pour contourner la résistance du glioblastome aux traitements

Mots clés : la barrière hémato-encéphalique, l'immunothérapie, pré-clinique, pompes à efflux ABC

Le glioblastome (GBM) est le cancer du cerveau le plus fréquent et le plus agressif chez l'adulte. Le traitement de référence des patients souffrant d'un GBM nouvellement diagnostiqué repose sur la chirurgie aussi sûre et maximale que possible suivie d'une radiochimiothérapie concomitante et d'une chimiothérapie adjuvante par témozolomide. Malgré ce protocole thérapeutique lourd, la survie globale médiane des patients est inférieure à 18 mois. La barrière hémato-encéphalique (BHE) et le micro-environnement immunodéprimé local limitent l'efficacité des traitements antitumoraux actuels utilisés contre les tumeurs cérébrales. Notre thèse est axée sur le contournement de la barrière hémato-encéphalique pour moduler l'immunité locale pour des traitements anti-tumoraux plus efficaces. Tout d'abord, nous avons passé en revue le rôle des membres de la superfamille des protéines ABC exprimés dans les cellules de la BHE et leur rôle dans la résistance des cellules de GBM à la chimiothérapie. Deuxièmement, nous avons étudié l'expression des protéines de points de contrôle immunitaires CD80 et CD86 et leurs impacts sur le pronostic des patients souffrant de glioblastome nouvellement diagnostiqués et traités avec le traitement de référence. La surexpression de CD86 est associée à un meilleur pronostic. Enfin, nous avons montré une efficacité spectaculaire des inhibiteurs de points de contrôle immunitaires ciblant PLD1 combinés à une ouverture, médiée par ultrasons, de la BHE chez des souris porteuses de glioblastome par rapport aux anti-PDL1 seuls. Les stratégies de modulations de la BHE et de l'immunité locale apparaissent comme des stratégies prometteuses pour accroitre notre arsenal thérapeutique contre le glioblastome.

Title : Modulation of the tumor microenvironment to overcome glioblastoma resistance

Keywords : Immune checkpoint, Glioblastoma, Blood Brain Barrier, ABC proteins

Glioblastoma (GBM) is the most frequent and the most aggressive primary brain cancer in adults. The current standard of care of newly diagnosed GBM includes maximal safe surgery followed by concurrent temozolomide (TMZ) and radiotherapy followed by adjuvant TMZ. Despite this intensive therapeutic regimen, the median overall survival is below 18 months. One of the main limitations of current anti-tumor treatments is the blood-brain barrier and the local immunosuppressed microenvironment typical to the setting of brain cancers. This thesis is focused on overcoming the blood-brain barrier to modulate local immunity to better anti-tumor treatments. Firstly, we reviewed the role of ABC proteins superfamily members expressed in the BBB cells and their role in GBM resistance to chemotherapy. Secondly, we have studied the expression of immune checkpoint proteins CD80 and CD86 and their impacts on the outcome in newly diagnosed glioblastoma patients treated with the standard of care. CD86 overexpression is associated with a better prognosis. Finally, we have shown the dramatic efficacy of immune checkpoint inhibitors targeting PD-L1 when combined with ultrasound-mediated BBB opening in glioblastoma-bearing mice compared to anti-PDL1 alone. BBB opening combined with immunity modulators are promising strategies to improve our therapeutic arsenal against glioblastoma.